# THE EFFECT OF CATALYST ZONING ON HYDRODEMETALATION OF A PETROLEUM RESIDUE

By

HASAN MOHAMAD QABAZARD

Bachelor of Science

The University of Tennessee

Knoxville, Tennessee

1979

Submitted to the Faculty of the Graduate College
of the Oklahoma State University
in partial fulfillment of the requirements
for the Degree of
MASTER OF SCIENCE
December, 1986

THE EFFECT OF CATALYST ZONING

ON HYDRODEMETALATION OF

A PETROLEUM RESIDUE

Thesis Approved:

Billy L. Crynes
Thesis Adviser

Mayis Seapan

Arland H. Johannes

Norman N. Durham
Dean of the Graduate College

# PREFACE

This study was concerned with the effect of catalyst zoning on the hydrodemetalation of a petroleum residue. A residue was hydrodemetalized over combinations of commercial Ni-Mo-$Al_2O_3$ catalysts in a two-zone, trickle-bed reactor system. Experiments were carried out varying catalyst activity in both the top and the bottom zones. The hydrodemetalation activities of five catalyst combinations were examined at 380°C, 10.3 MPa, and 1.0 $h^{-1}$ LHSV for 72 h. Analyses were performed on liquid products, and on spent and regenerated catalysts in an effort to determine the optimum hydrodemetalation combination.

Metal removal activities and coke deposition rates in graded catalyst beds were favored by higher total promotor and active metals contents and larger catalyst pore diameters. The upstream hydrodemetalation catalysts minimized physical property loss in the downstream catalyst in spite of increasing its coke content. Boiling point reduction activities were also favored by increasing the total promotor and active metals contents in graded catalyst beds.

I am especially indebted to my major advisor, Professor Billy L. Crynes for his intelligent guidance, concern, and invaluable help throughout my study. I am also thankful to Mr. R. Adarme for the excellent friendship and cooperation during the phases of this project. A special note of thanks to Mr. C. Baker for the invaluable assistance in the procurement of materials. A note of appreciation is also extended to the members of my thesis committee, Drs. M. Seapan and A. H. Johannes.

I am in great appreciation of Messrs. H. Wandke, J. L. Liu, L. Crynes, Randy Smejkal, and David Tice for their help in operating the experimental equipment. I would also like to take the opportunity to thank all of the faculty and staff at the School of Chemical Engineering for the advisement, cooperation, and understanding in the course of this work. A special note of appreciation to Mrs. Pamela Hartman for typing this manuscript.

I am deeply indebted to the valuable support and encouragement from the Kuwait Institute for Scientific Research. Financial support from the School of Chemical Engineering is appreciated.

I am thankful to the unforgettable friendship, encouragement and company of Dr. Saed Akashah, Dr. Suhal A-Fulaij, Meena Marafi, Haitham Al-Husaini, A. Arman, M. Abu-Arabi, S. L. Kuo, and Jeff and Marianne Mathis.

My father, who introduced me to the subject of engineering, my mother, my brothers and my sisters deserve my deepest love and appreciation for their constant support, moral encouragement, and understanding.

TABLE OF CONTENTS

LIST OF TABLES

LIST OF FIGURES

# CHAPTER I

## INTRODUCTION

Environmental restrictions on fossil fuels and deteriorating crude oil qualities have given substantial incentives for the development of specialized catalysts and reactor technologies for residue upgrading. Hydrotreating reactor zoning, operating different reactor zones with different catalyst properties, is an attempt to control upgrading costs and product quality. By properly balancing catalyst physical and chemical properties, activity decline inflected by poisons could be reduced and catalyst life could be prolonged. Petroleum residue upgrading objectives can vary; constraints imposed by its metal content must be weighed carefully to develop a practical choice in the selection of the catalysts.

In this set of experiments, a representative petroleum residue with a moderate metal content was hydrotreated using a trickle-bed reactor system with multiple catalyst zones. Three commercially available Ni-Mo-$Al_2O_3$ catalysts of different physical and chemical properties were used in five reactor-zoning combinations. The following objectives were addressed:

1. Evaluation of the effect of catalyst activity zoning on metal removal.

2. Comparison of the activities of the different catalyst zoning combinations for residue boiling point reduction.

3. Evaluation of the effect of zoning on spent catalyst coke content.

4. Study the effect of zoning on changes in the catalyst physical properties.

5. Investigation of the effect of zoning on metal deposition profiles within the catalyst bed and on the catalyst particles.

# CHAPTER II

# LITERATURE REVIEW

From the vast literature available on petroleum residue hydrotreating in general, and hydrodemetalation in particular, only the topics most closely related to the present study were discussed. These topics included:

1. Hydrotreating catalyst zoning.
2. Properties of petroleum residue.
3. Petroleum residue hydrotreating reactions in general, and hydrodemetallation reactions in particular.
4. Hydrotreating and hydrodemetallation catalysts.
5. Operating conditions.

## Catalyst Zoning

Improved hydrodemetalation (HDM) catalysts are reported to be most suitable for use upstream from active hydrotreating (HDT) catalysts in separate guard beds or in a graded catalyst system (Green and Broderick, 1981; Howell et al., 1985). The preliminary HDM step allows metal deposition to be the controlling deactivation mechanism while offering extended catalyst life (Bowes et al., 1984). Bimodal catalysts are also recommended to provide the necessary surface area and pore volume for HDM activity (Christman et al., 1985; Howell et al., 1985).

Guard beds consist of HDM catalysts placed in the entrance section of the reactor or in a separate vessel upstream of the main HDT catalyst bed (Green and Broderick, 1981). The catalyst may be a nearly spent catalyst. Possibly, it could be a lower cost version of the main catalyst, or a bed of adsorbants. Inexpensive guard beds made of scavenged, porous material with large diameter pores have been successfully used (Sei, 1980; Dooley and Crynes, 1985). Using a guard bed of HDM catalysts, Kwant et al. (1984) observed a 50 to 60% reduction in the residue metal content. Leach (1983a) reported reductions in the pressure drop rate with the use of trash baskets and guard reactors.

The higher operating severities required for heavy residue HDT result in very steep and uneven deposition profiles along the reactor length (Tamm et al., 1981; Green and Broderick, 1981). For optimum catalyst use, all positions in the bed should deactivate at the same rate. This requires the catalyst properties to be a function of bed height (Jacobsen et al., 1983). Several groups have described graded catalyst beds (Nielsen et al., 1981; Curtis et al., 1985; Howell et al., 1985). The graded catalyst bed is usually tailored by placing a low activity HDM catalyst upstream of a more active HDT catalyst (Howell et al., 1985; Gibson et al., 1983). Overall bed composition is designed for minimum bed volume at the desired conversion with equal fouling rates at all positions (Kwant et al., 1984). By properly balancing heteroatom removal and HDM activities, a graded catalyst bed can improve conversion and dramatically increase run length (Gibson et al., 1983; Higashi et al., 1985). Metal removal and the resulting asphaltene conversion allow milder conditions in the downstream HDT bed (Kwant et al., 1984). Severity limits of the downstream bed can also be pushed

upwards because of the removal of metal and coke precursors (Nielsen et al., 1981). Kwant et al. (1984) recommended dual catalyst beds for feed metals between 25-50 ppm, triple catalyst beds from 50-100 ppm and on stream catalyst replenishment for higher metal contents.

Sikonia (1980) hydrotreated a heavy residue over a dual catalyst bed. An HDM catalyst with good HDT activity was placed up stream of a highly active HDT catalyst. He reported increased unit efficiency and improved conversions with excellent distillate qualities even at higher severities. The first stage temperature was kept somewhat higher than that of the second stage. Jacobsen et al. (1983) established that the advantages of using multiple catalyst beds increase with increasing residue metal content and decreasing heteroatom reactivities. They recommended catalyst particle-size grading and void fraction grading for higher metal accommodation. Higashi et al. (1985) reported that although the initial activity of the graded bed is lower, its life is twice that of any single HDT catalyst bed. Gibson et al. (1983) used graded catalyst hydrotreating and concluded that by properly balancing heteroatom removal/HDM activities, conversion and life are improved over any single catalyst. They claimed 70% longer runs and recommended using non-cylindrical catalyst shapes. Banta (1984) patented the designs of dual and triple catalyst bed hydrotreaters. He used small and large pore diameter, quadrulobe shaped catalysts.

Green and Broderick (1981) carried out HDT of high metal feeds using dual and triple catalyst bed reactors. The reactors were designed for uniform fouling rates and high heteroatom conversion. They sited the merits of graded beds to be minimized by the limited available reactor volume. Relatively high HDT activity was sacrificed by using

the upstream HDM catalyst. Run length was determined by the upper temperature limit rather than by deactivation. Howell et al. (1985) emphasized this necessary trade-off between metal tolerance and conversion activity. They added that the full potential of grading can only be realized if adequate reactor volume is available. They used a system of two graded catalyst beds with HDM/HDT catalysts to upgrade very high metal feeds. Much higher initial temperatures were required for the desired activity. However, despite the initial reduction in activity, longer runs were sustained. Howell et al. (1985) concluded that the use of lower activity HDM catalysts will decrease product quality. Nielsen et al. (1981) used a 50% (volume) HDM pretreatment stage to minimize deactivation in subsequent HDT. Lower activity in the HDM stage required 25°C higher operating temperature to achieve the desired conversion. They concluded that higher operating severities led to lower utilization of the catalyst volume. However, Sosnowski and Turner (1981) operated the second HDT stage at temperatures significantly lower than in a single stage unit and well below any temperature that might impose thermodynamic limitations.

For lower coke production, Berg et al. (1983) recommended low temperature saturation of a high nitrogen content residue using a Ni-Mo/$Al_2O_3$ catalyst prior to high temperature HDT. Kokai et al. (1985) upgraded a high nitrogen-content residue using acidic/basic composite catalyst beds. They observed hydrodenitrogenation (HDN) activity to decrease in the following order: acidic/basic > acidic >> basic. Johnson and Tolberg (1983) upgraded a high-metal, high-nitrogen content shale oil by using an alumina pretreatment stage. They obtained higher

HDN activity with the initially-saturated, metal-free oil. Sikonia et al. (1983) also described HDM/HDN sequencing in shale oil upgrading.

Curtis et al. (1985) used two-stage reactors for coprocessing coal liquids with petroleum residua. Two sequences of inexpensive pyrite/Ni-Mo and Ni-Mo/Ni-Mo catalysts were tailored to optimize coal conversion and oil production. Conversions of the two sequences were found to be comparable, but the products from the pyrite/NiMo sequence were of slightly better quality. Bhan (1981) compared the reactivities of Co-Mo/$Al_2O_3$ and Ni-Mo/$Al_2O_3$ catalysts of similar pore diameters and their zonal combinations. He discovered no advantage in this type of grading in HDN of a coal liquid. Bhan (1983) used combinations of large and small pore size catalysts in coal liquids HDN. He also found no advantage in graded beds over single beds in HDN activity or deactivation. He recommended a low temperature section (260°C) for inorganic and carbonaceous residue removal prior to a higher temperature (400°C) HDN section. Beazer and Crynes (1985) hydrodenitrogenated a coal liquid using a high temperature reactor section (400-500°C) upstream of a low temperature section (400°C). Conversion was increased by increasing top section temperature, but early unacceptable coke deactivation was a problem for temperatures over 450°C.

This section on graded catalyst beds can be summarized as follows:

1. HDM catalysts are reported to be most suitable upstream from active HDT catalysts in separate guard beds or, in a graded catalyst bed.

2. Guard beds were used to reduce feed metal content and achieve reductions in pressure drop rates.

3. Graded catalyst beds are tailored by placing a low active-metal, HDM catalyst upstream of a very highly active HDT catalyst. The overall bed composition is designed for minimum bed volume at the desired conversion with equal deactivation rates at all positions.

4. By properly balancing heteroatom removal and HDM activities, a graded catalyst bed can improve conversion and increase run length.

5. Graded bed technology is also extended to shale oil and coal liquid upgrading and to temperature zoning.

## Properties of Petroleum Residue

Petroleum residue is a mixture of highly asphaltic molecules with a boiling point range between 350 to 600°C (650 to 1100°F). This refractory mixture is influenced by a large proportion of sterically-hindered, aromatic, heteroatom molecules. Consequently, residue constituents are nearly impossible to separate and identify (Richardson and Alley, 1975; Shiroto et al., 1983; Patmore et al., 1981). Petroleum residue is deficient in hydrogen; its hydrogen-to-carbon (H/C) atomic ratio does not exceed 1.5 (Bridge et al., 1981). Typical petroleum residue may contain the following:

up to 1 wt% mineral matter

up to 12 wt% asphaltenes

up to 1300 ppm vanadium, nickel and iron

4 to 5 wt% sulfur

up to 1 wt% oxygen

up to 1 wt% nitrogen.

Small amounts of copper, zinc and sodium are also found in some feed-stocks (Patmore et al., 1981; Shiroto et al., 1983).

Abbott et al. (1958) separated residue constituents into paraffins, naphthenes and aromatics. The paraffins are mixtures of both normal and branched alkanes, covering the molecular weight range. The naphthenes contain one or more 5- or 6-membered saturated rings. They may be separated or condensed. Paraffinic side chains give them some paraffinic character. Aromatics may be monoaromatics or polyaromatics with naphthenic rings and paraffinic side chains. McKay and Latham (1981) separated residue constituents into five fractions: acids, bases, neutral nitrogen compounds, and saturated hydrocarbons. Acids include phenols, carboxylic acids and pyrolic compounds. Bases include pyridines and amides that titrate as bases. Neutral nitrogen fractions also contain amides and pyrolic compounds. Schucker (1983) separated a petroleum residue into asphaltenes, polar aromatics, aromatics and saturates. He reported aromatics to be twice as reactive as asphaltenes or polar aromatics. Asphaltenes and polar aromatics contain much more nitrogen and sulfur functionalities and have higher molecular weights.

Sulfur is a major heteroatom (Rollman, 1977), and is found to be evenly distributed amoung compound classes with the exception of the saturated hydrocarbons which contain only traces (McKay and Latham, 1981). Sulfur compounds are usually lumped into aliphatic and thiophenic sulfur (Tarhan, 1983). The majority of the sulfur is contained in the thiophenic molecules which are concentrated in the highest boiling fractions (Schuit and Gates, 1973).

Nitrogen compounds appear in smaller concentrations than do sulfur compounds. Nitrogen compounds are not well characterized. They appear almost exclusively in 5- and 6-member ring-heterocycles (Rollmann, 1977). Inherent basicity is a distinguishing feature of most of these

compounds. They adsorb very strongly on catalyst acid sites thus deactivating these sites (Nagai et al., 1986; Ware and Wei, 1985a). Basicity also results in a $\sigma$- donor interaction of nitrogen with transition metals (Choi and Dines, 1985). The nitrogen atom free electrons coordinate in petroporphyrins to chemically trap metals and hold them firmly in place (Leach, 1983a).

Oxygen is not a significant component in petroleum residue (Rollmann, 1977). It is present in the medium boiling range fractions and in asphaltenes (Satterfield, 1980).

Metals in petroleum residue are generally associated with the heavier asphaltene constituents (Sie, 1980). They are present as organic complexes involving heteroatoms in functional groups. Metal concentrations are relatively small and they do not correlate with the distribution of heteroatoms (Jacobs and Filby, 1983).

Vanadium and nickel the most abundant metals, are present in metallo-porphyrin structures as well as in non-porphyrinic complexes. Porphyrins exist in stable homologous-series structures complexed with asphaltenes. Porphyrins are small components compared with the bulk of the metal containing compounds, and porphyrins are also more mobile. Porphyrin concentration in the residue indicates the relative ease of hydrodemetallation (Reynolds et al., 1985).

The majority of the metal containing components are non-porphyrinic, asphaltenic molecules (Jacobs and Filby, 1983). Non-porphyrins are extracted from all molecular weight ranges with some in the porphyrin size range. Non-porphyrins are larger than porphyrins and with different physical and chemical properties (Reynolds et al., 1985). In the asphaltene sheet structure, the non-porphyrins are

complexed in larger size structures through donor-acceptor interaction. The complexation includes porphyrin molecules as well (Jacobs and Filby, 1983). This complexation buries metal sites and decrease reactivity for hydrodemetalation (Reynolds et al., 1985).

The majority of petroleum residue was reported to have higher concentrations of V than Ni. The weight ratio is typically between 5:1 and 10:1 (Tamm et al., 1981; Satterfield, 1980). No more than one-third of the V and possibly one-third of the Ni are present in metalloporphyrin derivatives (Bowes et al., 1984). V occurs in most residua in vandyl ($V{=}O^{2+}$) form coordinated by nitrogen. Vandyl contributes greatly to the association of asphaltenes (Shiroto et al., 1983). V is a stronger catalyst poison than Ni. V compounds are three to five times more reactive but have only one-tenth of the effective diffisivity of the Ni compounds (Tamm et al., 1981). Although Ni porphyrins are of lower polarity than V porphyrins, the two metals are in similar chemical structures. The heteroatom association is similar in nature (Jacobs and Filby, 1983). Ni occurs in most residua as Ni(II) and has lower porphyrin concentrations than V (Ware and Wei, 1985a).

This section on petroleum residue properties can be summarized as follows:

1. Petroleum residue is a mixture of highly complicated molecules. These molecules are deficient in hydrogen and contain various amounts of sulfur, nitrogen, oxygen, and mineral matter.

2. Sulfur is a major heteroatom. Nitrogen compounds appear in smaller concentrations. Oxygen does not appear in significant quantities.

3. Vanadium and nickel, the most abundant metals, are associated with asphaltenic porphrin and non-porphrin complexes.

4. Several procedures were suggested to characterize petroleum residue constituents.

## Petroleum Residue Hydrotreating

Hydrotreating, a high cost process, has become a basic refinery tool (Whittington et al., 1981). HDT is combined with other refinery units to remove impurities, to increase feedstock flexibility and to improve gasoline yield and product quality (Howell et al., 1985). Residue HDT in combination with catalytic cracking was reported to offer the highest return on investment (Hohnholt and Fausto, 1985). This refinery scheme is predominant when transportation fuels are in demand (Christman et al., 1985).

The capabilities of catalytic cracking units are highly influenced by the nitrogen and metal levels on the catalyst. Only by residue HDT can the high molecular weight asphaltenes, porphyrins, and non-porphyrins be effectively processed to reduce heteroatoms and metals (Hohnholt and Fausto, 1985). In addition to heteroatom and metal removal, HDT converts some of the high molecular weight components of the residue allowing improved specific gravities and viscosities while increasing oil volumes (Hohnholt and Fausto, 1984 and 1985). Environmental benefits of using HDT technology result from the production of low sulfur fuels and lower levels of $SO_x$ emission in downstream operations (Bailey and Nager, 1967).

## HDT Reactions

Hydrotreating of petroleum residue consists of contacting the residue with hydrogen in the presence of a catalyst under suitable operating conditions (Leach, 1983a). Because the number of individual HDT reactions that occur simultaneously is so large it is customary to lump them into reaction groups such as hydrodenitrogenation (HDN), hydrodesulfurization (HDS), hydrogenation and hydrodemetalation (HDM). Major gaseous byproducts are methane, hydrogen sulfide ($H_2S$), ammonia, and water (Tarhan, 1983; Beret and Reynolds, 1985).

In the reaction mixture, each component inhibits the reaction rates of other components because of the competitive adsorption on a fixed number of active catalyst sites (Moore and Tyler, 1982). Maximum HDT activity is obtained with reactant molecules rapidly adsorbing on the catalyst surface with only moderately strong bonds (Sinfelt, 1985). The size and complexity of these molecules also inhibit their effective adsorption (Hohnholt and Fausto, 1985). Polar molecules are generally more strongly adsorbed than non-polar ones. As a result, hydrogenated reaction products are less strongly adsorbed than the reactants (Satterfield, 1980).

HDT reactions are largely believed to be first order in the organic reactant (Katti et al., 1984). They probably involve the formation and disappearance of intermediates (Aubert et al., 1986). Molecules interact differently with different reactions; i.e., they inhibit or enhance to varying extents (Satterfield et al., 1985). Nitrogen compounds might inhibit HDS while hydrogen sulfide might enhance HDN (Yang and Satterfield, 1984). HDM and HDS are generally the fastest reactions; they take place with relatively small hydrogen consumption.

HDS is one order of magnitude faster than hydrogenation of a typical aromatic hydrocarbon (Katti et al., 1984). Among sulfur compounds, mercaptans react 10-100 times faster than thiophenes (Hohnholt and Fausto, 1984). HDN and hydrogenation of monoaromatics are among the slowest reactions (Bailey and Nager, 1967). The reactivities of organo-oxygen compounds are poorly characterized (Li et al., 1984).

Under the more rigorous conditions required for the HDT of residue heteroatoms, saturation of most of the non-heteroatom molecules also takes place (Choi and Dines, 1985). The hydrogenation rate is significant. It consumes large quantities of hydrogen and it is limited by thermodynamic equilibrium (Chu and Wang, 1982; Katti et al., 1984). Hydrogenation enhances heteroatom and metal removal and increases the product H/C ratio (Hohnholt and Fausto, 1985). Hydrogen converts hydrocarbons from one functional group to another:

from asphaltenes to polar aromatics

from polar atomatics to neutral aromatics

from neutral aromatics to saturates.

The conversion of polar aromatics and asphaltenes proceeds faster than that of the saturates and aromatics. The last ring of a condensed aromatic is the most difficult to hydrogenate (Thompson and Holmes, 1985). The presence of sulfur on the hydrocarbon molecule was reported to enhance hydrogenation while nitrogen had the reverse effect (Scamangas et al., 1982).

Asphaltene conversion reactions are relatively fast. They greatly reduce metal and heteroatom content while keeping the atomic H/C ratio essentially unchanged (Shiroto et al., 1983). Reaction rates of larger asphaltenes are more rapid (Takeuchi et al., 1979). HDM is closely

related to asphaltene conversion and to the shift of distribution of molecular weights (Asaoka et al., 1983). Metals and heteroatoms in asphaltenes react differently depending on their position in the asphaltenic structure. Metals in the aromatic unit sheet are most refractory (Plumail et al., 1983).

Higher HDT temperatures promote thermal cracking, bond cleavage and the concurrent addition of hydrogen (Hohnholt and Fausto, 1985). Bonds with the lowest energies break first (Maloletnev et al., 1984). Thermal cracking reduces the boiling point and yields more reactor gas (Tsoung-Yuan Yan, 1984). Condensed ring structures undergo thermal degradation and polymerizaton to increased coke (Patmore et al., 1981). Thermal cracking was reported to be relatively minor below 400°C (Bunger, 1985).

## Residue Hydrodemetalation

### HDM Reactions

The dimensions of metal containing asphaltenes are of the same order of magnitude of the catalyst pore size; their conversion which accompanies or preceeds metal deposition is diffusion limited (Howell et al., 1985; Sie, 1980). Consequently, HDM is the least sensitive to intrinsic surface activity (Hung et al., 1986). V and Ni are removed chemically and by physical deposition (Hohnholt and Fausto, 1985). Chemically, metal sulfides accumulate in the pores and interstices of the catalyst particles (Gates et al., 1979). Metal sulfides are catalytically active. Both sulfides of V and Ni act as dehydrogenation agents. The deposits enhance HDM; however, these deposits contribute to asphaltene polymerization and condensation increasing coke and metal deposition by physical means (Hohnholt and Fausto, 1985; Higashi et al.,

1985; Krishna and Bott, 1985; Agrawal and Wei, 1984a).

Metal bearing heteroatoms undergo complicated and competing reactions. Organo-metallic bond cleavage is very fast if pore diffusion is not limiting (Ware and Wei, 1985a). Metal removal was seen to be first order with respect to concentration for large pore catalyst (Garcia and Pazos, 1982; Hohnholt and Fausto, 1984). HDM was seen to be first order for model compounds as well (Higashi et al., 1985). Several authors reported an apparent reaction order greater than one. This was attributed to varying stability and reactivity of organo-metallic compounds (Van Dongen et al., 1980).

Reaction rates for the removal of V, the most predominant metal, is always somewhat larger than that for Ni (Hung and Wei, 1980). V compounds are three to five times more reactive but have less than one-half the effective diffisivity of Ni componds (Tamm et al., 1981). Mohamad et al. (1985) reported that Ni was more easily removed than V at lower temperatures; the reverse is true at high temperatures. Vandyl porphyrins appear to be more polar than Ni porphyrins and have stronger affinity for the catalyst. As a result, Ni compounds pass through the reactor faster than V compounds (Hung and Wei, 1980). Hung and Wei (1980) sited vandyl compounds to supress Ni removal reactions with the reverse suppression less significant.

HDM takes place through complex, consecutive, and parallel reactions with hydrogenated intermediates (Agrawal and Wei, 1984a). Ware and Wei (1985a) suggested a possible reaction mechanism. The porphyrins react via a sequential mechanism: hydrogenaton of peripheral double bonds is followed by the final hydrogenolysis step which fragments the ring and removes the metal. Aromaticity is not

significantly interrupted. Porphyrin basicity and $H_2S$ concentration affect the degree of hydrogenation of different porphyrins. The overall HDM rate-limiting step is different for various porphyrins, but the global mechanism is similar. Steric and chemical factors influence the relative rates of hydrogenation, hydrogenolysis, and the complexity of the reaction pathway. The strength of interaction with the catalyst surface varies for porphyrins and their hydrogenated intermediates (Ware and Wei, 1985a). The HDM of non-porpyrins appears to be less rapid, possibly proceeding with a different mechanism (Reynolds et al., 1985).

Shifts in the overall HDM rate-limiting step are possible (Ware and Wei, 1985c). Nitrogen inhibits the hydrogenation of organo-metallic compounds. Catalyst sulfiding strongly enhances ring cleavage and shows less enhancement on hydrogenation (Ware and Wei, 1985b). Water vapor, added as such or generated in-situ, inhibits HDM (Tsoung-Yuan Yan, 1984). Cesium and sodium lower catalyst HDM activity and inhibit the metal deposition step. Iodine and chlorine promote metal deposition (Ware and Wei, 1985c).

## Metal Deposition

The pattern of metal deposition is interesting in catalyst deactivation and HDM kinetic studies (Tamm et al., 1981; Ware and Wei, 1985a). V and Ni compounds diffuse into cylindrical catalysts and deposit near the exterior of the pellet (Pereira et al., 1985). At the entrance of the catalyst bed, a maxima in metal deposition occurs inside the catalyst; the deposition profile is M shaped. At the middle and exit of the bed, the maxima moves to the external surface; metal deposition assumes a U shape (Agrawal and Wei, 1984b). The internal

maxima at the entrance is more pronounced for porphyrins with longer hydrogenation sequences and slower metal-removal steps. At the entrance, no metal depositing species are present in the oil. Organometallic molecules must diffuse and react before forming metal-depositing intermediates (Ware and Wei, 1985a).

Because of the higher reactivities and lower diffusivities of V compound, V deposits are steeper and more U shaped with less deposited in the center than on the edges of the catalyst pellet (Agrawal and Wei, 1984b; Ware and Wei, 1985a). Ni profiles are more uniform across the catalyst's cross-section (Agrawal and Wei, 1984b).

Metal deposition depends on the axial position of the catalyst pellet in the reactor (Ware and Wei, 1985a). The axial gradients of metal concentrations in the fixed bed are steeper for V. The ratio of Ni/V increases from entrance to exit. Metal deposits along the bed are proportional to the concentrations of the intermediate reaction species. The position of the maximum concentration of the intermediates, and hence the metal deposits, depend on the HDM conditions. For high HDM activity conditions (more hours on stream, more reactive feeds, more active catalyst and higher severities), decreasing V profiles are observed along the catalyst bed. For low activity conditions, the maximum V concentration is observed to move downwards (Pazos et al., 1983).

This section on petroleum residue hydrotreating can be summarized as follows:

1. During HDT, a large number of individual reactions occur simultaneously: HDS, HDN, HDM, hydrogenation, etc. These reactions probably involve the formation and disappearance of intermediates.

2. HDM and HDS are the fastest reactions. HDN and the hydrogenation of monoaromatics are among the slowest reactions.

3. During HDM, organo-metallic compounds undergo complex, consecutive, and parallel reactions with hydrogenated intermediates. Organo-metallic bond cleavage is fast if pore diffusion is not limiting.

4. V and Ni are removed chemically and by physical deposition. Metal deposits are catalytically active; they promote metal deposition and dehydrogenation reactions.

5. V removal is much faster than Ni removal. V compounds, however, have lower effective diffusivities than Ni compounds.

6. Metal compounds diffuse into the catalyst and deposit near the exterior of the particle. Ni deposition profiles are more uniform across the catalyst's cross-section.

7. Metal deposition also depends on operating severity and on the axial position in the reactor.

## Hydrotreating Catalysts

Sulfided HDT catalysts remove sulfur, nitrogen, and metals from complex hydrocarbons under the most adverse environments involving catalyst deactivation (Jespen and Rase, 1981). The solid catalysts are non-uniform with varying chemistry and morphology; hence, their activity varies with location on the surface (Satterfield, 1980). Ultimate activity, selectivity, and life of these catalysts are all affected by critical microstructural features. These features include surface area, pore structure, and catalyst particle size (Leach, 1983b).

HDT catalysts are usually mixtures of transition metal oxides (CoO or $NiO_2$-$MoO_3$) dispersed throughout an alumina support ($Al_2O_3$).

Molybdenum is called the "active metal". Ni or Co do not provide significant activity, but they improve the activity of Mo. Ni and Co are called "promoter metals" (Leach, 1983a). Ni and Co do not show the same catalytic activity (Bachelier et al., 1984). Katti et al. (1984) and Friedman et al. (1984) reported Co/Mo catalysts to have higher selectivity for hydrogenolysis than Ni/Mo catalysts. Thakur et al. (1985) cited the two catalysts' hydrogenolysis activities to be compatible, but Ni-Mo was five times more active in hydrogenation. Several authors agree (Johnson, 1983; Berg et al., 1983). Ni-Mo/$Al_2O_3$ commercial HDT catalysts will be discussed.

## Chemical Composition and Surface Morphology

Commercial HDT catalysts typically consist of mixtures of 3-5% $NiO_2$ (by weight) and 9-15% $MoO_3$ on alumina ($Al_2O_3$) support (Yang and Satterfield, 1983). $MoO_3$ is present in a well dispersed phase (Parham and Merrill, 1984). Ni appears in "free" and "fixed" forms (Zielinski, 1982). Alumina is used for its inertness, refractoriness and sintering resistance (Forzatti et al., 1984). HDT catalysts are manufactured in the oxide state; they must be converted to the sulfided state for activation (Leach, 1983a). In the sulfided state, there is a variety of possible morphologies and interactions that may occur between catalyst species. The final surface activity is a result of balanced valance states and chemical bond strengths (Johnstone et al., 1985; Laine et al., 1985). To correlate surface structure with catalytic activity, four models have been proposed: the Intercalation, the Monolayer, the Contact Synergy, and the Ni-Mo-S models (Thakur and Delmon, 1985). The

Ni-Mo-S model is generally preferred. It relates the activity of the catalyst to the amount of Ni associated in a so-called Ni-Mo-S phase (Bachelier et al., 1984; Topsøe and Topsøe, 1983).

Mo ions are believed to be grouped in a bimetallic cluster or a slab arrangement bound to the support (Bachelier et al., 1982). The Ni ions are located at the edges and defect sites of the slabs (Bachelier et al., 1984). The metal is highly dispersed on the support in slabs so small that most of the atoms are surface atoms (Sinfelt, 1985). Electron interactions between the metal and its support can be significant. The size of the clusters depend on this interaction (Leach, 1983b). Their sizes have been reported between 10 and 50 angstroms (Sinfelt, 1985). Increasing the Mo above an optimum level, possibly single atom-layer coverage, has no effect on catalytic activity. For higher Mo concentrations, change in dispersion is likely to occur with enlargement of the Mo clusters and a lower fraction of edge sites present for Ni accommodation (Bachelier et al., 1984; Akhtar, et al., 1985).

Ni-Mo/$Al_2O_3$ catalytic activity is markedly influenced by the presence of the promotor, Ni (Laine et al., 1985). The presence of Ni causes better Mo dispersion (Yang and Satterfield, 1983). Ni ions lose their individuality by association with the edges of the small Mo clusters thus increasing the activity of Mo sites and/or creating new sites (Laine et al., 1985; Bachelier et al., 1984). Upon increasing promoter concentration, activity increases to a maximum. Beyond this maximum, added Ni will have low catalytic participation (Wivel et al., 1981). For high HDT activity, Tischer et al. (1985) reported the

optimum Ni/Mo ratio to be 0.40. Bachelier et al. (1984) reported the optimum Ni/Mo ratio to be 0.60.

Surface Area

The surface area of a typical HDT catalyst is between 100 and 300 $m^2/g$ (Oleck and Sherry, 1984). Kinetic activity is directly proportional to the surface area exposed to the reacting fluids (Choi and Dines, 1985; Tsoun-Yuan Yan, 1984). For different feed compositions, catalytic activity is optimized between surface area and pore structure (Leach, 1983b).

Pore Structure

Pore structure strongly affects catalyst selectivity and life (Tarhan, 1983). Optimum catalyst pore structure depends on the molecular dimensions of the reacting molecules (Tamm et al., 1981). Pore volume is essential for improved diffusion and catalytic efficiency (Itoh et al., 1985). The mechanical properties of the catalyst particles are influenced strongly by pore volume (Leach, 1983b). Pore volume influences coke deposition and metal tolerance (Pazos et al., 1983; Plumail et al., 1983).

Small pore catalysts possess superior heteroatom removal activity because of their higher surface area (Bhan, 1983; Hannerup and Jacobsen, 1983). When coking is the predominant deactivation mechanism, these catalysts lose activity less rapidly due to the exclusion of the coke precursors. Under these conditions, they establish longer lives. Small pore catalysts accumulate less coke than large pore catalysts under identical conditions (Bhan, 1983). When metal deactivation dominates,

small pore catalysts lose activity very rapidly becasue of the low metal capacity and uneven distribution of metals (Jacobsen et al., 1983). Under these conditions, the life of the small pore catalyst becomes considerably short (Kwant et al., 1984). Increasing pore size improves catalyst effectiveness in the presence of metals if the surface area can be maintained (Tischer et al., 1985; Plumail et al., 1983). Catalysts with wide pores and large pore volume have lower heteroatom removal activity but extremely high HDM activity and high tolerance for metal deposition (Kwant et al., 1984; Van Zijll Langhout, et al., 1980; Nielsen et al., 1981). In the presence of metals, large pore catalysts give longer life up to a point. After this point, core poisoning works to reduce life (Hannerup and Jacobsen, 1983). Typical pore diameters of residue HDT catalysts range between 10 and 20 nm (Plumail et al., 1983; Bowes et al., 1984).

Oleck and Sherry (1984) reported that narrowly defined pore size distribution provides overall superior heteroatom removal and HDM activities. Tsakalis et al. (1984) established that catalysts with a more uniform pore size distribution will have higher initial activity. However, as deactivation sets in, the activity of the catalyst with the uniform size distribution will eventually exceed the activity of the non-uniform pore sizes distribution catalyst. Several authors have used bimodal pore size catalysts. Higher coke and metal capacities where obtained (Christman et al., 1985; Howell et al., 1985).

## Particle Size and Shape

Particle size and shape are important in determining catalyst strength, diffusional properties, and catalyst bed hydrodynamics

(Satterfield, 1980; Leach, 1983b). Decreasing particle size increases geometric surface area per unit-reactor-volume, shortens diffusional paths and enhances mass transfer (Rao and Drinkenburg, 1985). Small particles remove more metals per unit-reactor-length and have higher metal capacity (Tamm et al., 1981; Pereira et al., 1985). The improved metal distribution on the smaller particles increases catalyst life (Jacobsen et al., 1983). The optimum particle size depends on feed properties and process severity. The optimum particle size increases with increasing severity (Nielsen et al., 1981). Pressure drop considerations place a minimum limit on particle size (Moyse et al., 1985). Economic limitations also apply as the cost of forming smaller particles is higher (Satterfield, 1980).

The most common form of HDT catalysts is the cylindrical extrudate with particle diameter ranging from 1.6 to 3.2 mm (1/32 to 1/8 inch) (Leach, 1983a). Shaped catalysts are becoming more popular. Shaped catalyst particles possess higher ratio of external surface area per unit volume, higher crush strength and higher metal capacity (Banta, 1984). Shaped catalysts also shorten diffusion paths (Banta, 1984), improve liquid contacting (Satterfield, 1980), and lower the pressure drop build-up rate (Green and Broderick, 1981). The most common shapes are rings (Moyse, 1984), slabs (Rasmuson, 1985), and quadrulobe particles (Banta, 1984).

## Catalyst Sulfiding

The marked structural changes which occur during the sulfiding process are important in determining steady state activity (Laine et al., 1985). The surface of the catalyst undergoes a combination of

reduction and the replacement of oxygen by sulfur. Some oxygen, however, may be retained even after severe sulfiding (Yang and Satterfield, 1983). During sulfiding, the oxide structure is partially destroyed, and the fraction of the free Mo ions increase. The interaction between alumina and the metal is not destroyed (Bachelier et al., 1982). Parham and Merrill (1984) observed a transition of isolated Mo units to small $MoS_2$ like crystallites. The promoter maintains the dispersion of Mo during sulfiding (Laine et al., 1985). Bachelier et al. (1984) suggested that sulfiding enhances the activity of the sites and does not increase their concentrations. Laine et al. (1985) claimed that sulfiding increased Brønsted acid sites. Upon sulfiding, Ware and Wei (1985a) observed strong enhancement in ring cleavage and less enhancement in hydrogenation activity.

Ni/Mo catalysts appear to be non-stoichiometric. They sulfide to a larger extent than their individual components (Parham and Merrill, 1984; Bachelier et al., 1984). This non-stoichiometry is believed to result from the structural defects on the Mo crystallites. These surface defects are related to catalytic activity (Yang and Satterfield, 1983). Generally, the amount of sulfur required for the activation of NiMo/Al catalysts is calculated from the ratio $MoS_2$:$Ni_2S_3$ (Hallie, 1982). This amount was called one "theory" by Jepsen and Rase (1981). They recommended eight theories for complete sulfiding. Greater sulfiding not only implies higher activity but also less carbon deposition (Wivel et al., 1981).

Maximum activity and superior performance are obtained by converting the catalyst under controlled conditions (Wivel et al., 1981). Optimum temperature, typically between 300-400°C, could vary

with each catalyst (Banta, 1984; Tischer et al., 1985). Higher temperatures redistribute Mo ions and immobilize Ni ions thus lowering activity (Bachelier et al., 1984). Lower heating rates, 25-50°C/h, are also recommended (Anderson et al., 1980; Hallie, 1982). Slow heating rates preserve surface area by minimizing support sintering (Leach, 1983b). Higher heating rates appear to drive Ni deeper into the support and away from the Ni-Mo active phase (Topsøe and Topsøe, 1982). Hallie (1982) found little effect of pressure on the final activity of the sulfided catalyst. However, Yang and Satterfield (1983) concluded that higher steady state activity is achieved by sulfiding at higher pressures or for longer durations or both.

## Catalyst Deactivation

HDT catalysts decline in activity with time on stream. Deactivation mechanisms severely reduce catalyst pore volume and surface area which lead to modifications in reaction kinetics (Tsakalis et al., 1984). Several modes of deactivation such as sintering, irreversible poisoning, and metal and coke deposition, occur simultaneously (Kittrell et al., 1985; Johnstone et al., 1985).

Sintering is an important phenomenon in metallic catalysts. It is an irreversible phenomenon caused by support phase changes resulting from too high temperatures (above 700°C). Sintering degrades the physical characteristics of the particles (Leach, 1983b). It drastically reduces catalytic surface area leading to catalyst deterioration and crumbling (Satterfield, 1980; Friedman et al., 1984). Solid state reactions which usually accompany sintering change the chemical nature and composition of the catalyst constituents

(Forzatti et al., 1984). Poisons such as sodium salts and metal sulfides promote catalyst sintering (Collins et al., 1985).

Poisoning involves chemisorption of impurities on active sites (Leach, 1983a). Poisons also promote secondary reactions and lower selectivity by distributing themselves progressively downstream of the catalyst bed (Satterfield, 1980). Principal poisons are nitrogen, sulfur, metals and coke (Kittrell et al., 1985).

An active catalyst polymerizes the residue depositing adhesive carbonaceous matter (coke) on its surfaces. The diffusion of carbon and depositing metals was also reported to take place (Johnstone et al., 1985; Kuzeev et al., 1984). Coke deposition obstructs pore structure and drastically reduces activity (Katti et al., 1984). Coke deposition increases early in the run to an equilibrium level (Hannerup and Jacobsen, 1983). Coke equilibrium is related to the hydrogenation-dehydrogenation equilibrium and to metal deposition (Agrawal and Wei, 1984b; Krishna and Bott, 1985). Coke deposits distribute evenly over the catalyst bed (Sie, 1980). In-situ hydrogen sulfide apparently reduces coke formation (Seapan and Crynes, 1985).

Metal deposition controls catalyst life (Tamm et al., 1981; Green and Broderick, 1981). Unlike coking, metal deposition is nearly constant with time (Agrawal and Wei, 1984b). Metal deposition poisons the active surface and obstructs the pores of the catalyst (Kwant et al., 1984; Hohnholt and Fausto, 1984). Metal deposition leading to catalyst pore plugging appears as a wave which moves down the catalyst bed with increasing catalyst age (Moyse, 1984). Severe deposition between particles could completely block the catalyst bed (Kwant, et

al., 1984). Metal deposits also act as dehydrogenation agents promoting coke and gas yield while lowering selectivity (Krishna and Bott, 1985).

The relative rates of coke and metal deposition, the two main deactivation mechanisms operating simultaneously, determine the shape of the deactivation curve (Nielsen et al., 1981). Three zones could be identified on this curve: a period of rapidly decreasing activity, followed by a period of nearly constant rate, and a final period of rapidly accelerating deactivation (Leach, 1983a; Nielsen et al., 1981). The initial and final deactivation periods each constitute about one-quarter of the catalyst life; the constant deactivation period constitutes about one-half (Tamm et al., 1981). The extent of initial decline in activity is attributed to the combined effects of coke and metal deposits and the adsorption of poisons. The gradual deactivation is caused by the steady build up of coke and metals on the catalysts' surfaces (Agrawal and Wei, 1984b). Pore mouth poisoning is believed to play a major role in the initial deactivation; therefore, pore mouth plugging is probably responsible for the gradual deactivation (Sei, 1980). Tamm et al. (1981) reported that constriction of catalyst pores caused the final deactivation.

In a fixed bed hydrotreater, a deactivation front gradually moves in the direction of the flow (Sei, 1980). Tamm et al. (1981) drew an activity profile for a catalyst bed in the end-of-run condition. They sited the top one-third of the catalyst bed with one-third of the average bed activity. The bottom one-third was relatively unaffected by pore plugging and had sufficient activity. The middle one-third was in a state of transition as metal deposits began to obstruct the pore

structure. The amount of interstitial deposits was reported to decrease along the reactor length (Bhan, 1983).

## HDM Catalysts

There is a direct relationship between pore size, metal capacity, and selectivity for metal removal. With feeds of high metal contents, highly active catalysts with small pore size and large surface area are susceptible to rapid pore plugging. As pore diameter is increased, heteroatom removal activity decreases; however, HDM activity and catalyst metal capacity increase while pore plugging occurs less rapidly. Larger pore size catalysts possess greater metal capacity and higher stability (Howell et al., 1985). Large pore size HDM catalysts can handle up to 100% of the fresh catalyst's weight in deposited metals with negligible interstitial deposits and with lower rates of pressure drop (Higashi et al., 1985; Kwant et al., 1984). By changing pore diameter, catalyts can be tailored to provide the desired heteroatom removal/HDM selectivities (Howell et al., 1985). Green and Broderick (1981) used a catalyst with 15 nm pore diameter to hydrodemetallize a high metal content residue. They observed minimum diffusion restrictions and slower pore mouth plugging.

This section on hydrotreating catalysts can be summarized as follows:

1. HDT catalysts are mixtures of transition metal oxides, CoO or $Ni_2O_3$ and $MoO_3$, dispersed throughout a support, usually alumina. Mo is called the "active metal" and Ni or Co are called "promoter metals".

2. Several models have been proposed to correlate catalytic activity to surface chemistry and morphology.

3. Catalyst activity and life are affected by its microstructural features. For a set of operating conditions, activity is optimized between surface area and pore structure.

4. Particle size and shape are also important in determining catalyst performance.

5. For maximum activity, the catalyst should be sulfided under controlled conditions of temperature and pressure.

6. During HDT, the catalyst simultaneously undergoes several modes of deactivation. Deactivation severely reduces catayst pore volume and surface area and leads to modifications in reaction kinetics.

7. Low active-metal, large pore-size, HDM catalysts possess higher HDM activity, greater metal capacity, and higher stability.

## Operating Conditions

HDT operating conditions determine how hydrogen is incorporated in the residue and, thus, how usable the catalyst is (Beret and Reynolds, 1985). Typical operating temperatures for the HDM of petroleum residue are between 300 and 400°C (575 and 750°F). However, end-of-run temperatures of 440°C are common (Jacobsen et al., 1983). Operating pressures are between 5 and 15 MPa (700 and 2200 psig). The liquid hourly space velocity (LHSV) is usually 1.0 to 5.0 $h^{-1}$ (Geneste et al., 1983; Chillingworth and Potts, 1984; Banta, 1984). Hydrogen flow rates up to 1800 Std. $m^3$ $H_2/m^3$ oil (10000 SCF/BBL) are typical (Oleck and Sherry, 1984).

## Hydrogen Pressure

Hydrogen consumption is the primary operating cost in residue HDT (Hohnholt and Fausto, 1985). Typical hydrogen consumption rates range between 50 and 300 Std. $m^3$ $H_2/m^3$ oil (Nelson, 1977). The liquid must be "over-saturated" with hydrogen to reduce its concentration gradients in the catalyst pores (Van Zijll Langhout, et al., 1980). An excessive hydrogen flow rate maximizes heteroatom and metal removal while minimizing the production of unsaturates and coke. A very low hydrogen flow rate can lead to higher operating temperatures and shorter catalyst life (Leach, 1983a). High hydrogen purity ensures constant hydrogen concentration, reduces deactivation and prolongs catalyst life (Hohnholt and Fasuto, 1984).

There is a linear relationship between hydrogen pressure and the mole fraction of hydrogen in the liquid phase (Hung and Wei, 1980). Increasing hydrogen pressure enhances HDT reactions (Hohnholt and Fausto, 1985; Yang and Satterfield, 1984). This enhancement is especially significant for HDN (Mann et al., 1983). On the other hand, higher hydrogen pressures somewhat accelerate cracking reactions (Beret and Reynolds 1985). Very high hydrogen pressures convert monoaromatics lowering product octane quality (Johnson, 1983).

Operating pressure determines coke deposition equilibrium and the hydrogenation-dehydrogenation equilibrium (Sie, 1980). Coke deposition can be reduced by operating at sufficiently high hydrogen pressure (Kwant et al., 1984). Initial deactivation decreases while coke equilibrium is established at lower temperatures (Nielsen et al., 1981). However, higher pressures increase reactivities of organo-metallic compounds without affecting their diffusivities. This may lead

to pore diffusion interfering with reaction rates (Hannerup and Jacobsen, 1983; Woerde et al., 1982). Higher pressures move the position of the maximum metal deposition to the outer edge of the catalyst particles thus accelerating pore plugging and decreasing catalyst life (Pazos et al., 1983). At lower pressures, improved metal distribution and increased metal capacity lower the rate of deactivation (Agrawal and Wei, 1984b). Given process requirements and a catalyst, there is an optimum pressure that yields optimum metal distribution (Jacobsen et al., 1983).

## Temperature

Higher temperatures enhance hydrogenolysis, hydrogenation, and overall HDT activity (Mann et al., 1983; Beazer and Crynes, 1985; Mohamad et al., 1985). Consumption of hydrogen and the product H/C ratio are higher at increased temperatures (Bunger, 1985). Because hydrogenation reactions are reversible, conversion is limited at higher temperatures by thermodynamics (Chu and Wang, 1982). By increasing temperature, polynuclear-aromatic saturation increases to a maximum after which dehydrogenation becomes more significant (Beazer and Crynes, 1985). Temperatures above 350°C were reported to decrease thermal stability of the residue (Bunger, 1985). The transformation of asphaltenes is more rapid above 375°C; however, diffusional restrictions still persist. With increasing temperatures, product quantity increases but its quality declines (Howell et al., 1985).

The deactivation rate is a function of temperature (Buzzi-Ferraris et al., 1984). Excessive temperatures promote dehydrogenation and coke formation (Hohnholt and Fausto, 1985). Higher temperatures also

increase the adhesive strength of coke (Kuzeev et al., 1984). The metal capacity of the catalyst decreases at higher temperatures (Hannerup and Jacobsen, 1983). At higher temperatures, the uneven metal deposition on the outer catalyst surfaces promotes rapid pore plugging and shortens catalyst life. Lowering the temperature moves the maximum metal deposition into the catalyst pellet and axially away from the bed entrance. Consequently, better metal distribution and higher catalyst metal capacity results (Pazos et al., 1983; Tamm et al., 1981). Since chemical/physical transformations break-up and disable the catalyst, these transformations also impose constraints on the maximum temperature (Lee, 1982).

## Liquid Hourly Space Velocity

LHSV is a superficial measure of capacity usually calculated from inlet conditions. It is defined as the liquid flow per hour per volume of catalyst (Satterfield, 1980). Decreasing LHSV increases contact time; hence, decreasing LHSV increases HDM rates (Hohnholt and Fausto, 1985). The rate of HDM is inversely proportional to LHSV (Satterfield, 1980). Howell et al. (1985) reduced LHSV of residue HDT run by one-half and recorded four times longer catalyst life and more metal accumulation. Because of the higher superficial liquid velocities used, industrial scale reactors are more efficient than laboratory reactors. Keeping LHSV constant and increasing superficial liquid velocity in laboratory scale reactors will increase transfer rates and improve reactor efficiency (Garcia and Pazos, 1982; Ruether et al., 1980).

This section on operating conditions can be summarized as follows:

1. Higher hydrogen pressures enhance conversion but promote rapid pore plugging. Given process requirements and catalyst, there is an optimum pressure with a corresponding optimum metal distribution.

2. Higher operating temperatures increase conversion and catalyst deactivation rates. Dehydrogenation reactions become significant at higher temperatures as well.

3. HDM is inversely proportional to LHSV, the superficial contact time.

# CHAPTER III

# FEEDSTOCK AND CATALYST PROPERTIES

## Liquid Feedstock

Vacuum gas oil (VGO) and vacuum residue (VR) were received from CONOCO's Ponca City refinery. A mixture of 50 vol% VR in VGO was prepared by slowly mixing the VR in the VGO at 100°C. Table I presents the physical and chemical properties of the resulting residue. Distinctive features of this feed are its low sulfur content and moderately high nitrogen content. Its metal content is considered intermediate. The feedstock was prepared in the above manner to tailor a residue with a reasonable metal content to accent differences in the HDM activities of the different catalyst bed combinations used in this work. Feed properties were also tuned for ease of pumping in the available equipment.

## Fresh Catalyst

Three commercially available Ni-Mo-$Al_2O_3$ catalysts, Haldor Topsøe HT-TK-711, HT-TK-751, and HT-TK-771 were used. Table II presents the chemical compositions and physical properties of these catalysts. The three catalysts are presented in the order of increasing active metal, promotor metal and surface area. They are presented in the order of decreasing pore volume and average pore diameter. These new catalysts, which have never been tested in our laboratories, were recommended by

TABLE I

FEEDSTOCK PROPERTIES

| | |
|---|---|
| Specific Gravity at 16°C | 0.996 |
| API Gravity at 16°C | 10.6 |
| Elemental Analysis (%) | |
| S | 0.90 |
| N | 0.32 |
| C | 84.98 |
| H | 13.12 |
| Oxygen + Ash (by difference) | 0.68 |
| Metals (ppm) | |
| Ni | 43 |
| V | 58 |

| ASTM D-1160 Distillation* Volume Distilled (%) | Normal Boiling Point (°C) |
|---|---|
| IBP | 380 |
| 5 | 413 |
| 10 | 438 |
| 15 | 455 |
| 20 | 468 |
| 25 | 480 |
| 30 | 492 |
| 35 | 504 |
| 40 | 516 |
| 45 | 527 |

*Data corrected from 1.33 kPa (10 mmHg) to atmospheric pressure using ASTM D-2892 charts for petroleum hydrocarbons.

TABLE II

FRESH CATALYST PROPERTIES
(VENDOR)

| | HT-TK-711 | HT-TK-751 | HT-TK-771 |
|---|---|---|---|
| Main Functions | HDM | HDS/HDM | HDS |
| Chemical Composition (wt%) | | | |
| NiO | 2.0 | 2.3 | 3.4 |
| $MoO_3$ | 6.0 | 10.0 | 14.0 |
| $Al_2O_3$ | Balance | Balance | Balance |
| Physical Properties | | | |
| Geometry | 1.6 mm (1/6") Extrudates | | |
| Surface Area x $10^{-3}$, $m^2/kg$ | 140 (194*) | 170 (217*) | 200 (238*) |
| Pore Volume x $10^3$, $m^3/kg$ | 0.57 (0.79*) | 0.58 (0.78*) | 0.47 (0.53*) |
| Bulk Density, kg/L | 0.64 | 0.64 | 0.73 |
| Most Frequent Pore Diameter (MFPD), nm | 15.3 | 13.8 | 9.0 |
| Pore Size Distribution | | | |
| Pore Diameter Range, nm | % Pore Volume | | |
| 0 - 8.0 | 1.3 | 2.0 | 12.8 |
| 8.0 - 12.0 | 6.2 | 14.3 | 81.8 |
| 12.0 - 16.0 | 31.2 | 43.7 | 2.6 |
| 16.0 - 20.0 | 31.5 | 19.0 | 0.8 |
| 20.0 - 25.0 | 14.2 | 10.5 | 0.5 |
| 25.0 < | 15.6 | 10.5 | 1.5 |

* Determined in our laboratory.

the vendor for use in zoned catalyst beds. These markedly different catalysts were selected in order to clearly detect differences in catalytic activities of the different catalyst bed combinations.

Catalyst HT-TK-771 has relatively small pores with a very uniform pore-size distribution. This catalyst also possesses high active metal and promotor metal contents. This catalyst is said to be more active for heteroatom removal. HT-TK-771 was recommended by the vendor for use in the final stage of a zoned catalyst system. In this study, catalyst HT-TK-771 is called the HDS catalyst.

Catalyst HT-TK-711 was recommended by the vendor for use as a pretreatment stage in graded catalyst beds. This catalyst is said to be tailored for high HDM selectivity and increased metal capacity. Catalyst HT-TK-711 has a relatively wide pore structure with a non-uniform pore-size distribution. HT-TK-711 also has low active metal and promotor metal contents. Catalyst HT-TK-711 will be called the HDM catalyst.

Catalyst HT-TK-751 is an intermediate version. It contains intermediate active metal and promotor metal contents. HT-TK-751 will be called the HDS/HDM catalyst. This HDS/HDM version also possesses a wide pore structure with a uniform pore-dize distribution. The most frequent pore diameter (MFPD) of this catalyst is slightly smaller than that of the HDM catalyst. The HDS/HDM catalyst was recommended as an intermediate stage in graded catalyst beds.

Catalyst properties determined in our laboratories were different from the ones supplied by the vendor. This was possibly due to variations in equipment calibration or because of different instruments

and/or analysis methods used. Throughout this study, our data were used as a basis for comparison.

# CHAPTER IV

# EXPERIMENTAL EQUIPMENT AND ANALYSIS TECHNIQUES

## Reactor System and Experimental Procedure

A schematic diagram of the two-stage, trickle-bed reactor system used in this study is shown in Figure 1. This system was used earlier by Bhan (1983) and Beazer (1984). The only modification made here was heater tracing of feed and product lines to serve as feed preheating and to prevent line restriction by heavy residue.

Feed residue and hydrogen gas flowed cocurrently down the packed reactors. A continuous residue flow rate of 35 $cm^3/h$ was provided with a RUSKA positive displacement pump. Hydrogen was supplied from a cylinder to the top of reactor 1 through valve 1. Hydrogen pressure was controlled with a pressure regulator at 10.3 MPa (1500 psig). The flow of hydrogen was controlled at 1781 Std. $m^3$ $H_2/m^3$ oil (10000 SCF/BBL) by means of a high pressure flow meter and needle valve 10. Product oil and gas passed through the high pressure sample bombs where they were separated. The gases were scrubbed with a 50 vol% ethanolamine solution prior to venting. Temperatures of the reactors were separately controlled by two temperature programmer/controllers. Temperatures were monitored both inside the catalyst beds and outside the reactor walls.

Detailed descriptions of the reactor system and the experimental procedure are given in Appendices A and B.

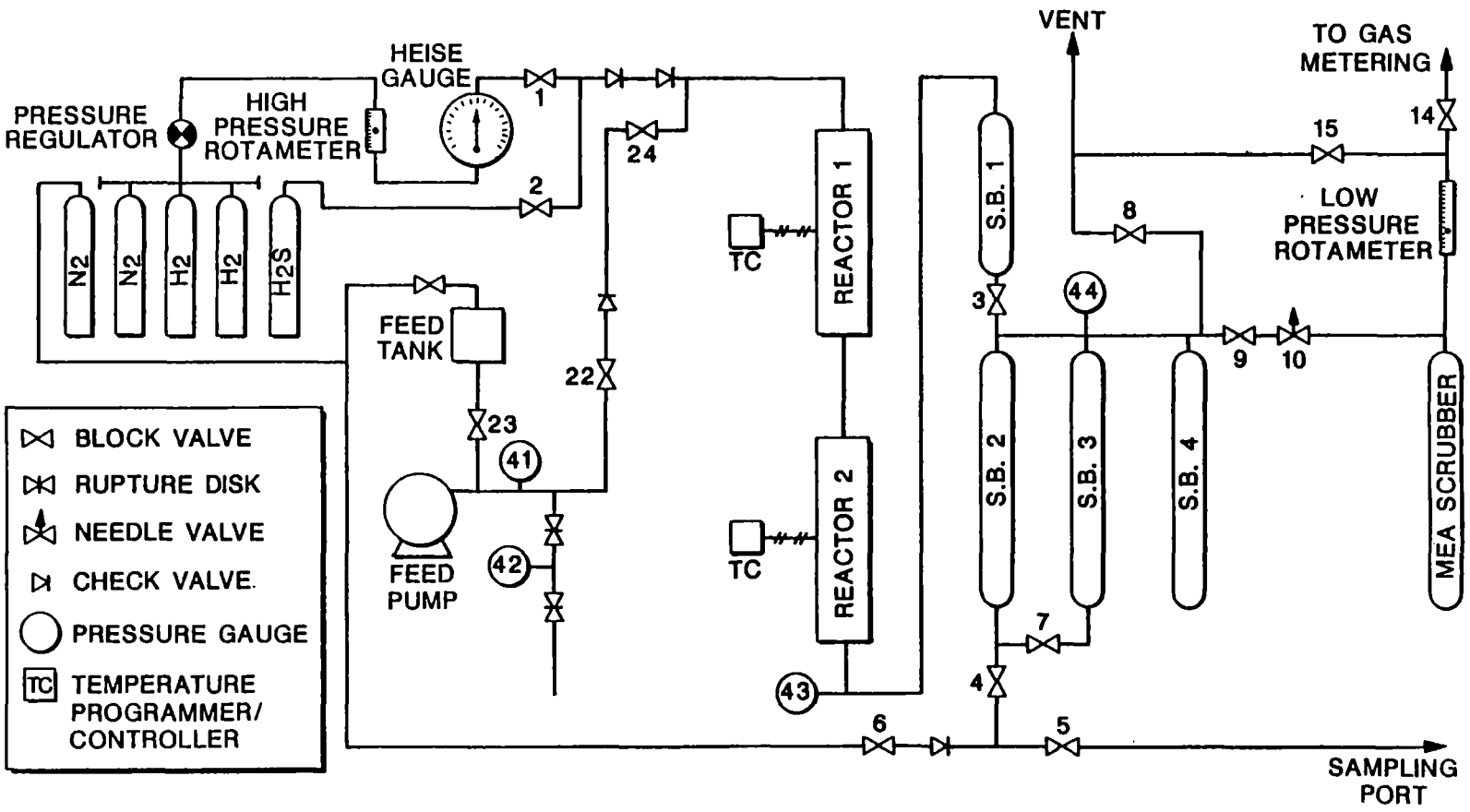


Figure 1. Process and Instrument Diagram of the Experimental Apparatus

Oil samples were collected every 6 h from sample bomb 2. After each run, the reactors were cut and the catalysts in each reactor were divided into four sections called, from top to bottom, 1Q, 2Q, 3Q, and 4Q.

## Product Characterization

Product liquid samples from all runs were analyzed for their vanadium and nickel contents. No equipment capabilities were availbale for the measurement of iron content. The 42 h product sample from each run was fractionated using procedures described in ASTM D-1160.

### Metal Analysis

Vanadium and nickel concentrations were measured in feed and product samples. The analytical equipment consisted of a Perkin-Elmer Model 403 double beam atomic absorption spectrophotometer and a Perkin-Elmer graphite furnace. Nickel and vanadium standards were purchased from Fisher Scientific Company. Standard solutions and samples were prepared by dilution with methyl-isobutyl ketone.

### ASTM D-1160 Distillation

The residue feed and the 42 h sample from each run were subjected to ASTM D-1160 distillation (Annual Book of ASTM Standards, Volume 05.01, 1985). 100 $cm^3$ of sample was fractionated at 1.33 kPa (10 mmHg) pressure. Vapor temperature was recorded versus percent volume distilled. Temperatures were corrected to atmospheric pressure by using ASTM D-2892 charts for petroleum hydrocarbons.

## Catalyst Characterization

Spent catalysts taken from the four sections in each reactor were extracted for 24 h with tetrahydrofuran in a Soxhlet extraction unit to remove any residual oil. Spent catalysts from each section were analyzed for coke content, and surface area and pore volume before and after regeneration at 600°C for 24 h. Because of the limited availability of the analytical equipment, only 1Q and 4Q catalyst sections from each reactor were analyzed for vanadium deposition.

### Coke Content

Coke content was defined as the percent loss in catalyst weight upon combustion at 600°C and for 24 h. Randomly selected catalyst pellets were weighed at ambient temperature before and after combustion. Coke percent was calculated with respect to the regenerated catalyst weight.

Upon combustion, some catalyst weight reduction porbably resulted from the oxidation of catalytic metal (Mo, Ni) and deposited metal (Ni, V, Fe) sulfides on the surfaces of catalyst pellets. Weight reduction due to metal sulfides' oxidation was estimated.

### Surface Area and Pore Volume

Selected spent and regenerated catalysts from each reactor section were analyzed for surface area, pore volume, and average pore diameter using a Quantachrome Autoscan - 60 Porosimeter.

## Vanadium Penetration

Two randomly selected catalyst pellets from 1Q and 4Q reactor sections were analyzed for vanadium penetration. A JOEL Model JSM-35 Scanning Electron Microscope (SEM) with a Microtrace Model 126-96 Silicon Energy Dispersive X-Ray Spectrometer (EDX) was used. At 60 times magnification of the pellet's cross-section, five small and equal surface areas along the radius of the pellet were analyzed for vanadium deposition. From edge to center, these selected areas were called $S_1$, $S_2$, $S_3$, $S_4$, and $S_5$, respectively. The concentration of vanadium in the selected areas was recorded as "counts". Counts only indicated the existence of V deposits; they gave no indication of the amounts of these deposits.

In metal deposition analysis, only V penetration was studied. The presence of iron in the microscope background and Ni in the fresh catalyst did not permit iron and Ni penetration analaysis.

# CHAPTER V

# PRECISION OF EXPERIMENTAL TECHNIQUES

Reactor performance, and the precision of product and catalyst characterization may have a major effect on experimental data. The performance of this system was previously discussed by Bhan (1983) and Beazer (1984).

## Reactor System Performance

The trickle-bed reactors were designed to give a good approximation to plug flow with minimum effects of back mixing. The reactor length-to-catalyst particle diameter ($L/d_p$) ratio was kept at 130 in both reactors for all the runs. To ensure a turbulent flow regime and to closely approach plug flow, Doraiswamy and Tajbl (1975) suggested an $L/d_p$ of greater than 30. To reduce radial temperature gradients and to ensure isothermality, they suggested a reactor diameter-to-catalyst particle diameter ($D_t/Dp$) ratio of greater than 4. Throughout the experimental runs, a $D_t/Dp$ of 7.5 was used. In addition, emphasis was placed on proper gas and liquid distribution with the use of mesh screens and redistributors. Proper distribution is essential to prevent radial dispersion (Do and Do, 1984).

Relatively good isothermal operation was achieved in spite of operational upsets, especially after sampling. A reactor operating temperature of 380°C was maintained by temperature programmer/

controllers. Variations in temperature with respect to time were less than 1°C for both reactors. In the first experimental run, CVR1, a deviation of 10°C existed between the top and the bottom in both reactors. The heating elements were rearranged afterwards to reduce this deviation to 5°C. Heating block temperatures were held to within 1°C of the desired temperature.

Pressure fluctuations during the experimental runs were also kept at a minimum. Experimental runs were carried out at 10.3 MPa with less than 50 kPa variation. The flow rate of hydrogen was maintained at 1781 ± 20 Std. $m^3$ $H_2/m^3$ oil. The oil flow rate was constant at 35 ± 1 $cm^3$ oil/h.

## Analytical Precision

### Product Characterization

The residue feed was analyzed seven times for nickel content and for vanadium content. The average feed metal content was 43.0 ± 2.5 ppm nickel and 58.0 ± 1.0 ppm vanadium. The nickel content of each liquid product sample was determined three times. Nickel content varied between 25.4 ppm to 34.5 ppm with standard deviations between ± 2.0 ppm to ± 6.0 ppm. These standard deviations were considered too high to facilitate any meaningful comparison between the Ni removal activity of different catalyst combinations. Thus, nickel data were presented for run CVR1 only. Vanadium removal was considered sufficient to describe the HDM process for subsequent runs. Vanadium content of the samples ranged between 21.0 ppm and 37.1 ppm with standard deviations between ± 0.4 ppm and ± 2.1 ppm. The higher standard deviations resulted from the determination of vanadium content on a nitrous-oxide flame in the atomic

absorption apparatus. The majority of the samples were analyzed using a graphite furnace. This kept standard deviations below ± 1 ppm.

The residue feed was distilled using the ASTM D-1160 method three times. The normal boiling point curves for the three runs were within 5°C deviation from each other. Because of the large liquid volume required for the distillation, product liquid samples could be distilled only once.

Catalyst Characterization

Coke content of each catalyst sample was determined three times, and ranged between 10.9% and 31.2% of the weight of the spent catalyst. Coke content standard deviations were observed around ± 2 wt%. Few standard deviations as low as ± 0.4 wt% and as high as ± 5.5 wt% were also observed.

Fresh catalyst samples were analyzed in triplicates for their surface area, pore volume, and the most frequent pore diameter. Table III presents the precision of the Quantachrome Porosimeter used for this purpose. Because of the small amount of catalyst samples available, spent and regenerated samples were analyzed only once.

## Reproducibility of Reactor Performance

The reliability of the experimental apparatus and procedure was concluded by Bhan (1981), Bhan (1983), and Beazer (1984). In our study, two identical runs were carried out. Vanadium content and the boiling curves of the product liquid samples for the duplicate runs varied within the range of the experimental error. Response to coke analysis

TABLE III

PRECISION OF CATALYST CHARACTERIZATION

| | Average and Standard Deviation | | |
|---|---|---|---|
| | Surface Area x $10^{-3}$ ($m^2/kg$) | Pore Volume x $10^3$ ($m^3/kg$) | Most Frequent Pore Diameter (nm) |
| Fresh Catalysts | | | |
| HT-TK-771 | 238 ± 2 (200*) | 0.53 ± 0.01 (0.47*) | 9.0 ± 0.0 |
| HT-TK-751 | 217 ± 2 (170*) | 0.78 ± 0.02 (0.58*) | 13.8 ± 0.0 |
| HT-TK-711 | 194 ± 2 (140*) | 0.79 ± 0.02 (0.57*) | 15.3 ± 0.1 |

*Vendor's data.

varied slightly, but the change in catalyst properties was reproduced. The two duplicate runs will be discussed in detail elsewhere.

# CHAPTER VI

## EXPERIMENTAL RESULTS

Seven experimental runs were carried out during this study; five catalyst bed combinations were tested. Table IV lists these catalyst combinations. Run CVR1 was a preliminary experiment to test operating conditions, and runs CVR4 and CVR7 were duplicate experiments to establish overall reproducibility. Runs CVR2, CVR3, and CVR5 were the graded bed experiments.

All experimental runs were conducted at a total pressure of 10.3 MPa (1500 psig) and 1.0 $h^{-1}$ LHSV. LHSV was defined as the residue flow per hour per volume of catalyst and was calculated from inlet conditions. Run CVR1 was carried out at two temperatures, 350 and 380°C (662 and 716°F), to determine the temperature at which reasonable conversion rates could be obtained. CVR1 was 114 h in duration. Subsequent runs were carried out at 380°C for a duration of 72 h.

### Run CVR1

CVR1 was a preliminary experiment to set reactor operating temperature at reasonable conversion rates and to check the suitability of the chosen pressure and LHSV. The HDS/HDM catalyst of Table II, HT-TK-751, was used in both reactor zones. This catalyst was chosen for its moderate active metal content and wide pore structure, i.e., large MFPD and high pore volume. This HDS/HDM catalyst was said to possess

TABLE IV

CATALYST COMBINATIONS USED IN THE EXPERIMENTAL RUNS

| Run | Reactor 1 (Top) | Reactor 2 (Bottom) | %wt Active and Promotor Metals Contents in the Combined Beds* | Average Pore Volume of the Combined Beds $m^3/kg$ | Average** MFPD, nm |
|---|---|---|---|---|---|
| CVR1 | HT-TK-751 | HT-TK-751 | 12.3 | 0.780 | 13.80 |
| CVR2 | HT-TK-751 | HT-TK-771 | 15.0 | 0.647 | 11.40 |
| CVR3 | HT-TK-711 | HT-TK-771 | 13.0 | 0.652 | 12.15 |
| CVR4 | HT-TK-751 | HT-TK-751 | 12.3 | 0.780 | 13.80 |
| CVR5 | HT-TK-711 | HT-TK-751 | 10.2 | 0.785 | 14.55 |
| CVR6 | HT-TK-771 | HT-TK-771 | 17.4 | 0.530 | 9.00 |
| CVR7 | HT-TK-751 | HT-TK-751 | 12.3 | 0.780 | 13.80 |

*Based on a volume of $1.75 \times 10^{-2}$ L per catalyst bed.

**Average MFPD = $\frac{\text{MFPD of reactor 1 + MFPD of Reactor 2}}{2}$.

moderate HDT activity with high HDM activity and high tolerance for metals. CVR1 lasted for 114 h. The reactor zones were operated at 350°C during the first 36 h, and during the second 36 h they were operated at 380°C. The temperature was reduced to 350°C during the rest of the run.

Table V presents the Ni content of the liquid products and the %wt Ni removal during run CVR1. Conversions between 25 and 40 %wt were achieved. No temperature trends were clear from the data of Table V, however, some of the higher conversions were achieved at 380°C. The experimental standard deviations for Ni content were too high to facilitate any comparison between the HDM activities of different catalyst combinations. Consequently, Ni data were presented for the run CVR1 only. V removal was considered sufficient to describe the HDM process.

Figure 2 presents the %wt V removal during CVR1. At 350°C, an initial deactivation period of about 24-30 h was apparent. V removal appeared to level at 45 %wt. However, as temperature was increased to 380°C, V removal appeared to increase to about 50 %wt. After about 72 h, V removal leveled at about 45 %wt. V removal of 50 %wt was considered acceptable and subsequent runs were carried out at 380°C.

Figure 3 shows ASTM boiling point curves for the feed and the 42 h liquid product sample of run CVR1. Initial boiling point was decreased by about 70°C. Boiling point reduction was at about 10-15°C for the 15 vol% and heavier fractions.

Table VI introduces the catalysts' physical property data for CVR1. The decrease in the catalysts' pore volume was similar for the different positions in the same reactor and for the two reactors.

TABLE V

NICKEL CONTENT AND %WT NICKEL REMOVAL FOR THE LIQUID PRODUCT SAMPLES OF RUN CVR1

| Sample Time (h) | Temperature (°C) | Ni (ppm) | %Wt Ni Removal |
|---|---|---|---|
| 6 | 350 | 32.3 ± 6.0 | 24.9 |
| 12 | | 28.4 ± 3.8 | 34.0 |
| 18 | | 30.7 ± 5.2 | 28.6 |
| 24 | | 30.1 ± 2.8 | 30.0 |
| 30 | | 31.4 ± 3.3 | 27.0 |
| 36 | | 28.4 ± 4.2 | 34.0 |
| 42 | 380 | 28.8 ± 3.0 | 33.0 |
| 48 | | 26.0 ± 2.8 | 39.5 |
| 54 | | 31.4 ± 2.9 | 27.0 |
| 60 | | 32.7 ± 5.7 | 26.9 |
| 66 | | 25.4 ± 5.4 | 40.9 |
| 72 | | 30.8 ± 6.0 | 28.4 |
| 78 | 350 | 34.5 ± 4.8 | 19.8 |
| 84 | | 30.9 ± 2.0 | 28.1 |
| 90 | | 31.0 ± 4.6 | 27.9 |
| 96 | | 29.2 ± 2.9 | 32.1 |
| 102 | | 32.8 ± 3.9 | 23.7 |
| 108 | | 30.1 ± 4.1 | 30.0 |
| 114 | | 31.0 ± 5.2 | 28.0 |

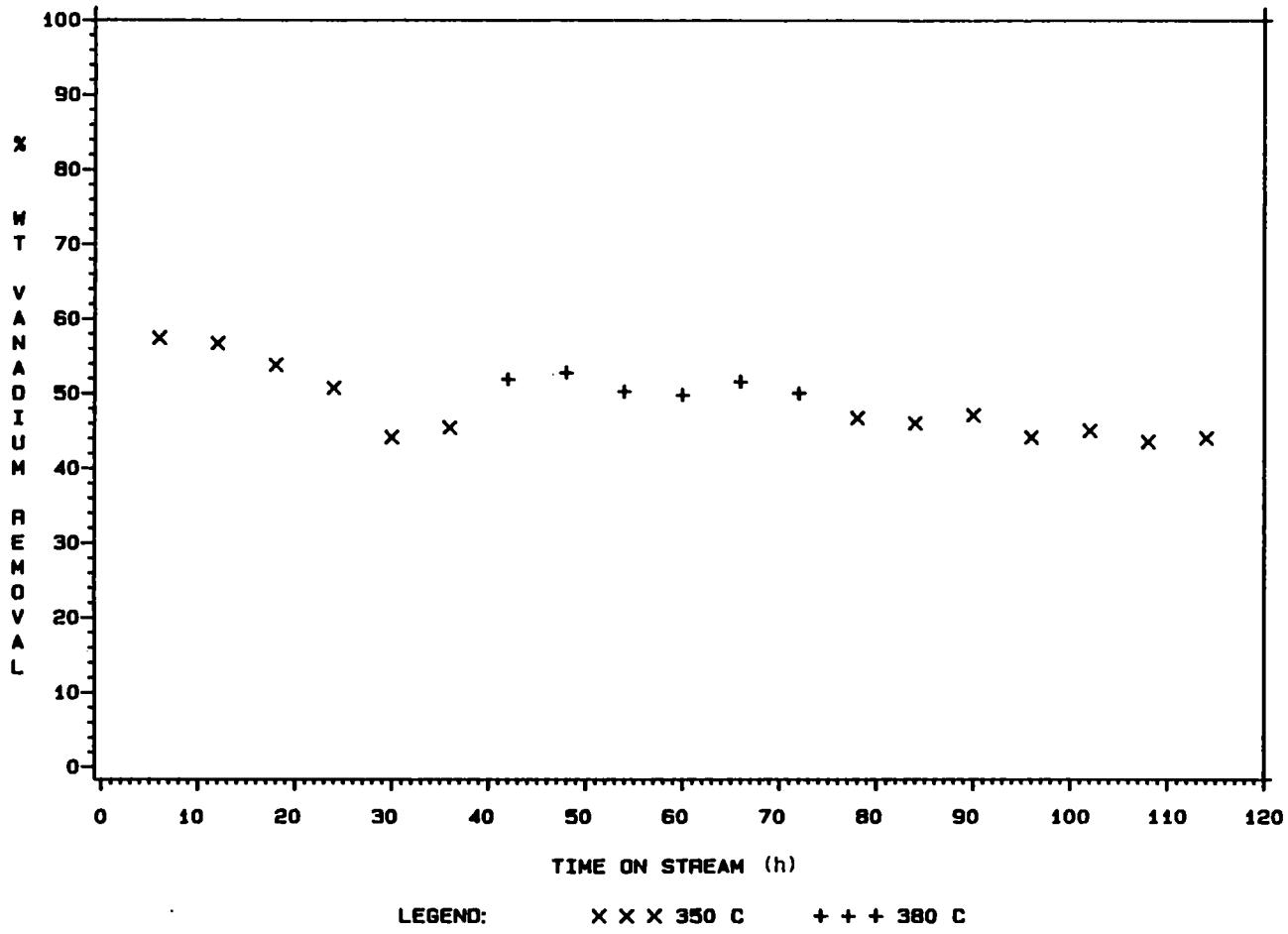


Figure 2. Percent Weight Vanadium Removal During Run CVR1

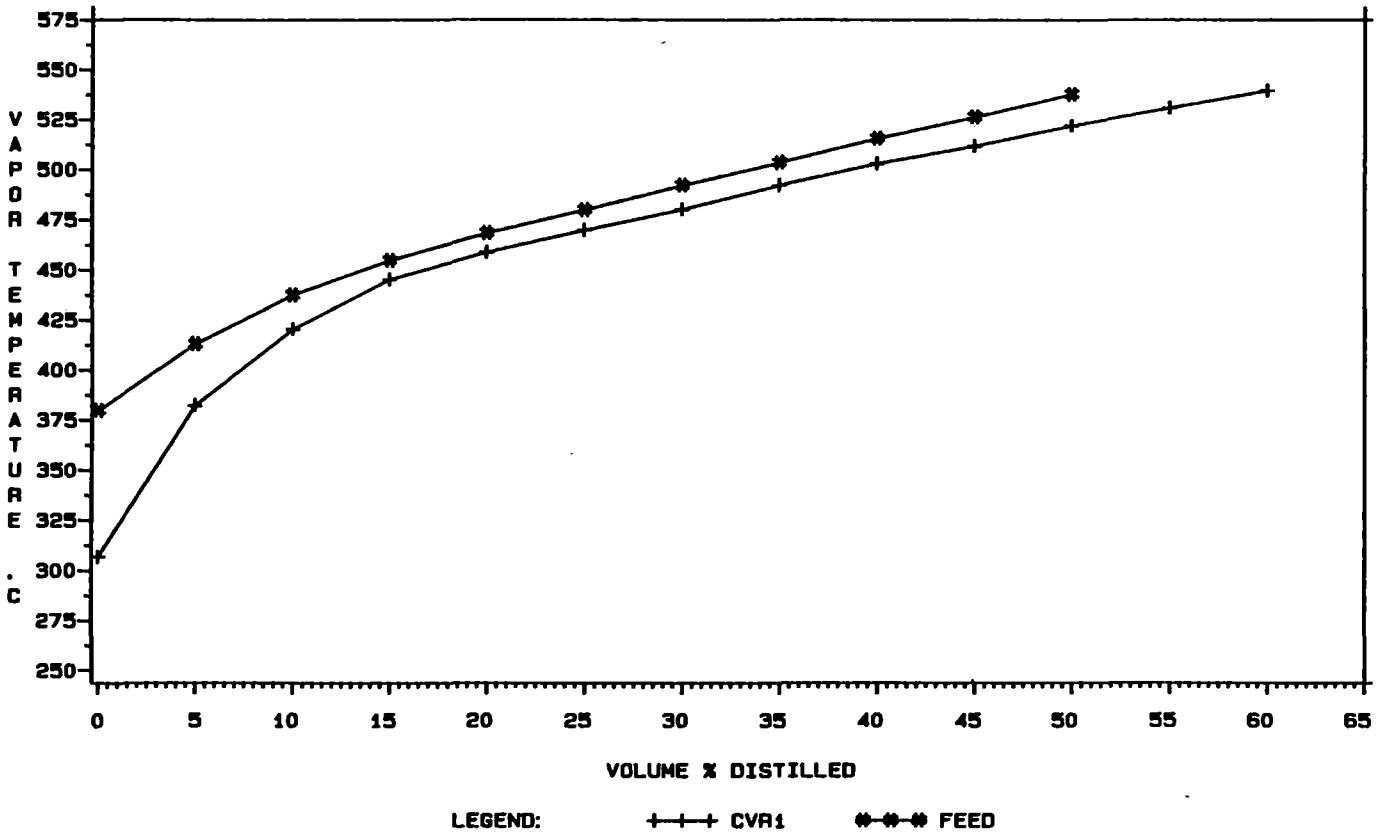


Figure 3. Boiling Point Curves for the Residue Feed and the 42 h Liquid Product Sample of Run CVR1

TABLE VI

REDUCTION IN THE PHYSICAL PROPERTIES OF CATALYST USED IN RUN CVR1*

| Reactor | Section | % Reduction in | | |
|---|---|---|---|---|
| | | Pore Volume | Surface Area | Most Frequent Pore Diameter |
| 1 | 1Q | 39.7 | 28.6 | 21.7 |
| | 2Q | 37.2 | 22.4 | 17.4 |
| | 3Q | 38.5 | 24.0 | 15.9 |
| | 4Q | 38.5 | 25.3 | 18.1 |
| Average for Reactor 1 | | 38.5 | 25.1 | 18.3 |
| 2 | 1Q | 38.5 | 25.8 | 20.3 |
| | 2Q | 38.5 | 26.7 | 17.4 |
| | 3Q | 38.5 | 26.3 | 16.7 |
| | 4Q | 35.9 | 23.0 | 18.8 |
| Average for Reactor 2 | | 37.9 | 25.5 | 18.3 |

*See Table III for experimental error.

Reductions in catalysts' surface area and MFPD were also similar in the two reactors. In reactor 2, however, maximum reduction in surface area appeared somewhat beyond the entrance. The HDS/HDM catalyst seemed to have lost physical properties to the same extent in both reactors.

Table VII summarizes coke content analysis for the catalyst of CVR1. Coke was evenly distributed in both reactors. Average coke content was also similar in both reactor zones.

Table VIII presents results from the catalyst EDX analysis, and indicates the extent of V penetration into the catalyst particles. In reactor 1, V penetrated to the third selected area on the catalyst cross-section for all reactor sections except 3Q. V penetrated to a lesser extent in this section. In reactor 2, V penetration decreased from top to bottom. V penetration was deeper at top of reactor 2 than at top of reactor 1.

Runs CVR4 and CVR7

The HDS/HDM catalyst of Table II, HT-TK-751, was packed in both reactor zones for both CVR4 and CVR7. The two runs were duplicates to establish overall equipment operation and analysis reproducibility. Both runs were used as bases for comparison.

Figure 4 presents %wt V removal during runs CVR4 and CVR7. Within the range of error in V content determination, V removal rates were similar in both experiments. A 24 h to 30 h period of rapid initial deactivation was apparent on both curves of Figure 4, then V removal leveled at about 50 %wt. V removal data from run CVR 7 were used for subsequent comparisons.

TABLE VII

COKE CONTENT* OF SPENT CATALYST USED IN RUN CVR1

| Reactor | Section | Coke %** |
|---|---|---|
| 1 | 1Q | 24.3 ± 2.4 |
| | 2Q | 22.0 |
| | 3Q | 16.9 |
| | 4Q | 27.9 ± 2.2 |
| Average Reactor Coke Content: | | 23.4 ± 4.5 |
| 2 | 1Q | 22.6 ± 1.0 |
| | 2Q | 22.5 |
| | 3Q | 21.5 ± 1.1 |
| | 4Q | 22.3 ± 2.9 |
| Average Reactor Coke Content: | | 22.2 ± 1.9 |
| Overall Coke Content: | | 22.8 ± 3.4 |

*% Weight of regenerated catalyst.
**Adjusted for metal sulfide oxidation.

TABLE VIII

VANADIUM PENETRATION THROUGH SPENT CATALYST OF RUN CVR1

| Reactor | Section | Vanadium Counts in Selected Areas* | | | | |
|---|---|---|---|---|---|---|
| | | $S_1$ | $S_2$ | $S_3$ | $S_4$ | $S_5$ |
| 1 | 1Q | 3415 | 1667 | 755 | --** | -- |
| | 2Q | 734 | 656 | 404 | -- | -- |
| | 3Q | 1722 | 785 | -- | -- | -- |
| | 4Q | 6659 | 2884 | 785 | -- | -- |
| 2 | 1Q | 5010 | 2468 | 997 | 818 | -- |
| | 2Q | 2449 | 913 | -- | -- | -- |
| | 4Q | 535 | -- | -- | -- | -- |

*See V penetration analysis in Chapter IV for definitions.
**non-detectable.

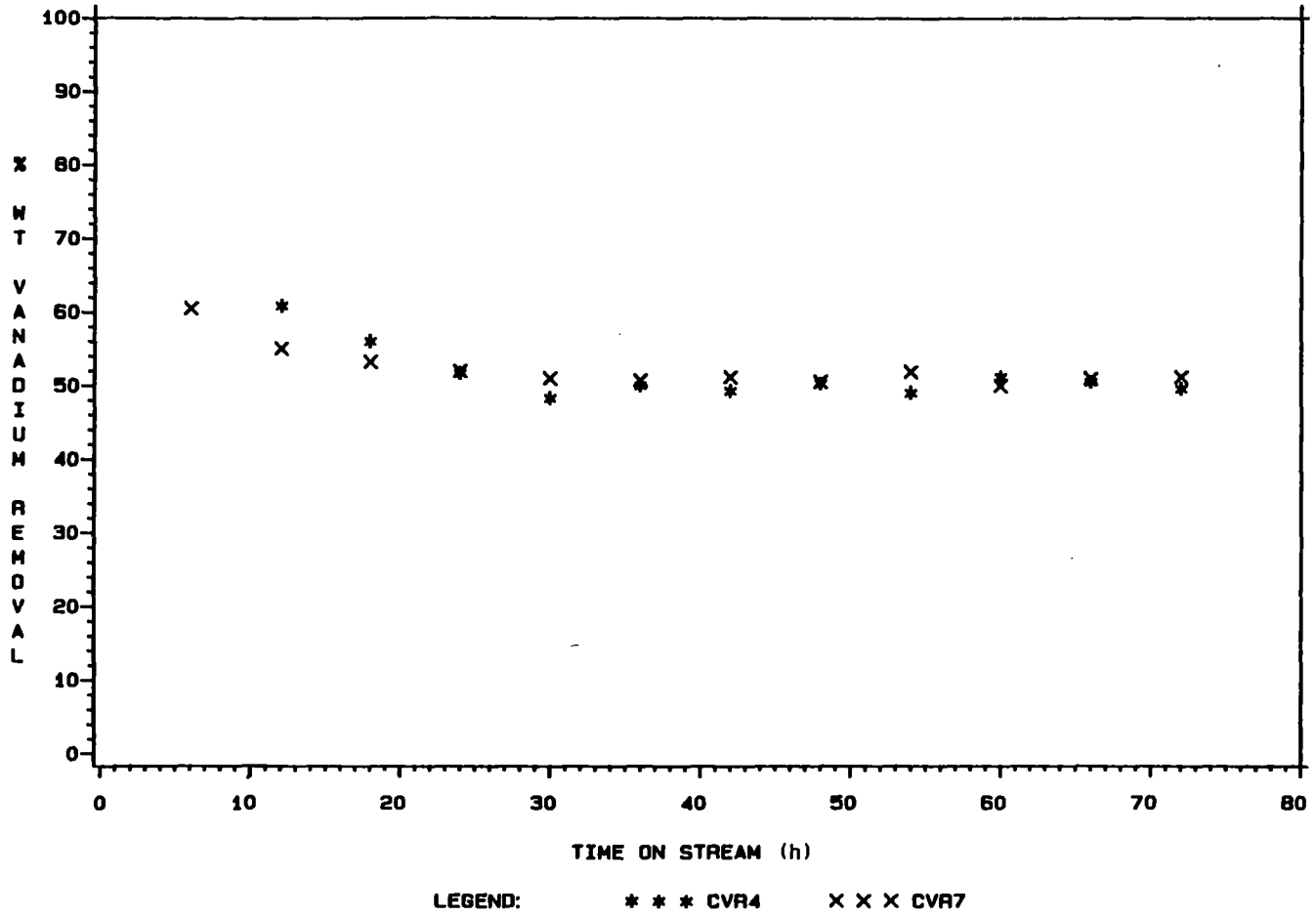


Figure 4. Percent Weight Vanadium Removal During Runs CVR4 and CVR7

Figure 5 shows ASTM boiling point curves for the residue feed and the 42 h liquid product samples of CVR4 and CVR7. Within the range of experimental error, boiling point reduction was identical in both runs. Initial boiling point was reduced by about 100°C. Boiling points of the lighter fractions (0-25 vol%) were displaced by about 30-70°C. Boiling points of the heavier fractions (above 30 vol%) were displaced by less than 20°C. Boiling point reduction decreased with increasing boiling point. Also, boiling point reduction appeared to be more pronounced in runs CVR4 and CVR7 than in run CVR1 with the identical catalyst. The boiling point curve for the 42 h liquid product sample of run CVR4 was taken as a basis for comparison in subsequent discussions.

Tables IX and X summarize spent catalysts' deactivation data for runs CVR4 and CVR7, respectively. Reduction in pore volume seemed to decrease along reactor length in both reactors for both runs. In CVR4, loss of catalysts' pore volume was slightly higher in reactor 1. The opposite was true for CVR7. Loss of pore volume was, on the average, comparable in both reactors for both runs. Reduction in surface area decreased along reactor length and its average was comparable in both reactors for the two runs. Reduction in the MFPD followed similar patterns. In general, catalysts' physical property losses decreased along reactor length and their magnitudes were comparable in both reactors. A comparison of Tables IX and X with table VI revealed spent catalyst physical properties of similar magnitudes for CVR1, CVR4, and CVR7 in spite of the fact that CVR1 was carried out for 58% longer duration.

Table XI presents coke content analysis for the catalysts of runs CVR4 and CVR7. Within the range of experimental standard deviations, no

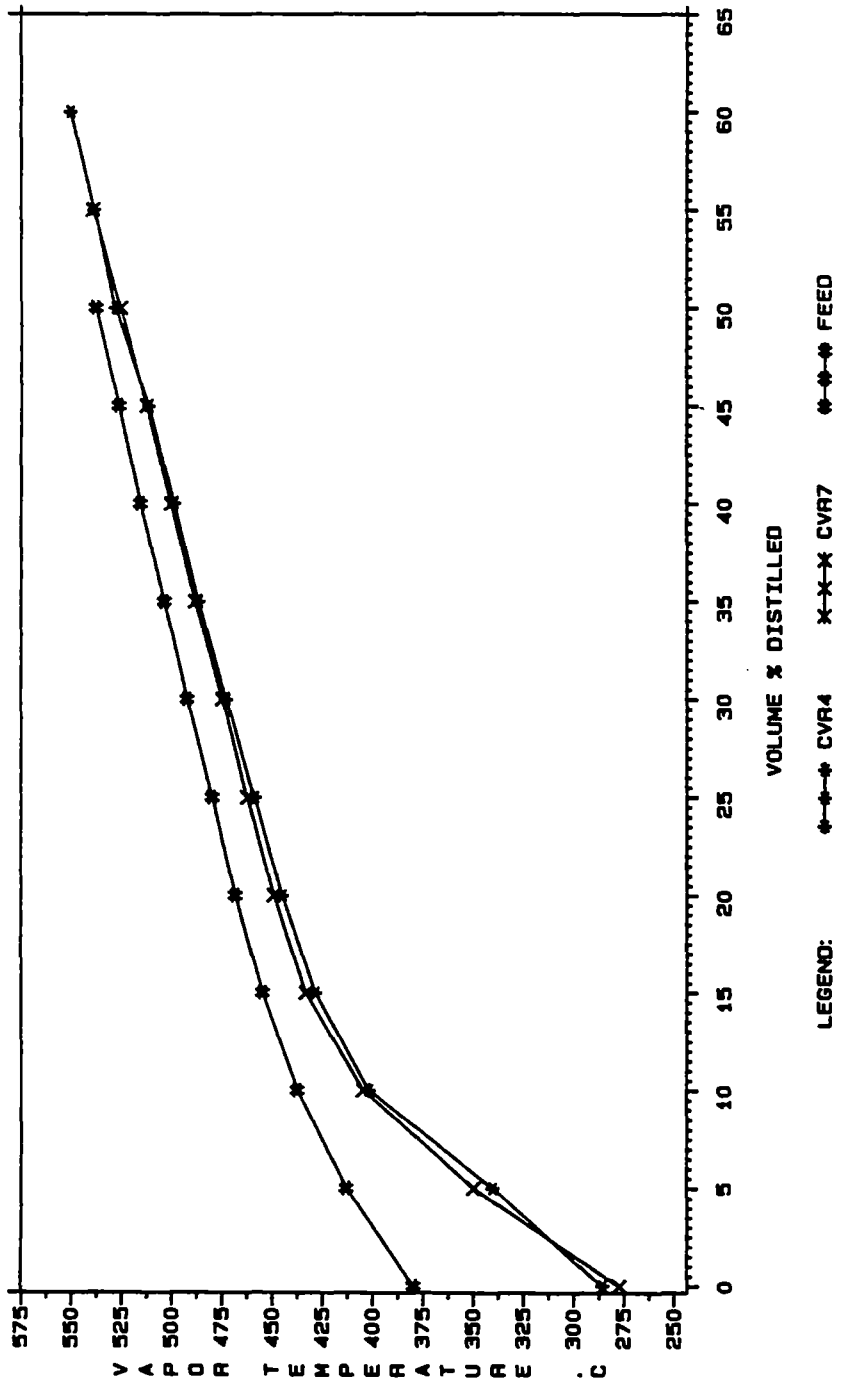


Figure 5. Boiling Point Curves for the Residue Feed and the 42 h Liquid Product Sample of Runs CVR4 and CVR7

TABLE IX

REDUCTION IN THE PHYSICAL PROPERTIES OF CATALYST USED IN RUN CVR4*

| Reactor | Section | % Reduction in | | |
|---|---|---|---|---|
| | | Pore Volume | Surface Area | Most Frequent Pore Diameter |
| 1 | 1Q | 42.3 | 30.9 | 21.7 |
| | 2Q | 39.7 | 28.1 | 18.1 |
| | 3Q | 34.6 | 22.5 | 16.7 |
| | 4Q | 35.9 | 23.5 | 15.2 |
| Average for Reactor 1 | | 38.1 | 26.3 | 17.9 |
| 2 | 1Q | 41.0 | 30.9 | 17.4 |
| | 2Q | 37.2 | 26.7 | 16.7 |
| | 3Q | 34.6 | 24.4 | 15.9 |
| | 4Q | 33.3 | 19.8 | 14.5 |
| Average for Reactor 2 | | 36.5 | 25.5 | 16.1 |

*See Table III for experimental error.

TABLE X

REDUCTION IN THE PHYSICAL PROPERTIES OF CATALYST USED IN RUN CVR7*

| Reactor | Section | % Reduction in | | |
|---|---|---|---|---|
| | | Pore Volume | Surface Area | Most Frequent Pore Diameter |
| 1 | 1Q | 39.7 | 28.6 | 18.8 |
| | 2Q | 35.9 | 24.9 | 17.4 |
| | 3Q | 33.3 | 23.5 | 15.9 |
| | 4Q | 33.3 | 22.1 | 15.9 |
| Average for Reactor 1 | | 35.6 | 24.8 | 17.0 |
| 2 | 1Q | 39.7 | 26.3 | 20.3 |
| | 2Q | 37.2 | 25.8 | 16.7 |
| | 3Q | 35.9 | 24.9 | 14.5 |
| | 4Q | 34.6 | 24.0 | 13.0 |
| Average for Reactor 2 | | 36.9 | 25.3 | 16.1 |

*See Table III for experimental error.

TABLE XI

COKE CONTENT* OF SPENT CATALYST USED IN RUNS CVR4 and CVR7

| Reactor | Section | Coke %** | |
|---|---|---|---|
| | | CVR4 | CVR7 |
| 1 | 1Q | 24.9 ± 1.5 | 19.1 ± 0.4 |
| | 2Q | 21.7 ± 3.2 | 15.9 ± 2.4 |
| | 3Q | 22.7 ± 1.7 | 16.6 ± 2.5 |
| | 4Q | 17.7 ± 0.8 | 19.3 ± 2.5 |
| Average Reactor Coke Content: | | 21.8 ± 3.2 | 17.7 ± 2.4 |
| 2 | 1Q | 25.0 ± 5.4 | 19.9 ± 1.3 |
| | 2Q | 22.0 ± 1.3 | 17.8 ± 2.2 |
| | 3Q | 17.8 ± 1.3 | 21.0 ± 1.2 |
| | 4Q | 21.1 ± 1.1 | 17.0 ± 1.7 |
| Average Reactor Coke Content: | | 21.5 ± 3.6 | 18.9 ± 2.2 |
| Overall Coke Content: | | 21.6 ± 3.4 | 18.3 ± 2.3 |

*% Weight of regenerated catalyst.
**Adjusted for metal sulfide oxidation.

regular patterns of coke deposition were detected between catalyst sections and between reactors in both runs. From Table XI, for both CVR4 and CVR7, coke was evenly distributed along catalyst beds and the amounts of coke were similar in both reactors. The catalyst of CVR4 might have accumulated slightly higher amounts of coke than the catalyst of CVR7. Coke deposition during CVR4 appeared to be slightly lower than coke deposition during CVR1 (Table VII).

Table XII shows the physical properties of fresh catalysts after combustion at 600°C (1112°F) for 42 h. Slight differences in physical properties from the fresh catalysts were apparent when comparing with data of Table III, however, no regular patterns were clear. Fresh catalysts' combustion data were used as a basis for the determination of the extent of spent catalyst regeneration.

Table XIII presents the physical properties of the regenerated catalyst of run CVR4. Since it was a duplicate run, regenerated catalysts' physical properties were not presented for CVR7. Comparing with Table XII, all physical properties of the catalysts were recovered upon regeneration. Regenerated pore volume and MFPD seemed slightly higher than for the combusted fresh catalyst. This might have been due to experimental error. No regular patterns of physical properties were seen in both reactors of Table XIII.

Tables XIV and XV list V penetration data for runs CVR4 and CVR7, respectively. V penetration was less pronounced in the catalyst of run CVR4 than of run CVR7. V penetrated to a deeper extent in the top reactor of both runs. In CVR4, the catalyst showed more uniform V penetration profiles along the lengths of both reactors. In CVR7, V penetration decreased along reactors' length. V penetration in these

TABLE XII

PHYSICAL PROPERTIES OF FRESH CATALYST AFTER COMBUSTION AT 600°C FOR 24 h

| Catalyst | Surface Area $x10^{-3}$ $m^2/kg$ | Pore Volume $x\ 10^3$ $m^3/kg$ | Most Frequent Pore Diameter nm |
|---|---|---|---|
| HT-TK-711 | 197 ± 6 | 0.81 ± 0.2 | 15.7 ± 0.2 |
| HT-TK-751 | 207 ± 1 | 0.78 ± 0.02 | 14.4 ± 0.2 |
| HT-TK-771 | 233 ± 2 | 0.53 ± 0.01 | 9.3 ± 0.1 |

TABLE XIII

PHYSICAL PROPERTIES OF REGENERATED CATALYST OF RUN CVR4*

| Reactor - Section | | Surface Area x $10^{-3}$ $m^2/kg$ | Pore Volume x $10^3$ $m^3/kg$ | Most Frequent Pore Diameter nm |
|---|---|---|---|---|
| 1 | 1Q | 203 | 0.77 | 15.0 |
| | 2Q | 205 | 0.77 | 14.4 |
| | 3Q | 206 | 0.77 | 14.6 |
| | 4Q | 213 | 0.79 | 14.6 |
| Average for Reactor 1 | | 207 | 0.78 | 14.7 |
| 2 | 1Q | 207 | 0.77 | 14.5 |
| | 2Q | 209 | 0.78 | 14.6 |
| | 3Q | 207 | 0.79 | 15.0 |
| | 4Q | 207 | 0.76 | 14.4 |
| Average for Reactor 2 | | 208 | 0.78 | 14.6 |

*See Table XII for experimental error.

TABLE XIV

VANADIUM PENETRATION THROUGH SPENT CATALYST OF RUN CVR4

| Reactor | Section | Vanadium Counts in Selected Areas* | | | | |
|---|---|---|---|---|---|---|
| | | $S_1$ | $S_2$ | $S_3$ | $S_4$ | $S_5$ |
| 1 | 1Q | 8663 | 5746 | 1752 | -- | -- |
| | 4Q | 6279 | 3931 | 1652 | -- | -- |
| 2 | 1Q | 1505 | -- | -- | -- | -- |
| | 4Q | 1790 | -- | -- | -- | -- |

*See V penetration analysis in Chapter IV for definitions.

TABLE XV

VANADIUM PENETRATION THROUGH SPENT CATALYST OF RUN CVR7

| Reactor | Section | Vanadium Counts in Selected Areas* | | | | |
|---|---|---|---|---|---|---|
| | | $S_1$ | $S_2$ | $S_3$ | $S_4$ | $S_5$ |
| 1 | 1Q | 7961 | 6316 | 3500 | 1538 | -- |
| | 4Q | 980 | 775 | -- | -- | -- |
| 2 | 1Q | 1095 | 1003 | -- | -- | -- |
| | 4Q | 1032 | -- | -- | -- | -- |

*See V penetration analysis in Chapter IV for definitions.

runs assumed similar patterns to the ones obtained from run CVR1 but in CVR1, V penetration in reactor 2 was more pronounced (Table VIII).

Run CVR6

In run CVR6, both reactors were packed with the highly active HDS catalyst HT-TK-771. Among the catalyst beds tested, the combined catalyst beds of CVR6 had the highest %wt active metals content, the lowest catalyst pore volume, and the smallest average MFPD (Table IV). Run CVR6 was conducted to evaluate the effect of using a small pore size, high surface area, and high active metal content-catalyst on residue metal removal. This run was also used as a basis for comparison.

Figure 6 presents a comparison of the %wt V removal for runs CVR6 and CVR7. Diffusional limitations in the HDM reactions were very clear. In spite of its higher promotor and active metals contents, the HDS catalyst of CVR6 had about 12 %wt lower V removal activity than the larger pore size, HDS/HDM catalyst of CVR7. No clear activity decline intervals could be seen from the curve for CVR6, however, this curve appeared to have a negative slope over the run duration.

Figure 7 is a comparison of ASTM boiling point curves for the residue feed and the 42 h liquid product samples of runs CVR4 and CVR6. The initial boiling point was reduced by 20°C more in run CVR6 than in CVR4. The higher active metal catalyst of CVR6 also appeared to cause similar or slightly more boiling point reduction for most residue feed fractions.

Table XVI presents reduction in the physical properties of the catalyst used in CVR6. Pore volume and surface area could not be

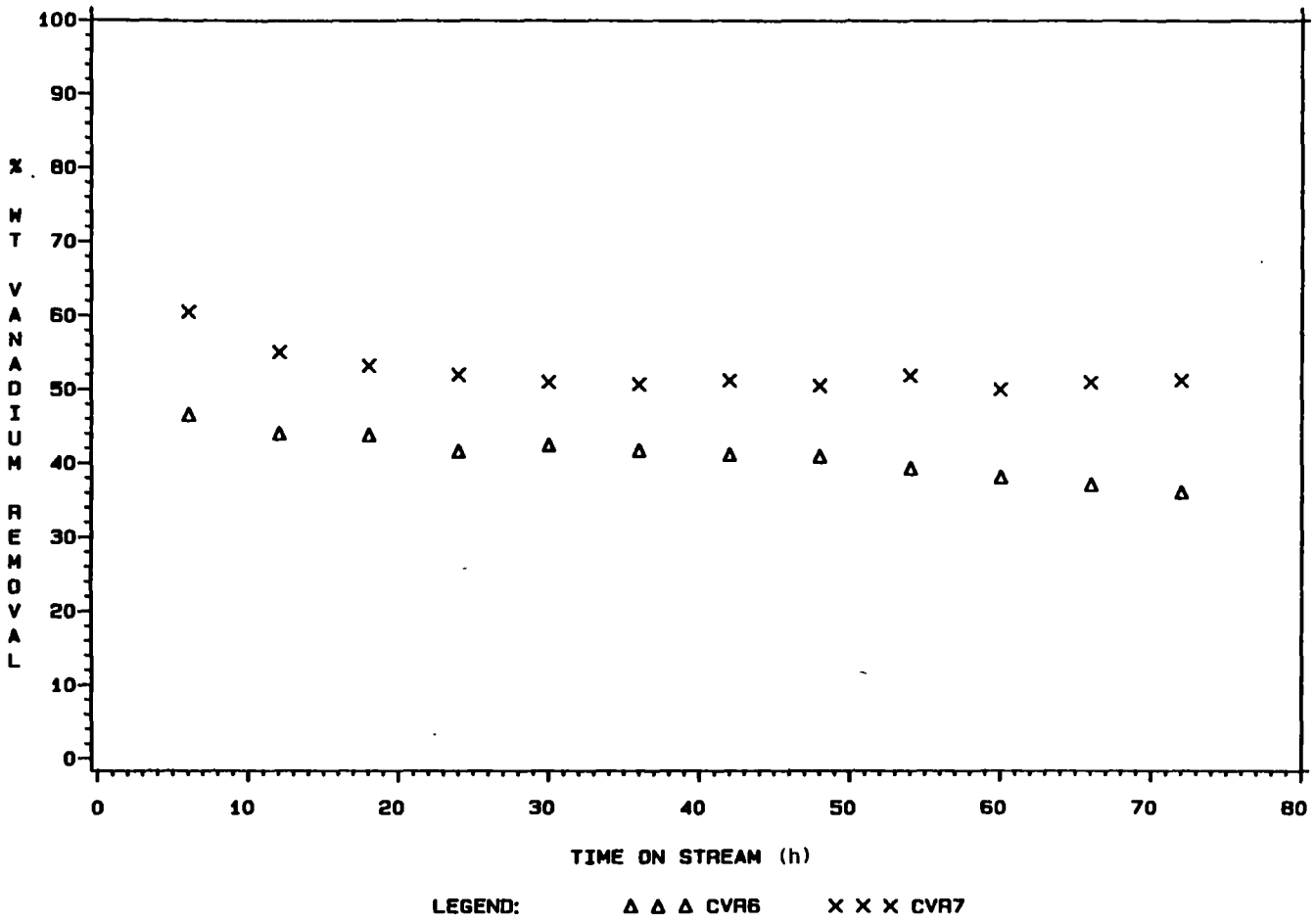


Figure 6. Percent Weight Vanadium Removal During Runs CVR6 and CVR7

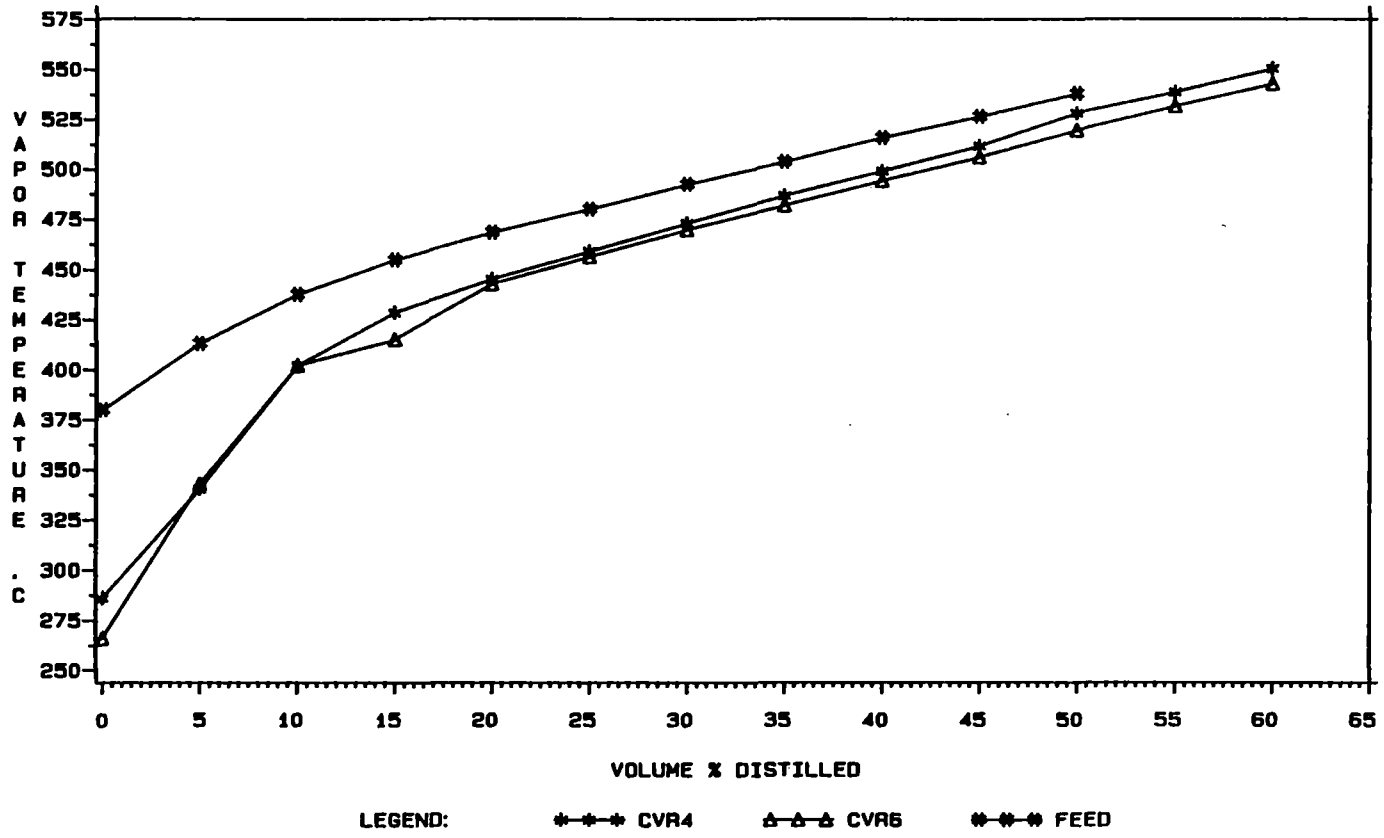


Figure 7. Boiling Point Curves for the Residue Feed and the 42 h Liquid Product Samples of Runs CVR4 and CVR6

TABLE XVI

REDUCTION IN THE PHYSICAL PROPERTIES OF CATALYST USED IN RUN CVR6*

| Reactor | Section | % Reduction in** | | |
|---|---|---|---|---|
| | | Pore Volume | Surface Area | Most Frequent Pore Diameter |
| 1 | 1Q | 47.0 | 16 | 50.0 |
| | 2Q | 38.0 | 6 | 45.6 |
| | 3Q | 38.0 | 1 | 43.3 |
| | 4Q | 43.0 | 20 | 43.3 |
| Average for Reactor 1 | | 41.5 | 10.8 | 45.6 |
| 2 | 1Q | 34.0 | 1 | 47.8 |
| | 2Q | 36.0 | 2 | 44.4 |
| | 3Q | 49.0 | 21 | 43.3 |
| | 4Q | 43.0 | 17 | 40.6 |
| Average for Reactor 2 | | 40.5 | 10.3 | 44.0 |

*See Table III for experimental error.
**Due to the extreme irregularities in the physical property curves from the porosimeter, these data are only approximate.

accurately determined for this spent catalyst due to the extreme irregularities in the physical property curves obtained from the porosimeter. Data listed in the above table are only approximate. Nevertheless, data of Table XVI showed that the HDS catalyst achieved high reductions in pore volume in spite of little loss in surface area. The HDS catalyst of CVR6 was deactivated to a much larger extent than the wide pore-size, HDS/HDM catalyst of runs CVR4 and CVR7 (Tables IX and X).

Table XVII presents the coke content of spent catalyst used in run CVR6. Within the range of experimental error, no regular patterns of coke deposition were seen within the reactors. The average coke content in both reactors was also comparable; coke seemed to be evenly distributed. Coke deposited on this small pore-size catalyst to a consistently lesser extent than on the HDS/HDM catalyst of runs CVR4 and CVR7 (13.8 vs. 21.6 and 18.3%, Table XI).

Table XVIII presents the physical properties of the regenerated catalyst of CVR6. The spent catalyst fully recovered physical properties after combustion. Some of the properties listed in the above table exceeded those for the combusted fresh HT-TK-771 catalyst of Table XII. This was attributed to experimental error. No general patterns could be seen in Table XVIII except that the catalyst in reactor 2 recovered properties to a slightly higher extent than the catalyst in reactor 1.

Table XIX lists data for V penetration into the spent catalyst of CVR6. V was only detected on and very close to the surface of catalyst particles in very high counts. V was nonexistent on the catalyst cross-section after the first selected area. This was in marked contrast to

TABLE XVII

COKE CONTENT* OF SPENT CATALYST USED IN RUN CVR6

| Reactor | Section | Coke %** |
|---|---|---|
| 1 | 1Q | 14.6 ± 2.9 |
| | 2Q | 10.9 ± 0.5 |
| | 3Q | 11.4 ± 1.5 |
| | 4Q | 14.6 ± 7.1 |
| Average Reactor Coke Content: | | 12.9 ± 3.9 |
| 2 | 1Q | 15.0 ± 0.3 |
| | 2Q | 11.9 ± 1.3 |
| | 3Q | 15.9 ± 0.8 |
| | 4Q | 14.1 ± 1.3 |
| Average Reactor Coke Content: | | 14.2 ± 1.6 |
| Overall Coke Content: | | 13.8 ± 2.8 |

*% Weight of regenerated catalyst.
**Adjusted for metal sulfide oxidation.

TABLE XVIII

PHYSICAL PROPERTIES OF REGENERATED CATALYST OF RUN CVR6*

| Reactor | Section | Surface Area x $10^{-3}$ $m^2/kg$ | Pore Volume x $10^3$ $m^3/kg$ | Most Frequent Pore Diameter nm |
|---|---|---|---|---|
| 1 | 1Q | 223 | 0.49 | 9.1 |
| | 2Q | 234 | 0.52 | 8.8 |
| | 3Q | 240 | 0.54 | 9.0 |
| | 4Q | 229 | 0.53 | 9.4 |
| Average for Reactor 1 | | 232 | 0.52 | 9.1 |
| 2 | 1Q | 264 | 0.6 | 9.2 |
| | 2Q | 242 | 0.53 | 9.0 |
| | 3Q | 249 | 0.56 | 9.1 |
| | 4Q | 233 | 0.52 | 9.1 |
| Average for Reactor 2 | | 247 | 0.55 | 9.1 |

*See Table XII for experimental error.

TABLE XIX

VANADIUM PENETRATION THROUGH SPENT CATALYST OF RUN CVR6

| Reactor | Section | Vanadium Counts in Selected Areas* | | | | |
|---|---|---|---|---|---|---|
| | | $S_1$ | $S_2$ | $S_3$ | $S_4$ | $S_5$ |
| 1 | 1Q | 1481 | -- | -- | -- | -- |
| | 4Q | 3789 | -- | -- | -- | -- |
| 2 | 1Q | 6164 | -- | -- | -- | -- |
| | 4Q | 3600 | -- | -- | -- | -- |

*See V penetration analysis in Chapter IV for definitions.

runs CVR4 and CVR7 (Tables XIV and XV). Evidently the small pore size prevented penetration of the V containing molecules.

Run CVR2

CVR2 was the first of the graded-bed experiments. Reactor 1 was packed with the HDS/HDM catalyst, HT-TK-751, while reactor 2 was packed with the HDS catalyst, HT-TK-771. Excluding the catalyst combination of run CVR6, the combination of run CVR2 had the highest active and promotor metals contents, the lowest pore volume, and the smallest average MFPD among the catalyst combinations (Table IV). This combination was chosen to investigate the effect of protecting the high activity, small pore, low metal tolerance, HDS catalyst with an upstream intermediate activity, wide pore, HDS/HDM catalyst.

Figure 8 shows V removal curves for runs CVR2, CVR6, and CVR7. Although considerable HDM activity was sacrificed in CVR2 by placing the HDS catalyst in reactor 2, V removal rate matched that obtained in CVR7. However, initial activity might have been slightly lower. By the same token, placing the HDS/HDM catalyst in reactor 1 increased V removal rate from that obtained in CVR6 by about 15 %wt. After the initial deactivation period of 20 h or so in CVR2, no HDM activity loss was observed; run CVR6 showed activity loss throughout the run duration.

Figure 9 presents the boiling point curves for the 42 h liquid product samples of runs CVR2, CVR4, and CVR6. Reduction of the initial boiling point was similar in CVR2 and CVR4. Excluding the initial few points for the lighter components, reduction of boiling points in run CVR2 fall between those obtained from runs CVR4 and CVR6. The active

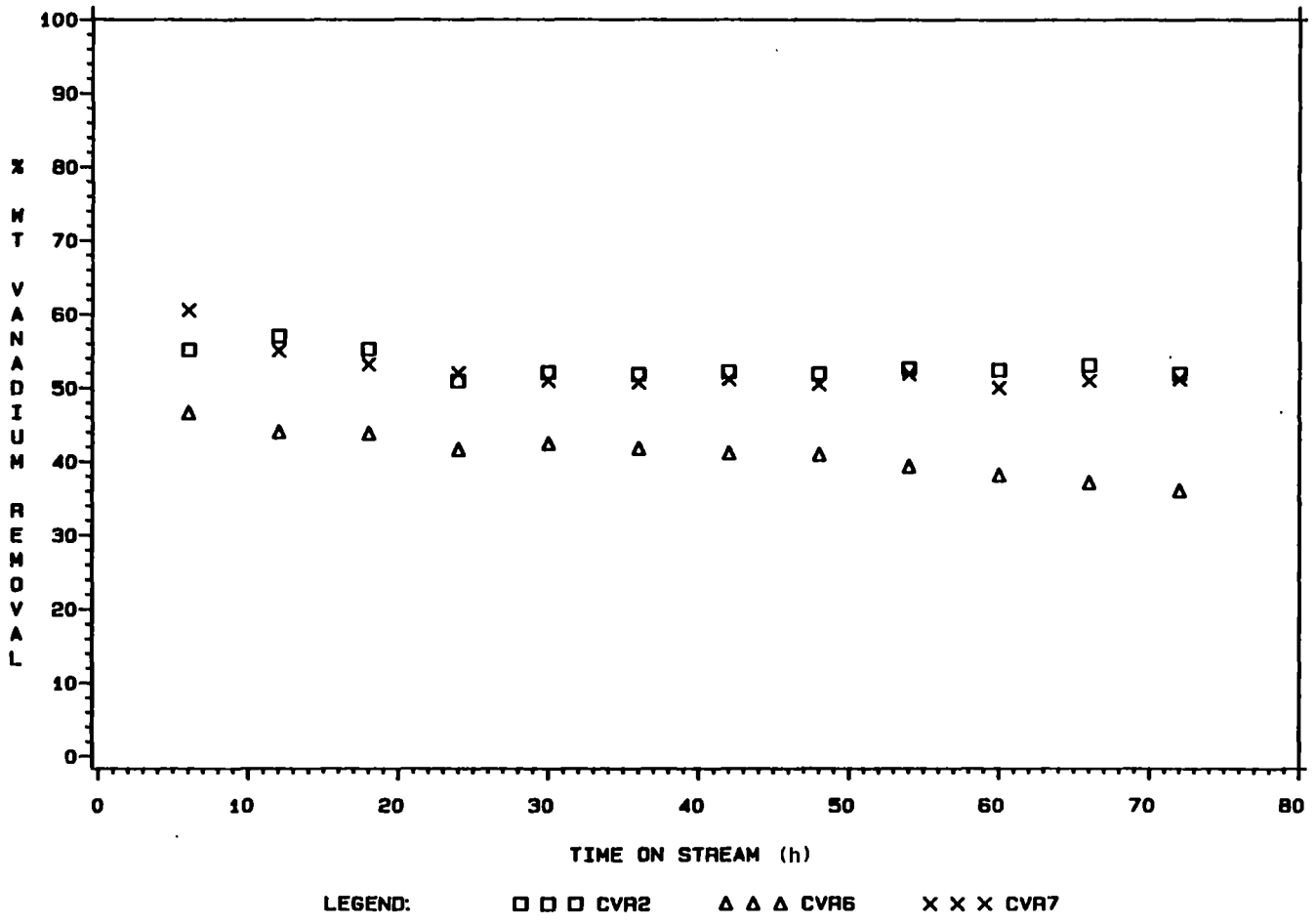


Figure 8. Percent Weight Vanadium Removal During Runs CVR2, CVR 6, and CVR7

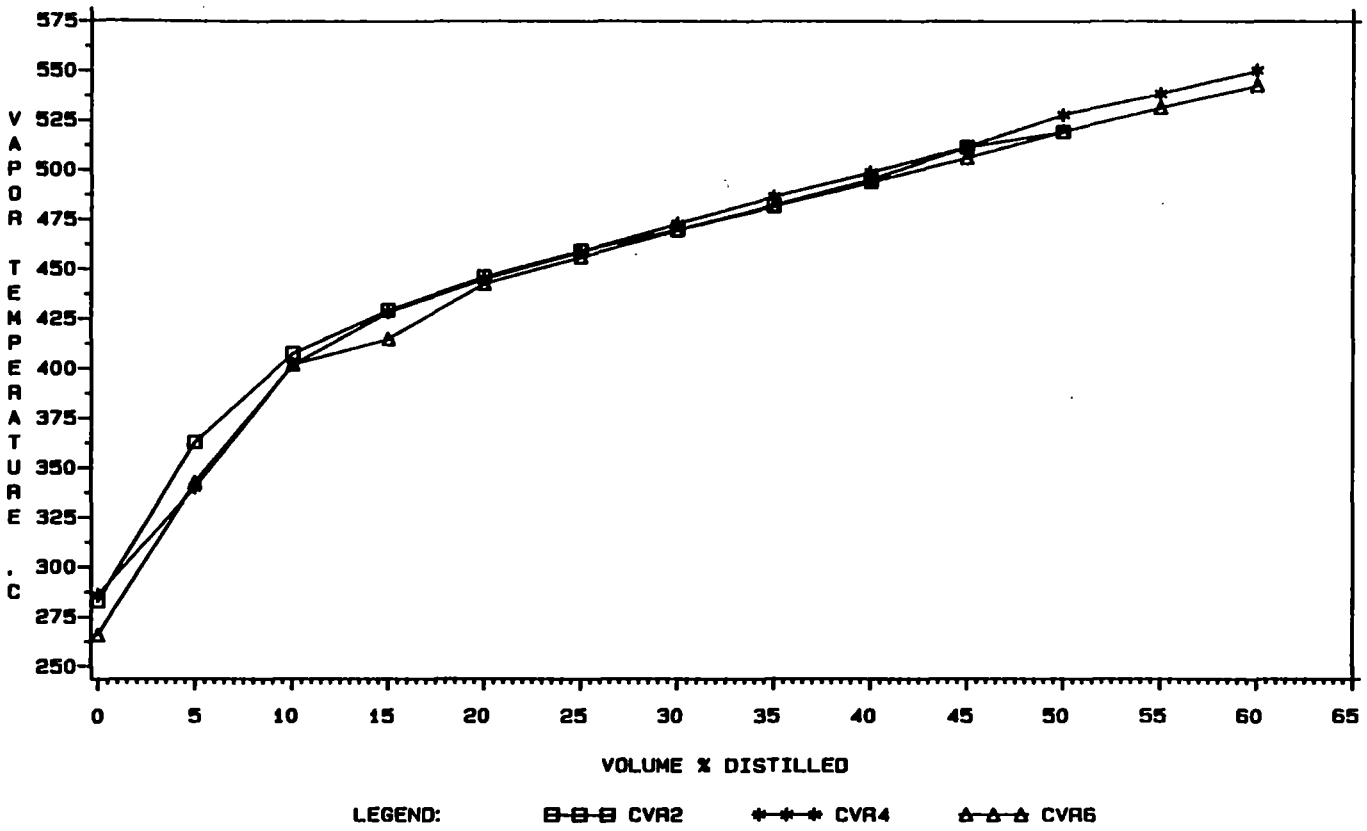


Figure 9. Boiling Point Curves for the 42 h Liquid Product Samples of Runs CVR2, CVR4, and CVR6

metal content of catalyst combination of CVR2 also fell between the active metal content of combinations of runs CVR4 and CVR6.

Table XX presents reductions in the physical properties of the catalysts used in run CVR2. In reactor 1, reductions in physical properties decreased along the length of the reactor. Loss of catalyst physical properties were similar in this reactor and in reactor 1 of runs CVR4 and CVR7 with the same type of catalyst (Tables IX and X). In this run, loss of catalyst physical properties also decreased along the length of reactor 2. Pore plugging of the HDS catalyst in CVR2 was less rapid than in both reactors of CVR6 (Table XVI). The spent catalyst in reactor 1 had higher physical properties' values than the catalyst in reactor 2.

Table XXI lists data on coke content of spent catalysts used in run CVR2. Within the range of experimental error, no difference in coke deposition was found between the different reactor sections of both reactors. Also, both reactors seemed to have accumulated similar amounts of coke deposits. The important observation here was that the HDS catalyst in reactor 2 accumulated considerably higher coke deposits than in reactor 2 of CVR6 (Table XVII). The overall coke content of the catalysts for this run was somewhat higher than for runs CVR4 and CVR7 (Table XI) and considerably higher than for run CVR6. Standard deviations for coke content analysis of this run were also high.

The physical properties of regenerated catalyst of run CVR2 are listed in Table XXII. The recovered physical properties in the above table exceeded those for the combusted fresh catalysts (Table XII). The regenerated catalyst in reactor 1 had the same physical properties of the regenerated catalyst in reactor 1 of CVR4 (Table XIII). The regenerated

TABLE XX

REDUCTION IN THE PHYSICAL PROPERTIES OF CATALYST USED IN RUN CVR2*

| Reactor | Section | % Reduction in | | |
|---|---|---|---|---|
| | | Pore Volume | Surface Area | Most Frequent Pore Diameter |
| 1 | 1Q | 48.7 | 38.3 | 16.7 |
| | 2Q | 43.6 | 32.3 | 15.9 |
| | 3Q | 33.3 | 23.5 | 15.9 |
| | 4Q | 29.5 | 18.4 | 13.0 |
| Average for Reactor 1 | | 38.8 | 28.1 | 15.4 |
| 2 | 1Q | 54.7 | 39.1 | 40.0 |
| | 2Q | 54.7 | 25.6 | 44.4 |
| | 3Q | 47.2 | 13.4 | 43.3 |
| | 4Q | 43.4 | 13.9 | 40.6 |
| Average for Reactor 2 | | 50.0 | 23.0 | 42.1 |

*See Table III for experimental error.

TABLE XXI

COKE CONTENT* OF SPENT CATALYST USED IN RUN CVR2

| Reactor | Section | Coke %** |
|---|---|---|
| 1 | 1Q | 31.2 ± 3.0 |
| | 2Q | 29.3 ± 4.6 |
| | 3Q | 19.2 ± 4.2 |
| | 4Q | 23.5 ± 5.7 |
| Average Reactor Coke Content: | | 25.8 ± 6.3 |
| 2 | 1Q | 24.8 ± 0.7 |
| | 2Q | 22.2 ± 2.5 |
| | 3Q | 26.2 ± 2.5 |
| | 4Q | 25.6 |
| Average Reactor Coke Content: | | 24.6 ± 2.3 |
| Overall Coke Content: | | 25.2 ± 4.63 |

*% Weight of regenerated catalyst.
**Adjusted for metal sulfide oxidation.

TABLE XXII

PHYSICAL PROPERTIES OF REGENERATED CATALYST OF RUN CVR2*

| Reactor | Section | Surface Area x $10^{-3}$ $m^2/kg$ | Pore Volume x $10^3$ $m^3/kg$ | Most Frequent Pore Diameter nm |
|---|---|---|---|---|
| 1 | 1Q | 210 | 0.80 | 14.8 |
| | 2Q | 210 | 0.74 | 14.4 |
| | 3Q | 210 | 0.78 | 14.8 |
| | 4Q | 201 | 0.76 | 14.8 |
| Average for Reactor 1 | | 208 | 0.77 | 14.7 |
| 2 | 1Q | 244 | 0.52 | 9.4 |
| | 2Q | 230 | 0.51 | 9.3 |
| | 3Q | 232 | 0.50 | 9.3 |
| | 4Q | 228 | 0.53 | 9.6 |
| Average for Reactor 2 | | 232 | 0.52 | 9.4 |

*See Table XII for experimental error.

catalyst in reactor 2 had similar properties to the regenerated catalyst in the same reactor of run CVR6 (Table XVIII).

V penetration data for the catalysts of this run are presented in Table XXIII. For reactor 1, V penetration into the catalyst particles was similar to that occurring in reactor 1 of CVR4 (Table XIV). V penetration was even along the length of the reactor. V penetration into the catalyst of reactor 2 was less pronounced. V seemed to have penetrated to the same extent into the catalyst of reactor 2 and into the same type of catalyst used in CVR6 (Table XIX).

Run CVR3

In run CVR3, the wide-pore, low active-metal content HDM catalyst, HT-TK-711, was packed in reactor 1. Reactor 2 was packed with the HDS catalyst HT-TK-771. This combination was selected to investigate the deactivation behavior of the active HDS catalyst when protected with an upstream, high metal tolerance HDM catalyst.

V removal curves for runs CVR3, CVR6, and CVR7 are presented in Figure 10. Placing the HDM catalyst in reactor 1 during run CVR3 increased HDM activity by about 8 %wt more than in run CVR6. HDM activity in this run, however, seemed to be similar to, or a little lower than in CVR7. Initial HDM activity decline during CVR3 lasted for about 30 h after which V removal activity leveled at about 46 wt%.

Figure 11 shows the boiling point curves for the 42 h liquid product samples of runs CVR3, CVR4, and CVR6. In CVR3, the initial boiling point was reduced by 6°C less than in CVR4 and by 14°C more than in CVR6. The boiling points of the first 15 to 20 vol% of the residue, the lighter components, were reduced less in this run than in runs CVR4

TABLE XXIII

VANADIUM PENETRATION THROUGH SPENT CATALYST OF RUN CVR2

| Reactor | Section | Vanadium Counts in Selected Areas* | | | | |
|---|---|---|---|---|---|---|
| | | $S_1$ | $S_2$ | $S_3$ | $S_4$ | $S_5$ |
| 1 | 1Q | 7643 | 6790 | 1325 | -- | -- |
| | 2Q | 3576 | 1732 | 720 | -- | -- |
| | 4Q | 3750 | 2348 | 910 | -- | -- |
| 2 | 1Q | 2639 | -- | -- | -- | -- |
| | 3Q | 2400 | -- | -- | -- | -- |
| | 4Q | 934 | -- | -- | -- | -- |

*See V penetration analysis in Chapter IV for definitions.

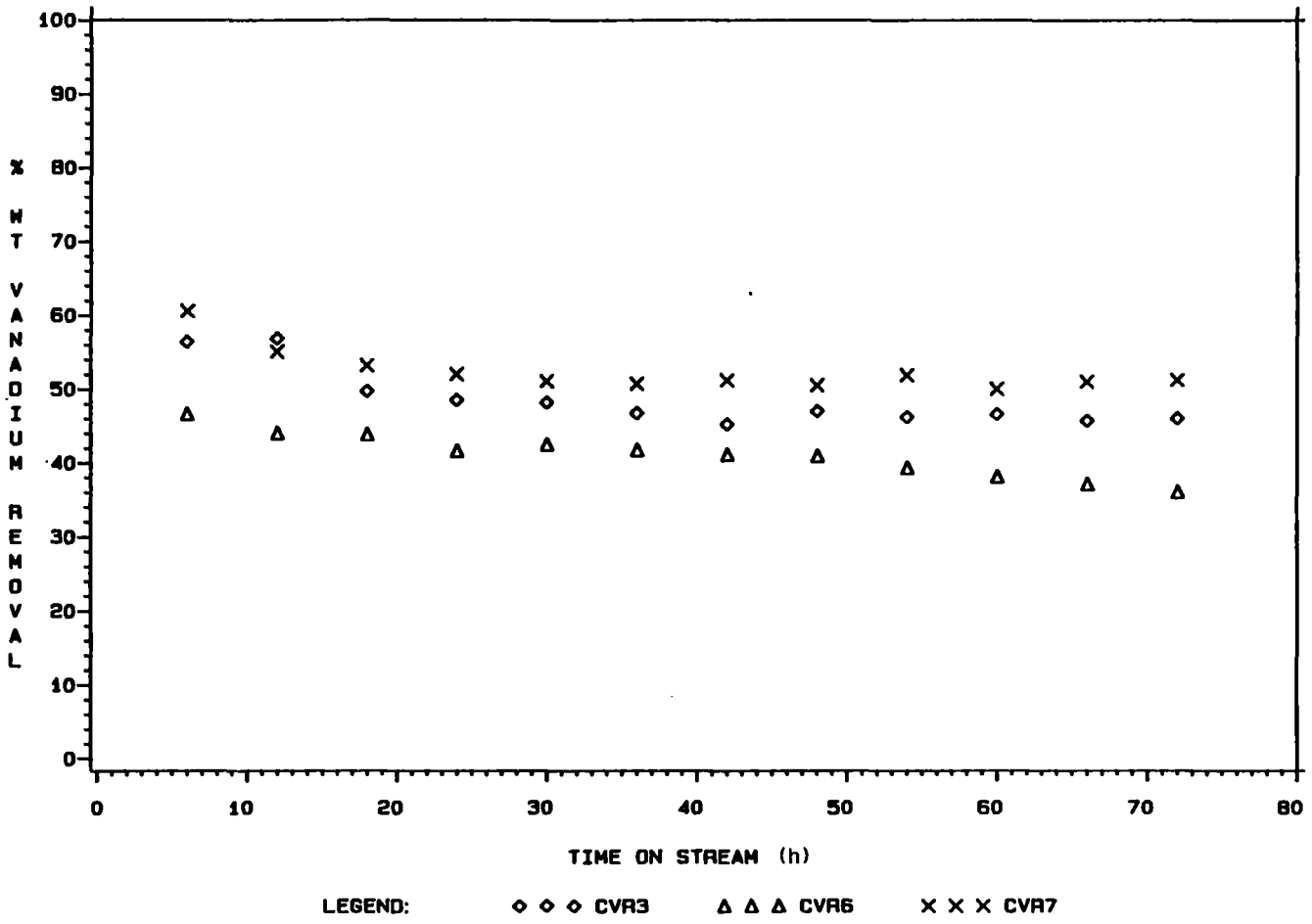


Figure 10. Percent Weight Vanadium Removal During Runs CVR3, CVR6, and CVR7

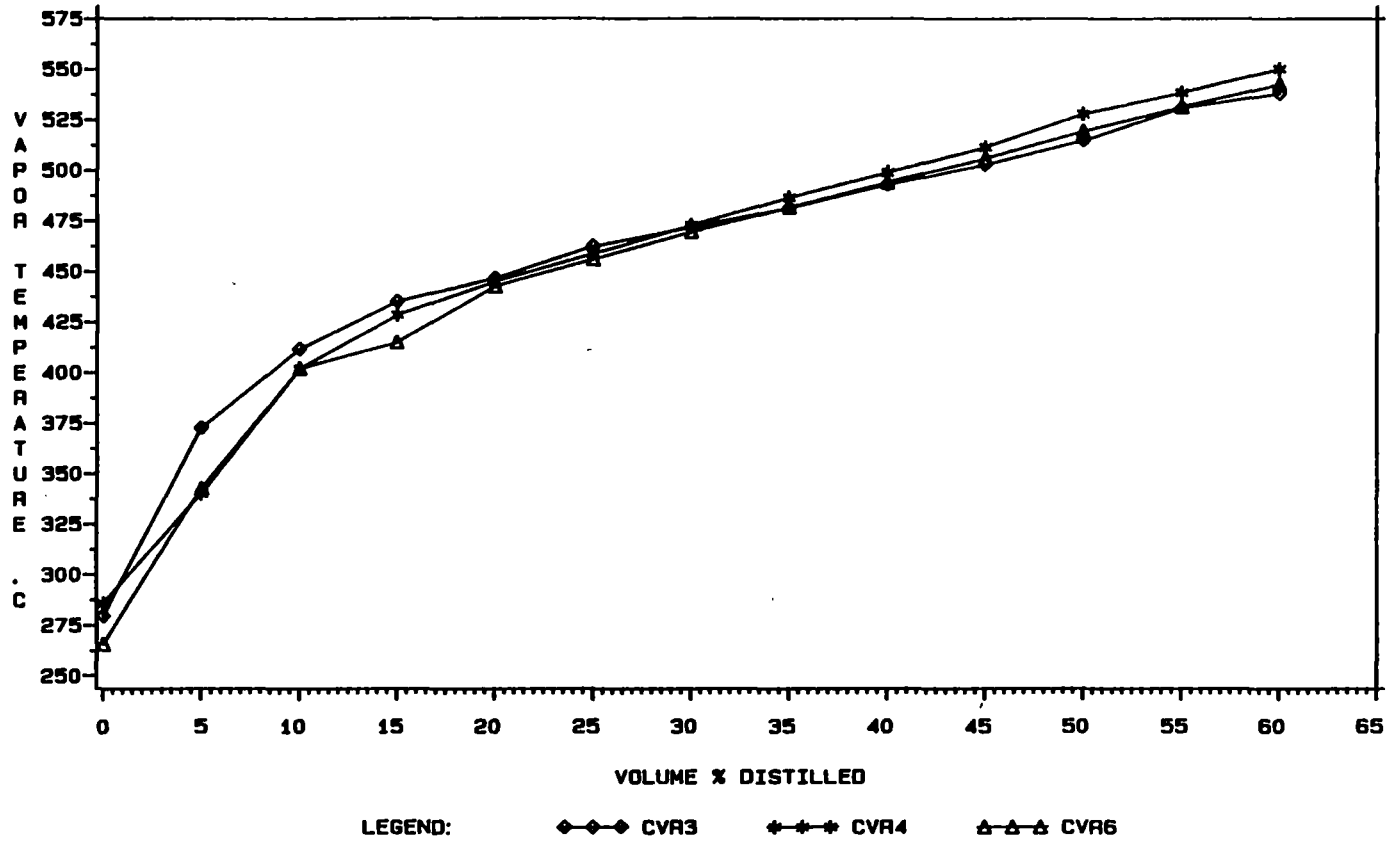


Figure 11. Boiling Point Curves for the 42 h Liquid Product Samples of Runs CVR3, CVR4, and CVR6

and CVR6. Reduction in the boiling points of the heavier components was between those obtained from CVR4 and CVR6 and similar to one obtained from CVR2.

Table XXIV shows reductions in the physical properties of catalysts used in CVR3. Reductions in the physical properties of the HDM catalyst in reactor 1 were slightly lower and somewhat more uniform than reductions that occurred to HDS/HDM catalyst properties in the same reactor of runs CVR2, CVR4, and CVR7 (Tables XX, IX, and X respectively). The active HDS catalyst in reactor 2, however, lost physical properties to a lesser extent than the same catalyst used in runs CVR2 and CVR6 (Tables XX and XVI respectively). This catalyst lost a small percentage of its surface area, an average of 11.6%, in spite of 44% pore volume loss.

Table XXV presents data for coke content on the spent catalyst of run CVR3. No particular pattern of coke deposition could be described in either reactor. Both reactors accumulated similar amounts of coke. The coke content of the HDM catalyst in reactor 1 resembled the coke content of the HDS/HDM catalyst in reactor 1 of runs CVR2, CVR4, and CVR7 (Tables XXI and XI). The active HDS catalyst in reactor 2 accumulated coke to a higher extent than the same catalyst in run CVR6 (Table XVII). Coke deposition seemed less in reactor 2 of CVR3 than in reactor 2 of CVR2. The overall catalyst coke content for this run was similar to those of runs CVR4 and CVR7, lower than that for CVR2, and higher than that for CVR6.

Catalyst regeneration data for this run are listed in XXVI. The catalysts in both beds seemed to fully recover their physical properties after regeneration.

TABLE XXIV

REDUCTION IN THE PHYSICAL PROPERTIES OF CATALYST USED IN RUN CVR3*

| Reactor | Section | % Reduction in | | |
|---|---|---|---|---|
| | | Pore Volume | Surface Area | Most Frequent Pore Diameter |
| 1 | 1Q | 38.0 | 25.8 | 17.7 |
| | 2Q | 34.6 | 27.3 | 15.0 |
| | 3Q | 30.8 | 22.7 | 13.7 |
| | 4Q | 35.9 | 25.8 | 15.0 |
| Average for Reactor 1 | | 34.8 | 25.4 | 15.4 |
| 2 | 1Q | 49.1 | 26.9 | 37.2 |
| | 2Q | 43.4 | 9.7 | 33.3 |
| | 3Q | 41.5 | 4.2 | 31.1 |
| | 4Q | 43.4 | 5.5 | 31.1 |
| Average for Reactor 2 | | 44.4 | 11.6 | 33.2 |

*See Table III for experimental error.

TABLE XXV

COKE CONTENT* OF SPENT CATALYST USED IN RUN CVR3

| Reactor | Section | Coke %** |
|---|---|---|
| 1 | 1Q | 21.4 ± 1.9 |
| | 2Q | 24.2 ± 0.6 |
| | 3Q | 19.3 ± 3.3 |
| | 4Q | 20.8 ± 3.1 |
| Average Reactor Coke Content: | | 21.4 ± 2.8 |
| 2 | 1Q | 20.1 ± 0.6 |
| | 2Q | 21.8 ± 2.4 |
| | 3Q | 19.7 ± 2.8 |
| | 4Q | 16.2 ± 0.8 |
| Average Reactor Coke Content: | | 19.5 ± 2.7 |
| Overall Coke Content: | | 20.5 ± 2.9 |

*% Weight of regenerated catalyst.
**Adjusted for metal sulfide oxidation.

TABLE XXVI

PHYSICAL PROPERTIES OF REGENERATED CATALYST OF RUN CVR3*

| Reactor | Section | Surface Area x $10^{-3}$ $m^2/kg$ | Pore Volume x $10^3$ $m^3/kg$ | Most Frequent Pore Diameter nm |
|---|---|---|---|---|
| 1 | 1Q | 187 | 0.8 | 16.2 |
| | 2Q | 181 | 0.83 | 17.0 |
| | 3Q | 196 | 0.83 | 15.8 |
| | 4Q | 186 | 0.8 | 16.0 |
| Average for Reactor 1 | | 188 | 0.82 | 16.3 |
| 2 | 1Q | 220 | 0.53 | 9.9 |
| | 2Q | 225 | 0.52 | 9.8 |
| | 3Q | 224 | 0.54 | 9.8 |
| | 4Q | 236 | 0.54 | 9.0 |
| Average for Reactor 2 | | 226 | 0.53 | 9.6 |

*See Table XII for experimental error.

Table XXVII gives an indication of the extent of V penetration into the catalyst particles used in run CVR3. V penetration in reactor 1 resembled data obtained from reactor 1 of runs CVR2, CVR4, and CVR7 (Tables XXIII, XIV, and XV respectively). V penetration in reactor 2 catalyst was similar to V penetration into the catalyst of run CVR6 (Table XIX).

Run CVR5

In this run, reactor 1 was packed with the HDM catalyst, HT-TK-711. The HDS/HDM catalyst, HT-TK-751, was used in reactor 2. This combination was used to investigate the effect of the upstream HDM catalyst on the HDT performance of the downstream HDS/HDM catalyst. Among the catalyst combinations investigated, the combination in this experiment had the lowest active metal content and the most open pore structure (Table IV).

Figure 12 presents V removal curves for runs CVR5, CVR6, and CVR7. Initial HDM activity was the highest in CVR5. Initial V removal activity decline lasted for 24 to 30 h, after which HDM activity was constant at 47 %wt V removal. V removal activity was similar for the combinations of CVR5 and CVR7. V removal in CVR5 was higher than in CVR6.

Figure 13 presents the boiling point curves for the 42 h liquid product samples of runs CVR4, CVR5, and CVR6. Boiling point reduction activity in run CVR5 was lower than in runs CVR4 and CVR6.

Table XXVIII presents reduction in the physical properties of catalysts used in CVR5. In both reactors, properties' loss seemed to decrease from top to bottom. The catalyst in reactor 2 lost more

TABLE XXVII

VANADIUM PENETRATION THROUGH SPENT CATALYST OF RUN CVR3

| Reactor | Section | Vanadium Counts in Selected Areas* | | | | |
|---|---|---|---|---|---|---|
| | | $S_1$ | $S_2$ | $S_3$ | $S_4$ | $S_5$ |
| 1 | 1Q | 5729 | 3612 | 1032 | 1006 | -- |
| | 4Q | 1258 | 878 | 984 | -- | -- |
| 2 | 1Q | 1127 | -- | -- | -- | -- |
| | 4Q | 1074 | -- | -- | -- | -- |

*See V penetration analysis in Chapter IV for definitions.

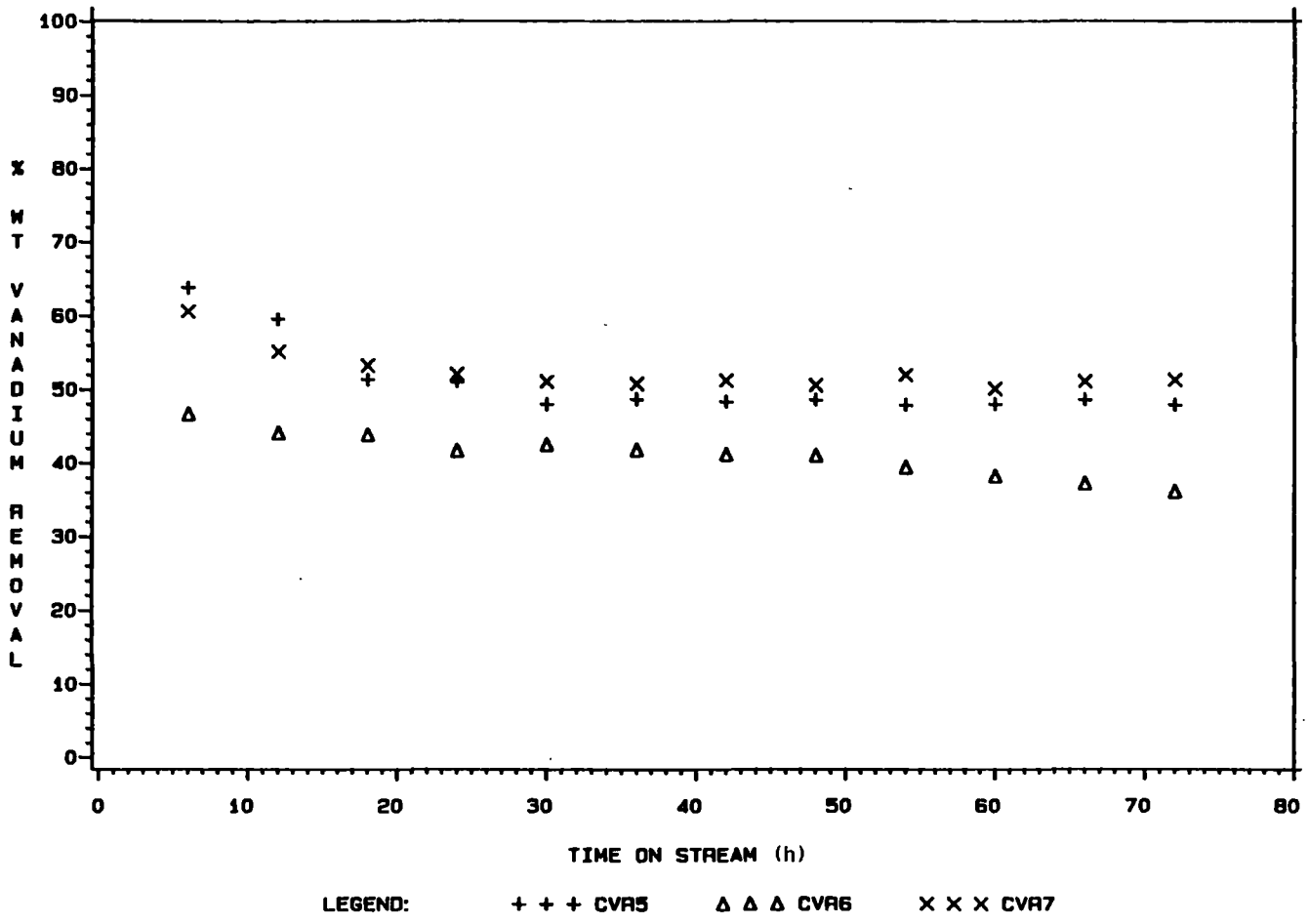


Figure 12. Percent Weight Vanadium Removal During Runs CVR5, CVR6, and CVR7

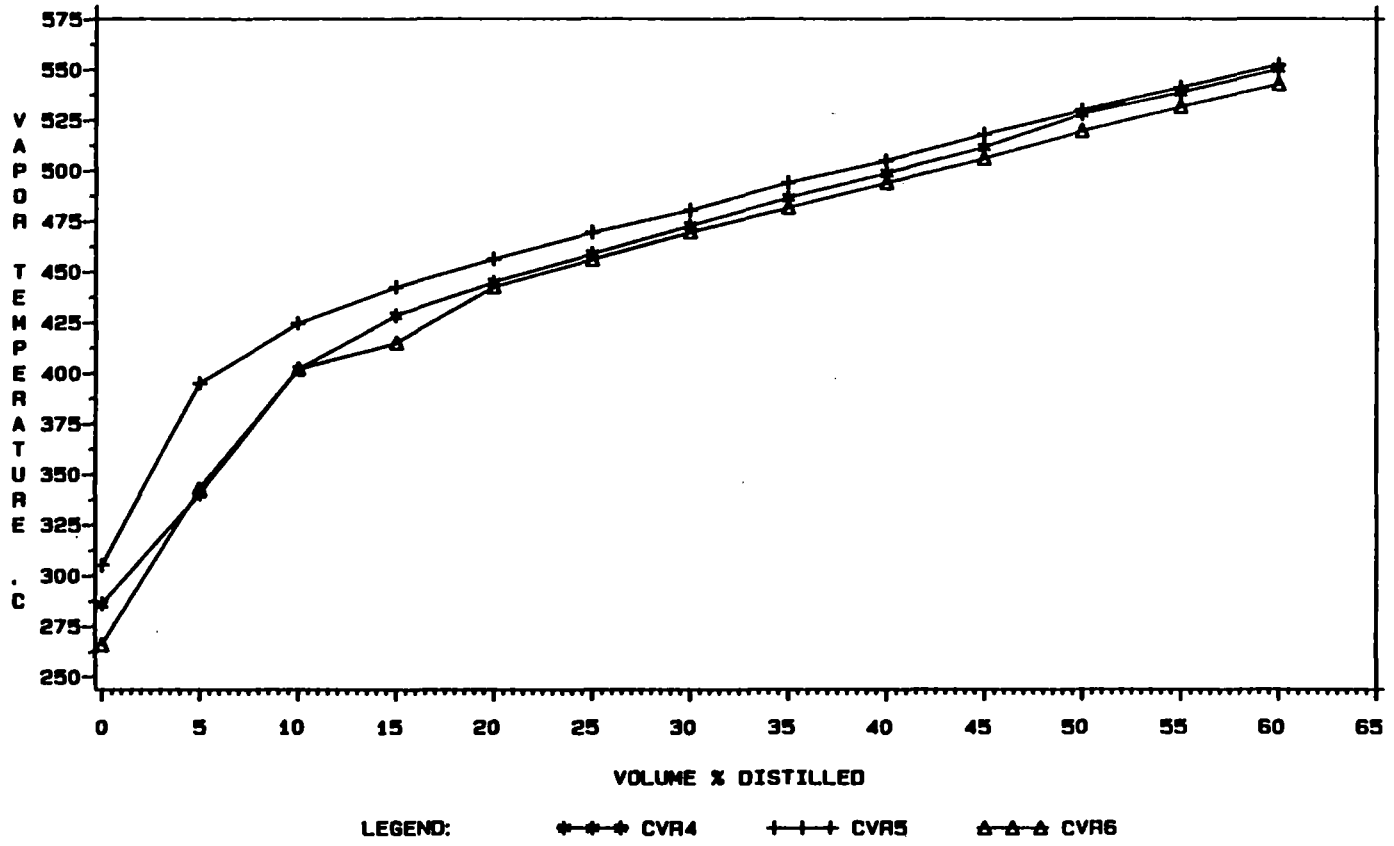


Figure 13. Boiling Point Curves for the 42 h Liquid Product Samples of Runs CVR4, CVR5, and CVR6

TABLE XXVIII

REDUCTION IN THE PHYSICAL PROPERTIES OF CATALYST USED IN RUN CVR5*

| Reactor | Section | % Reduction in | | |
|---|---|---|---|---|
| | | Pore Volume | Surface Area | Most Frequent Pore Diameter |
| 1 | 1Q | 36.7 | 23.2 | 21.6 |
| | 2Q | 35.4 | 24.7 | 17.0 |
| | 3Q | 32.9 | 19.6 | 15.0 |
| | 4Q | 35.4 | 20.1 | 15.0 |
| Average for Reactor 1 | | 35.1 | 21.9 | 17.2 |
| 2 | 1Q | 42.3 | 31.8 | 20.3 |
| | 2Q | 43.6 | 34.1 | 18.8 |
| | 3Q | 37.2 | 27.2 | 16.7 |
| | 4Q | 35.9 | 27.2 | 17.4 |
| Average for Reactor 2 | | 39.8 | 30.1 | 18.3 |

*See Table III for experimental error.

physical properties than the catalyst in reactor 1. Catalyst physical property loss in reactor 1 matched that in reactor 1 of run CVR3 (Table XXIV). The rate of catalyst physical property loss in reactor 2 was slightly higher than in reactor 2 of runs CVR4 and CVR7 (Tables IX and X).

Table XXIX presents data on the coke content of spent catalysts of runs CVR5. In both reactors, coke deposited in similar quantities; maximum deposition was observed at the entrance sections. Coke deposition in reactor 1 was similar to that in reactor 1 of CVR3 (Table XXV). Coke content in reactor 2 of runs CVR5, CVR4, and CVR7 were also similar (Table XI). Overall coke deposition was similar to the ones in runs CVR3, CVR4, and CVR7, higher than run CVR6 (Table XVII), and lower than in CVR2 (Table XXI).

Physical properties for the regenerated catalysts of run CVR5 are presented in Table XXX. Physical properties of both catalysts were fully recovered upon regeneration.

Table XXXI describes the extent of penetration of V into the catalyst particles of CVR5. V penetration into the HDM catalyst of reactor 1 was similar to reactor 1 in runs CVR5 and CVR3 (Table XXVII). Catalyst in reactor 2 achieved higher V penetrations in this run than in runs CVR4 and CVR7 (Tables XIV and XV) and lower than in run CVR1 (Table VIII).

TABLE XXIX

COKE CONTENT* OF SPENT CATALYST USED IN RUN CVR5

| Reactor | Section | Coke %** |
|---|---|---|
| 1 | 1Q | 20.7 ± 1.3 |
| | 2Q | 17.6 ± 3.7 |
| | 3Q | 17.0 ± 1.2 |
| | 4Q | 18.1 ± 0.8 |
| Average Reactor Coke Content: | | 18.4 ± 2.3 |
| 2 | 1Q | 24.4 ± 0.4 |
| | 2Q | 24.1 ± 5.5 |
| | 3Q | 18.6 ± 0.4 |
| | 4Q | 15.9 ± 2.0 |
| Average Reactor Coke Content: | | 20.8 ± 4.5 |
| Overall Coke Content: | | 19.6 ± 3.7 |

*% Weight of regenerated catalyst.
**Adjusted for metal sulfide oxidation.

TABLE XXX

PHYSICAL PROPERTIES OF REGENERATED CATALYST OF RUN CVR5*

| Reactor - Section | | Surface Area x $10^{-3}$ $m^2/kg$ | Pore Volume x $10^3$ $m^3/kg$ | Most Frequent Pore Diameter nm |
|---|---|---|---|---|
| 1 | 1Q | 188 | 0.78 | 15.8 |
| | 2Q | 197 | 0.82 | 16.0 |
| | 3Q | 187 | 0.79 | 16.4 |
| | 4Q | 189 | 0.79 | 15.6 |
| Average for Reactor 1 | | 190 | 0.80 | 16.0 |
| 2 | 1Q | 201 | 0.79 | 14.8 |
| | 2Q | 210 | 0.79 | 14.6 |
| | 3Q | 212 | 0.77 | 14.4 |
| | 4Q | 217 | 0.61 | 14.2 |
| Average for Reactor 2 | | 210 | 0.74 | 14.5 |

*See Table XII for experimental error.

TABLE XXXI

VANADIUM PENETRATION THROUGH SPENT CATALYST OF RUN CVR5*

| Reactor | Section | Vanadium Counts in Selected Areas | | | | |
|---|---|---|---|---|---|---|
| | | $S_1$ | $S_2$ | $S_3$ | $S_4$ | $S_5$ |
| 1 | 1Q | 2616 | 1731 | 1098 | -- | -- |
| | 4Q | 2045 | 1503 | 830 | -- | -- |
| 2 | 1Q | 1007 | 1258 | -- | -- | -- |
| | 4Q | 1342 | 728 | -- | -- | -- |

*See V penetration analysis in Chapter IV for definitions.

# CHAPTER VII

# DISCUSSION

A summary of the experimental results is shown in Table XXXII, and a discussion of these results follows. It is appropriate to mention here that HDS results from these experiments were reported by Adarme (1986).

## Product Characterization

### Metal Analysis

Because of the relatively high experimental error in Ni content analysis, Ni data were presented for run CVR1 only. V removal was considered sufficient to describe the HDM process. High V removal rates, up to 65 %wt, were obtained. Excessive flow of hydrogen, the use of Ni-Mo catalysts, and the extensive sulfiding procedure (Appendix B) probably promoted optimum hydrogenation activity (Van Zijill Langhout, 1981; Thakur et al., 1985). Hydrogenation was found to be the first step in HDM reactions (Ware and Wei, 1985a). High concentrations of metallo-porphyrins in the feed were indicated by the apparent ease of metal removal (Reynolds et al., 1985).

Diffusion limitations in HDM reactions were very clear when V removal curves of CVR6 and CVR7 were examined (Figure 6). Because of the higher pore volume and larger MFPD of the HDS/HDM catalyst and in

TABLE XXXII

SUMMARY OF THE EXPERIMENTAL RESULTS

| Run | CVR2 | CVR3 | CVR4/7 | CVR5 | CVR6 |
|---|---|---|---|---|---|
| Catalyst Used* | | | | | |
| Top: | HDS/HDM | HDM | HDS/HDM | HDM | HDS |
| Bottom: | HDS | HDS | HDS/HDM | HDS/HDM | HDS |
| Vanadium Removal: | High | Intermediate | High | Intermediate | Low |
| Boiling Point Reduction: | Intermediate | Intermediate | Intermediate | Low | High |
| % Reduction in Physical Properties | | | | | |
| - Pore Volume | | | | | |
| Top: | Intermediate | Low | Intermediate | Low | High |
| Bottom: | High | Intermediate | Low | Intermediate | Intermediate |
| - Surface Area | | | | | |
| Top: | High | Intermediate | Intermediate | Intermediate | Low |
| Bottom: | Intermediate | Low | Intermediate | High | Low |
| - MFPD | | | | | |
| Top: | Low | Low | Low | Low | Very high |
| Bottom: | High | Intermediate | Low | Low | Very high |

TABLE XXXII (Continued)

| Run | CVR2 | CVR3 | CVR4 | CVR5 | CVR6 |
|---|---|---|---|---|---|
| Coke Content | | | | | |
| Top: | High | Intermediate | Intermediate | Intermediate | Low |
| Bottom: | High | Intermediate | Intermediate | Intermediate | Low |
| Catalyst Regeneration | ---------- | ---------- | fully regenerated | ---------- | ---------- |
| Vanadium Penetration** | | | | | |
| Top: | 3S | 3-4S | 3S | 3S | 1S |
| Bottom: | 1S | 2S | 1S | 2S | 1S |

* HDS catalyst = HT-TK-771
  HDS/HDM catalyst = HT-TK-751
  HDM catalyst = HT-TK-711
**See V penetration analysis in Chapter IV for definition.

spite of its lower active metal content it achieved higher rates of HDM than the HDS catalyst.

Because of the added HDM activity, the three graded catalyst bed combinations of runs CVR2, CVR3, and CVR5 yielded higher V removal rates than the HDS catalyst of CVR6 (Figures 8, 10 and 12 respectively). The high V removal rates of the HDS/HDM catalyst in CVR4 and CVR7 were only matched by the catalyst combination of CVR2; the HDS/HDM catalyst placed upstream of the HDS catalyst. While catalyst beds of runs CVR4 and CVR7 contained more open pore structure, the active metal content of the combination of CVR2 was higher. In general, placing the HDS/HDM catalyst in the top reactor enhanced the overall HDM activity of the catalyst combination.

Figure 14 is a comparison between V removal activities of the graded-bed catalyst combinations. During the first 24 h, differences between V removal activities were not clear. However, CVR3 catalyst combination appeared to possess lower HDM activity than the catalysts of CVR2. Reactor 1 of CVR3 contained more favorable HDM catalyst properties but the HDS/HDM catalyst of CVR2 contained more active metal.

Catalyst combinations of run CVR3 and CVR5 provided nearly similar HDM activities. The combination of CVR5 had the lowest active metal content of all other combinations, but it had the most favorable HDM catalytic properties. Because of its higher pore volume and larger average MFPD, the initial activity of CVR5 combination was the highest. But, as the more limited active metal sites were occupied by poisons and coke, V removal activity initially declined at higher rates than in other experimental runs. Initial, rapid activity decline was

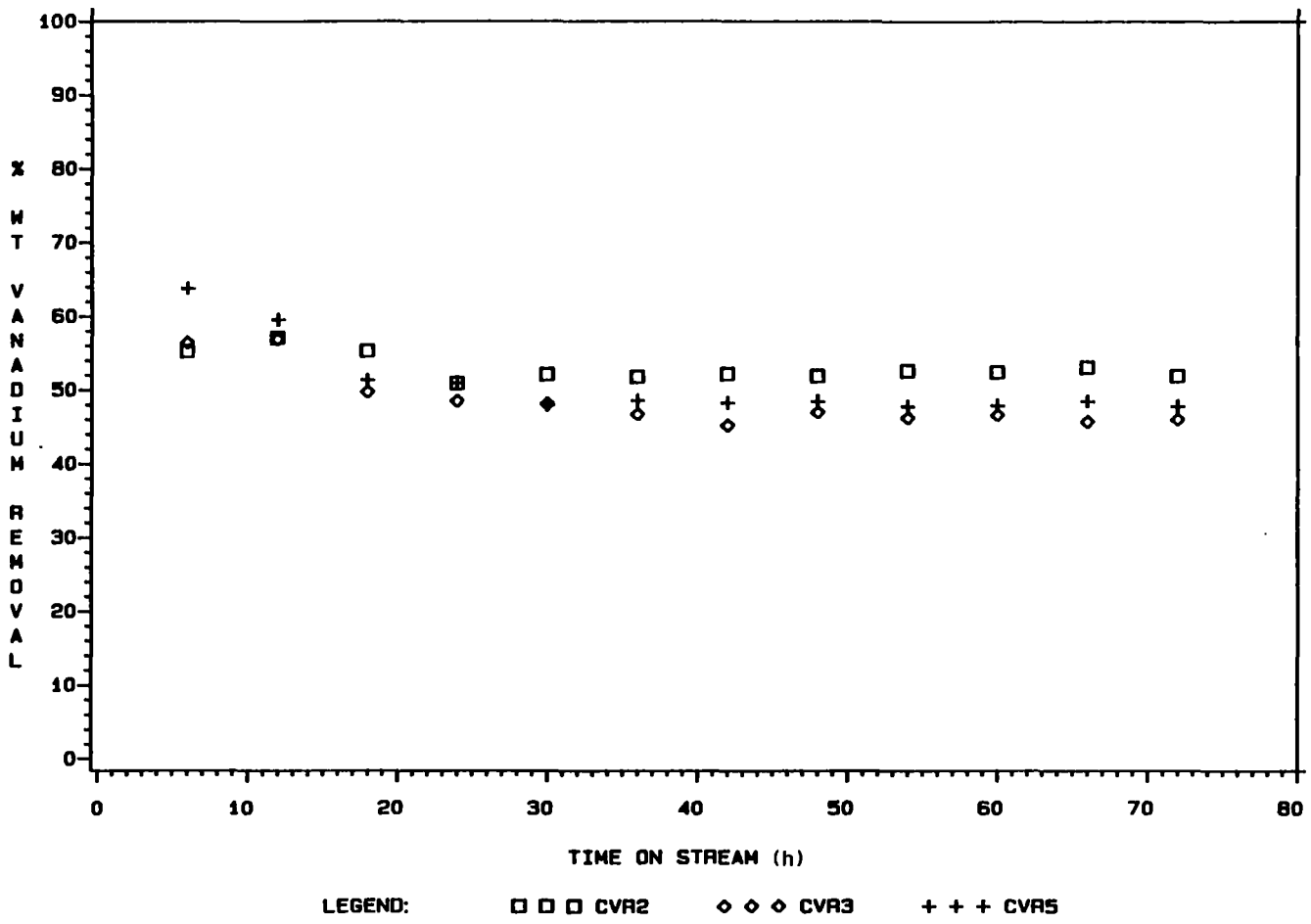


Figure 14. Percent Weight Vanadium Removal During Runs CVR2, CVR3, and CVR5

apparent for all the runs. This initial activity decline lasted for 24 to 30 h on the average.

In run CVR1, the HDM dependence on temperature was not clear for Ni and V analysis. This was probably due to the diffusional limitations in the HDM reactions (Table V and Figure 2).

ASTM D-1160 Distillation

Thermal cracking was reported to be minor below 400°C (Bunger, 1985). Boiling point reduction of the feed residue during the HDM experiments reflected conversion via hydrocracking and HDT reactions. Boiling point reduction has been closely related to HDM (Asaoka et al., 1983).

The shift of boiling points, and hence, of residue molecular weight distribution was, in general, proportional to the total active plus promoter metals concentrations in the catalyst combination. The catalyst combinations of runs CVR2 and CVR3 had metal contents between those for CVR4 and CVR6 combinations. Boiling point reduction activities in CVR2 and CVR3 also appeared to fall between the ones obtained in CVR4 and CVR6 (Figures 9 and 11). Figure 15 is a comparison between boiling point reduction activities of the graded-bed catalyst combinations. The catalyst combination of CVR5 had the least boiling point reduction activity; it also had the lowest total active and promoter metals contents. In contrast, the combination of run CVR6 with the highest total active and promotor metals contents had the greatest boiling point reduction activity.

In spite of samples taken at the same temperature, less boiling point reduction was achieved for the 42 h sample of CVR1 than of CVR4

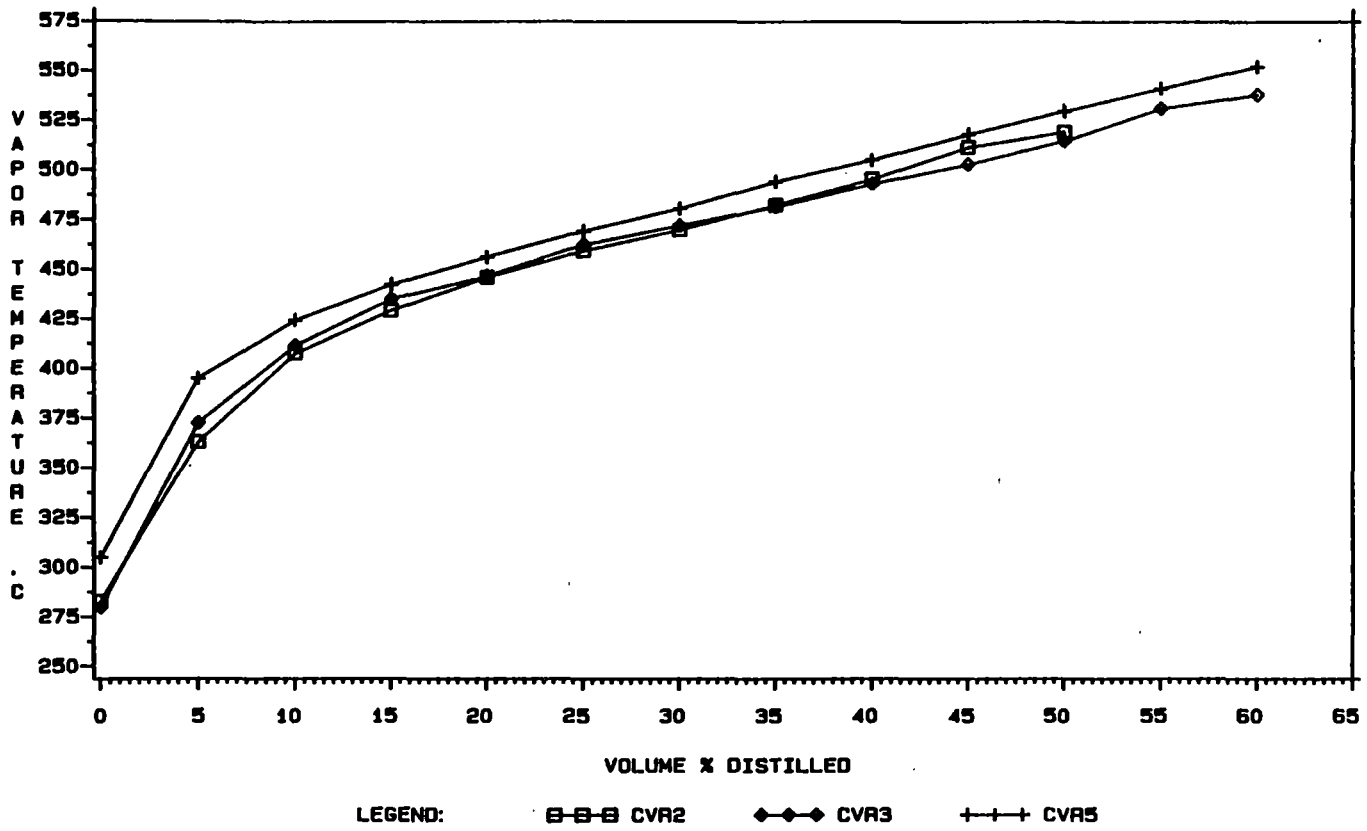


Figure 15. Boiling Point Curves the 42 h Liquid Product Samples of Runs CVR2, CVR3, and CVR5

and CVR7. Because the catalyst in CVR1 was subjected to lower severities prior to the 42 h sample collection, it inflicted milder boiling point reduction on this sample compared with the 42 h sample of runs CVR4 and CVR7. Catalyst previous history appeared to play a role in determining boiling point reduction activity.

## Catalyst Characterization

The feed metal content (101 ppm Ni+V) was not as high as desired for this study. Feed metals in the range of 300 to 400 ppm Ni+V were desired. But difficulty in procurement forced a compromise in feed properties. When an average of 50 %wt metal removal was assumed, only a negligible 1.3 g was calculated to deposit on the catalyst during the 3-day runs. With estimated total bed metal capacities of 35 to 50 g, this 1.3 g was only 2.6 to 2.7 of the bed limits. Hence, although both metals and coke deactivation exist, pore-mouth plugging by coke probably was the major cause in the deactivation of catalysts.

### Spent Catalyst Physical Properties

The reproducibility of the catalyst physical property changes were excellent. For the HDS/HDM catalyst, changes in catalysts' physical properties were reproduced in reactor 1 of runs CVR2, CVR4, and CVR7 and in reactor 2 of runs CVR4 and CVR7 within ± 10%. For the HDM catalyst, physical property changes were reproduced in reactor 1 of runs CVR3 and CVR5 within ± 10%.

Losses in the physical properties of the HDS/HDM catalyst were similar in reactor 1 and reactor 2. This large pore catalyst with the narrowly defined pore-size distribution acquired somewhat even physical

property profiles. Even distribution of deactivation species was reported to improve catalyst effectiveness and life (Howell et al., 1985).

Reductions in the physical properties of the HDS catalyst in CVR6 were so pronounced that no reliable porosimeter curves could be obtained. Generally, physical property reductions for the HDS catalyst decreased from the top to the bottom of the reactors. Changes were steeper for this catalyst than for the HDS/HDM catalyst. Pore plugging by coke appeared to be the dominating deactivation mechanism. The catalyst lost the least amount of surface area but achieved the highest pore volume and MFPD reductions. Excluding coke precursors and metal compounds from its inner surfaces, the HDS catalyst deposited these precursors on its outer surfaces in high rates which led to increased pore plugging by metals and coke. Similar results were obtained by Bhan (1983) when upgrading a coal derived liquid using small pore catalysts. According to the above findings and the results of Howell et al. (1985), one can conclude that the HDS catalyst was not utilized very effectively.

The HDM catalyst in reactor 1 of runs CVR3 and CVR5 showed the least change of catalyst physical properties. This large pore-size, wide pore-size distribution catalyst also acquired much more uniform physical property profiles along catalyst beds. The HDM catalyst was the most effectively used among the three catalysts.

At the end of run conditions, no dramatic activity profiles such as described by Tamm et al. (1981) were observed. Catalyst physical properties slightly increased from the top to the bottom in all reactors during all experimental runs except CVR1. Much more uniform activity

profiles were achieved in both reactors of CVR1. The extents of catalyst physical property reductions were also identical in both reactors of CVR1. Lower operating severity might have resulted in more even end-of-run activity profiles. These results seemed to agree with the results of Tamm et al. (1981) and Green and Broderick (1981). Because of this lower severity and in spite of 58% longer duration, physical property changes in CVR1 were similar to those in CVR4 and CVR7.

In run CVR6, the HDS catalyst in reactor 1 did not seem to help reduce the catalyst physical property losses in reactor 2. Almost the same levels of property reductions were achieved in both reactors. The HDS catalyst in reactor 1 did not effectively reduce the amounts of larger coke precursors and metal species on the surfaces of the downstream HDS catalyst. The HDS catalyst in reactor 1, therefore, did not reduce pore plugging of the catalyst in reactor 2.

In CVR2, losses in the catalyst physical properties of the HDS catalyst in reactor 2 were considerably reduced by placing the HDS/HDM catalyst upstream of it in reactor 1. The HDS/HDM catalyst with its wider pores, probably caused considerable molecular size reduction and improved diffusion conditions in the downstream catalyst bed, thus, reducing catalyst pore plugging.

Loss of catalyst physical properties of the HDS catalyst were lower in CVR3 than in CVR6 and CVR2. While both the HDM and the HDS/HDM catalysts in reactor 1 improved the performance of the downstrean HDS catalyst in reactor 2, lower conversion activity of the HDM catalyst probably caused the HDS catalyst in reactor 2 of run CVR3 to exclude more metals and coke precursors from its pores. Because of its larger

MFPD, the HDM catalyst might have reduced the sizes of larger molecules more effectively than the HDS/HDM catalyst, thus decreasing their concentrations on the surfaces of the downstream catalyst and, thereby reducing pore plugging.

The HDS/HDM catalyst in reactor 2 of run CVR5 lost slightly more catalyst physical properties than in reactor 2 of runs CVR4 and CVR7. The upstream HDS/HDM catalyst had more conversion activity and accumulated more deactivating species than the upstream HDM catalyst of CVR5. This is a reverse of what was found when placing these two catalysts upstream of the small pore HDS catalyst.

## Coke Content

Relatively high amounts of coke were accumulated on the catalyst surfaces; up to 25 wt%. Coke deposition obstructed catalyst pores and drastically reduced pore volume.

Coke content standard deviations were sometimes too high to facilitate reasonable comparisons. However, within the range of this experimental error, no regular patterns of coke deposition were observed between catalyst sections in any particular reactor. Coke deposits seemed to evenly distribute throughout the catalyst beds. These results agreed with the findings of Sei (1980). In addition, no differences in coke contents of reactors 1 and 2 were observed in any of the experimental runs.

Coke contents of the HDM catalyst in reactor 1 of runs CVR3 and CVR5 were similar. They resembled those for the HDS/HDM catalyst in runs CVR1, CVR2, and CVR7. Coke content of the HDS catalyst in CVR6 was considerably lower. The small pore catalyst seemed to exclude coke

precursors from its pores. Although the HDS catalyst accumulated lower amounts of coke, it lost the most pore volume and MFPD. Larger pore catalysts possessed higher tolerance for coke deposition. They achieved lower losses in pore volume and MFPD, hence, coke was more effectively distributed on their surfaces.

When the HDS/HDM catalyst, in CVR2, or the HDM catalyst, in CVR3, were placed upstream from the HDS catalyst, the HDS catalyst coke content increased considerably. Lower physical property reductions were obtained in spite of this increase in coke content. The upstream, wide pore catalysts seemed to decrease the sizes of larger molecules, including the coke precursors, and improved their diffusion into the HDS catalyst pores. Improved diffusion properties probably led to more efficient distribution of coke on the downstream catalyst surfaces. The upstream, wide pore catalysts increased the HDS catalyst coke capacity.

Among the runs with the graded-bed combinations, CVR2 had the highest coke deposition rates. The catalyst combination in this run also contained the highest active metal content. Similar coke accumulation rates in runs CVR3 and CVR5 demonstrated a balance between increased coking due to more active metal content versus increased coking due to the more open pore structure and the higher capacity for coke.

## Catalyst Regeneration

Upon combustion, spent catalysts fully recovered their original properties. Some of the measured properties exceeded those for the combusted fresh catalysts by 1 to 2 percents. This was believed to be the result of experimental error in catalyst characterization.

No regular patterns of physical properties were seen for any of the regenerated catalysts. Similar physical properties were seen for the regenerated HDM catalyst in both CVR3 and CVR5. Similar physical properties were also seen for the regenerated HDS/HDM catalyst in all runs. The regenerated HDS catalyst in reactor 2 of runs CVR2, CVR3, and CVR6 recovered slightly more properties than the regenerated catalyst of reactor 1 of run CVR6.

Vanadium Penetration

The HDS/HDM and the HDM catalysts achieved relatively deep V penetration profiles within the catalyst particles. These profiles were more even along reactor 1 and showed less penetration in reactor 2. Deeper metal penetration is said to reflect higher catalyst effectiveness in the presence of metals (Plumail et al., 1983).

V penetration into the HDM and the HDS/HDM catalysts was similar. It could not be concluded, therefore, which of the two catalysts had higher effectiveness in the HDM reactions.

V was only detected on and very close to the surface of the HDS catalyst particles. V penetration into the HDS catalyst was similar in runs CVR2, CVR3, and CVR6. V was nondetectable after the $S_1$ area of the particle cross-sections tested. By excluding high molecular weight asphaltenes and coke precursors from its pore volume, the HDS catayst also excluded metal depositing species. The HDS catalyst was not effectively used in the HDM process.

# CHAPTER VIII

# CONCLUSIONS AND RECOMMENDATIONS

## Conclusions

Within the range of operating conditions and catalysts used in this study the following conclusions could be drawn regarding the use of graded-catalyst beds for the HDM of the petroleum residue.

1. Overall metal removal activities of graded-catalyst bed combinations appeared to be favored by more open pore structures (high pore volumes and large MFPD) and higher total active and promotor metals contents. Catalyst combinations with physical properties that favored HDM resulted in slightly lower HDM rates due to lower total active and promotor metals contents.

2. Boiling point reduction activity was also favored by increasing the total active and promotor metals contents of the catalyst bed combination.

3. At the end-of-run conditions, catalyst physical property losses appeared to decrease from the top to the bottom of catalyst beds. The small pore-size, highly active HDS catalyst achieved the steepest physical property profiles. Pore plugging was probably the dominating deactivation mechanism for this catalyst. Also, metal penetration into the HDS catalyst particles was minimal. The large pore-size, HDS/HDM catalyst with the narrowly defined pore-size distribution possessed more uniform physical property profiles than the

HDS catalyst. Metal penetration profiles were deeper for this catalyst. The large pore-size, wide pore-size distribution, HDM catalyst with the lowest intrinsic surface activity achieved the most uniform physical property profiles.

4. Physical property losses of the HDS catalyst in the single catalyst bed were severe. In graded-catalyst beds, the upstream HDS/HDM catalyst reduced physical property losses of the downstream HDS catalyst. The HDS/HDM catalyst reduced residue molecular size-distribution and probably improved diffusion conditions downstream, thus, decreasing HDS catalyst pore plugging. The HDM catalyst provided the best HDS catalyst protection. The HDM catalyst probably reduced the concentrations of larger residue molecules on the surfaces of the downstream small-pore catalyst.

5. When a downstream HDS/HDM catalyst was to be protected, an upstream HDS/HDM catalyst provided a better catalyst protection than an upstream HDM catalyst.

6. Coke deposits were evenly distributed throughout catalyst beds. Large pore catalysts accumulated the highest amounts of coke deposits but suffered the least rates of pore plugging. The distribution of coke on catalytic surfaces was more efficient for large pore than for small pore catalysts.

7. In graded catalyst beds, upstream large pore catalysts increased the coke content of the HDS catalyst considerably in spite of decreasing its pore plugging rate. More efficient distribution of coke on catalytic surfaces and, hence, improved residue diffusion conditions downstream were evident.

8. The graded-catalyst bed experiments demonstrated a trade-off between increased coking due to more open pore structure versus increased coking due to increased catalyst active metal content The graded-bed combination with the highest total active and promotor metals contents achieved the highest coke levels.

## Recommendations For Future Work

1. To compensate for the low intrinsic surface activity of the HDM catalyst, the possibility of operating HDM catalyst beds at higher temperatures (up to 450°C) should be investigated.

2. Information on catalyst activity decline that might result from using the three catalysts in triple-bed combinations for the HDT of a petroleum residue seem attractive.

3. Longer experimental runs (up to 30 days) with higher feed metal contents (300 to 400 ppm Ni+V) should be conducted to study the long-term effect of metal deposition on graded-beds' performance.

# BIBLIOGRAPHY


Abbott, M. D., R. C. Archibald, and R. W. Dorn; American Petroleum Institute, Division of Refining, Vol. 38 (1958).

Adarme, R.; M.S. Thesis, Oklahoma State University, Stillwater, Oklahoma (1986).

Agrawal, R. and J. Wei; Ind. Eng. Chem. Proc. Des. Dev., Vol. 23, No. 3 (1984a).

Agrawal, R. and J. Wei; Ind. Eng. Chem. Proc. Des. Dev., Vol. 23, No. 3 (1984b).

Akhtar, S. et al.; Quarterly Technical Report DOE/PETC/QTR-85/1, U. S. Dept. of Energy, Pittsburgh (1985).

Anderson, L. R. et al.; NPRA Q&A-6, Oil and Gas Journal, June (1980).

Annual Book of ASTM Standards, Volume 05.01 (1985).

Asaoka, S. A., S. Nakata, Y. Shiroto, and C. Takeuchi; Ind. Eng. Chem. Proc. Des. Dev., Vol. 22, No. 2 (1983).

Aubert, C., R. Durand, P. Geneste, and C. Moreau; Journal of Catalysis, Vol. 97, pp. 169-176 (1986).

Bachelier, J., M. J. Tilliette, J. C. Duchet, and D. Cornet; Journal of Catalysis, Vol. 76, pp. 300-315 (1982).

Bachelier, J., M. J. Tilliette, J C. Duchet, and D. Cornet; Journal of Catalysis, Vol. 87, pp. 292-304 (1984).

Bailey, W. A., Jr., and M. Nager; The Seventh World Petroleum Congress, Mexico City (1967).

Banta, F.; U. S. Patent No. 4447314, May 8 (1984).

Beazer, J. R.; M.S. Thesis, Oklahoma State University, Stillwater, Oklahoma (1984).

Beazer, J. R. and B. L. Crynes; Fuel Processing Tech., Vol. 11, pp. 241-250 (1985).

Beret, S., and J. G. Reynolds; Symposium on New Chem. Heavy Ends, American Chemical Society, Div. of Pet. Chem., Chicago (1985).

Berg, J. W. et al.; NPRA Q&A-4, Oil and Gas Journal, July (1983).

Bhan, O. K., M.S. Thesis, Oklahoma State University, Stillwater, Oklahoma (1981).

Bhan, O. K., Ph.D. Dissertation, Oklahoma State University, Stillwater, Oklahoma (1983).

Bowes, E., S. D. Brandes, M. Farcasiu, and E. Scott; U.S. Patent No. 4486298, December (1984).

Bridge, A. G., G. D. Gould, and J. F. Berkman; Oil and Gas Journal, January (1981).

Bunger, J. W.; Symposium on Mechanism of Coke Formation, American Chemical Society, Div. of Pet. Chem., Chicago (1985).

Buzzi-Ferraris, G., M. Morbidelli, P. Forzatti, and S. Carra; International Chemical Engineering, Vol. 24, No. 3, July (1984).

Chillingworth, R. S., and J. D. Potts; U. S. Department of Energy Report DOE/PC/60047-T6 (1984).

Choi, H. W., and M. B. Dines; Fuel, Vol. 64, January (1985).

Christman, R. D., E. Pasek, and R. W. Plesko; Symposium on Dev. in HDM Catalysts, American Chemical Society, Div. of Pet. Chem., Miami (1985).

Chu, C. I., and I. Wang; Ind. Eng. Chem. Proc. Des. Dev., Vol. 21, No. 2 (1982).

Collins, J. M., et al.; NPRA Q&A-2, Oil and Gas Journal, March (1985).

Curtis, C. W., K. J. Tsai, and J. A. Guin; Symposium on New Chemistry of Heavy Ends, American Chemical Society, Div. of Pet. Chem., Chicago (1985).

Do, H. D., and D. D. Do; Chemical Engineering Journal, No. 29 (1984).

Dooley, K. A., and B. L. Crynes, Submitted to Liquid Fuel Technology, April (1985).

Doraiswamy, L. K., and D. G. Tajbl; "Laboratory Catalytic Reactors", Marcel Dekker (1975).

Forzatti, P., G. Buzzi-Ferraris, M. Morbidelli, and C. Carra; International Chemical Engineering, Vol. 24, No. 1, January (1984).

Friedman, S. et al.; Quarterly Technical Report DOE/PETC/QTR-84/4, U. S. Dept. of Energy, Pittsburgh (1984).

Garcia, W., and J. M. Pazos; Chemical Engineering Science, Vol. 37, No. 10, pp. 1589-1591 (1982).

Gates, B. C., Katzer, and Schuit; "Chemistry of Catalytic Processes", McGraw-Hill, New York (1979).

Geneste, P., J. L. Olive, and S. Biyoko; Journal of Catalysis, Vol. 83, pp. 245-247 (1983).

Gibson, K. R., D. C. Green, and D. P. Teichman; Chemical Engineering Progress, May (1983).

Green, D. C., and D. H. Broderick; Chemical Engineering Progress, December (1981).

Hallie, H.; Oil and Gas Journal, December (1982).

Hannerup, P. N., and A. C. Jacobsen; American Chemical Society, Div. of Pet. Chem., Seattle (1983).

Higashi, H., K. Shironno, G., Sato, Y. Nishimura, and S. Egashira; Symposium on Development of HDM Catalysts, American Chemical Society, Div. of Pet. Chem., Miami (1985).

Hohnholt, J. F., and C. Fausto; Symposium on Petroleum Residue Upgrading, American Institue of Chemical Engineers, Annual Meeting (1984).

Hohnholt, J. F., and C. Fausto; Chemical Engineering Progress, June (1985).

Howell, R. L., C. Hung, K. Gibson, and H. C. Chen; Oil and Gas Journal, July (1985).

Hung, C., R. L. Howell, and D. R. Johnson; Chemical Engineering Progress, March (1986).

Hung, C. W., and J. Wei; Ind. Eng. Chem. Proc. Des. Dev., Vol. 19, No. 2 (1980).

Itoh, R., M. Sekino, and H. Muto; Synfuels' Fifth Worldwide Symposium, Washington, D. C., November (1985).

Jacobs, F. S., and R. H. Filby; Symposium on Advances in Separation Technology, American Chemical Society, Div. of Pet. Chem., Seattle (1983).

Jacobsen, A, C., P. N. Hannerup, B. Cooper, J. Bartholdy, and A. Nielsen, American Institute of Chemical Engineers, Spring National Meeting, Houston (1983).

Jepsen, J. S., and H. F. Rase; Ind. Eng. Chem. Prod. Res. Dev., Vol. 20, No. 3 (1981).

Johnson, A. D.; Oil and Gas Journal, May (1983).

Johnson, D. R., and R. S. Tolberg; "Shale Oil Upgrading and Refining", Edited by S. A. Newman, Butterworth Publishers, Boston (1983).

Johnstone, R. A. W., A. H. Wilky, and I. D. Entwistle; Chemical Reviews, Vol. 85, No. 2 (1985).

Katti, S. S., D. Westerman, B. Gates, T. Youngless, and L. Petrakis; Ind. Eng. Chem. Proc. Des. Dev., Vol. 23, No. 4 (1984).

Kittrell, J. R., P. S. Tam, and J. W. Eldridge; Hydrocarbon Processing, August (1985).

Kokai Tokkyo Koko JP; Chemical Abstract, 102:116473k, Vol. 102 (1985).

Krishna, A. S., and D. J. Bott; Ind. Eng. Chem. Proc. Des. Dev., Vol. 24, No. 4 (1985).

Kuzeev, I. R., R. G. Sharafiev, Yu M. Abyzgil'din, and M. V. Kretinim; Khimyai Tekhnologiya Topliv; Mosel, No. 1, pp. 27-28, January (1984).

Kwant, P. B., J. B. Wijffels, and W. C. Van Zijill Langhout; Petroleum Refining Conference on the Japan Petroleum Institute, Tokyo (1984).

Laine, J., J. Brite, J. Gallardo, and F. Severino; Journal of Catalysis, Vol. 91, pp. 64-68 (1985).

Leach, B. E., Editor; "Applied Industrial Catalysis", Vol. 1, Academic Press, New York (1983a).

Leach, B. E., Editor; "Applied Industrial Catalysis", Vol. 2, Academic Press, New York (1983b).

Lee, H.; Chemical Engineering Science, Vol. 37, No. 10, pp. 1539-1545 (1982).

Li, C. L., S. S. Katti, and B. C. Gates; Journal of Catalysis, Vol. 85, pp. 256-259 (1984).

Maloletnev, A. S., A. A. Krichko, M. K. Yulin, and A. M. Gyul'maiev; Kimiya; Tekhnologiya Topliv; Masel, No. 11, pp. 12-14, November (1984).

Mann, R. S., I. S. Sambi, and K. C. Khulbe; Symposium on Processing Heavy Oils and Residua, American Chemical Society Div. of Pet. Chem., Seattle (1983).

Mohammad, A. H., A. A. Abbas, and A. S. Al-Mayah; Fuel, Vol. 64, July (1985).

McKay, J. F., and D. R. Latham; Symposium on Characterization of Heavy Ends in Petroleum, American Chemical Society, Div. of Fuel Chem., New York (1981).

Moore, H. J., and A. Lamont Tyler; AIChE Symposium Series, Vol. 78, No. 216 (1982).

Moyse, B. M.; Oil and Gas Journal, December (1984).

Moyse, B. M., A. Albjerg, and B. H. Cooper; Oil and Gas Journal, March (1985).

Nagai, M., T. Sato, and A. Aiba; Journal of Catalysis, Vol. 97, pp. 52-58 (1968).

Nelson, W. L.; Oil and Gas Journal, February 28 (1977).

Nielsen, A., B. Cooper, and A. Jacobsen; Symposium on Residue Upgrading, American Chemical Society, Div. of Pet. Chem., March 29-April 3 (1981).

Oleck, S. M., and H. S. Sherry, ; U. S. Patent No. 448677, May (1984).

Parham, T. G., and R. P. Merrill; Journal of Catalysis, Vol. 85, pp. 295-310 (1984).

Patmore, D. J., C. P. Khulbe, and K. Belinko; Symposium on Residue Upgrading and Coking, American Chemical Society, Div. of Pet. Chem., Atlanta (1981).

Pazos, J. M., J. C. Gonzalez, and A. J. Gullen; Ind. Eng. Chem. Proc. Des. Dev., Vol. 22, No. 4 (1983).

Pereira, C. J., J. W. Beekman, W. C. Chang, R. G. Donnelly, and L. L. Hegedus; Symposium on Developments in HDM Catalysts, American Chemical Society, Div. of Pet. Chem., Miami (1985).

Plumail, J. C., Y. Jacquin, G. Martino, and H. Toulhoat; Symposium on Processing Heavy Oils and Residua, American Chemical Society, Div. of Pet. Chem., Seattle, March (1983).

Rao, V. G.m and A. A. Drinkenburg; AIChE Journal, Vol. 31, No. 7, July (1985).

Rasmuson, A.; Chemical Engineering Science, Vol. 40, No. 7, pp. 1115-1122 (1985).

Reynolds, J. G., W. R. Biggs, and J. C. Fetzer; Liquid Fuels Technology, Vol. 3, No. 4, pp. 423-448 (1985).

Richardson, R. L., and S. K. Alley; Symposium, American Chemical Engineering Society ,Div. of Pet. Chem., Philadelphia (1975).

Rollman, L. D.; Journal of Catalysis, Vol. 46, No. 3, March (1977).

Ruether, J. A., C. S. Yang, and W. Hayduk; Ind. Eng. Chem. Proc. Des. Dev., Vol. 19, No. 1 (1980).

Satterfield, C. N.; "Heterogeneous Catalysis in Practice", McGraw-Hill Book Company, New York (1980).

Satterfield, C. N., C. M. Smith, and M. Ingalls; Ind. Eng. Chem. Proc. Des. Dev., Vol. 24, No. 4 (1985).

Scamangas, A., N. Papayannakos, and J. Marangozis; Chemical Engineering Science, Vol. 37, No. 12 (1982).

Schucker, R. C.; Ind. Eng. Chem. Proc. Des. Dev., Vol. 22, No. 4 (1983).

Schuit, G. C. A., and B. C. Gates; AIChE Journal, Vol. 19, No. 3, May (1973).

Seapan, M., and B. L. Crynes; Quarterly Report No. 8, DOE/PC/60813-8, Department of Energy, Pittsburgh, August (1985).

Shiroto, S. Nakata, Y. Fukul, and C. Takeuchi; Ind. Eng. Chem. Proc. Des. Dev., Vol. 22, No. 2 (1983).

Sie, S. T.; "Catalyst Deactivation", Delmon and Froment, Editors, Elservier Scientific Publishing Company, Amsterdam (1980).

Sikonia, J. G.; Hydrocarbon Processing, June (1980).

Sikonia, J. G., T. G. Board, J. R. Wilcox, and L. Hilfman; "Shale Oil Upgrading and Refining", S. A. Newman, editor, Butterworth Publishers, Boston (1983).

Sinflet, J. H.; Scientific American, Vol. 253, No. 3, September (1985).

Sosnowski, J., and D. Turner; Chemical Engineering Progress, February (1981).

Takeuchi, C., M. Nakamura, and Y. Shiroto; Symposium on Advances in Petroleum Processing, American Chemical Society, Div. of Pet. Chem., Honolulu, April (1979).

Tamm, P. W., H. F. Harnsberger, and A. G. Bridge; Ind. Eng. Chem. Proc. Des. Dev., Vol. 20, No. 2 (1981).

Tarhan, M. O.; "Catalytic Reactor Design", McGraw-Hill, New York (1983).

Thakur, D. S., and B. Delmon; Journal of Catalysis, Vol. 91, pp. 308-317 (1985).

Thakur, D. S., P. Grange, and B. Delmon; Journal of Catalysis, Vol. 91, pp. 318-326 (1985).

Thompson, L. F., and S. A. Holmes; Fuel, Vol. 64, January (1985).

Tischer, R. E., N. K. Narain, G. J. Stiefel, and D. L. Cillo; Symposium on Catalytic Processes in Coal Conversion, American Chemical Society, Div. of Pet. Chem., Chicago (1985).

Topsøe, N. Y., and H. Topsøe; Journal of Catalysis, Vol. 75, pp. 354-374 (1982).

Topsøe, N. Y., and H. Topsøe; Journal of Catalysis, Vol. 84, pp. 386-401 (1983).

Tsakalis, K. S., T. T. Tsotsis, and G. J. Stiegel; Journal of Catalysis, Vol. 88, pp. 188-202 (1984).

Tsoung-Yuan Yan; Ind. Eng. Chem. Proc. Des. Dev., Vol. 23, No. 3 (1984).

Van Dongen, R. H., D. Bode, H. Van Der Fijk, and J. Van Klinken; Ind. Eng. Chem. Proc. Des. Dev., Vol. 19, No. 4 (1980).

Van Zijill Langhout, W. C., C. Ouwerkerk, and K. M. A. Prouk; Oil and Gas Journal, December (1980).

Ware, R. A., and J. Wei; Journal of Catalysis, Vol. 93, pp. 100-121 (1985a).

Ware, R. A., and J. Wei; Journal of Catalysis, Vol. 93, pp. 122-134 (1985b).

Ware, R. A., and J. Wei; Journal of Catalysis, Vol. 93, pp. 135-151 (1985c).

Whittington, E. L., V. E. Pierce, and B. B. Bansal; Chemical Engineering Progress, February (1981).

Wivel, C., R. Canadia, B. S. Clausen, S. Mørup, and H. Topsøe; Journal of Catalysis, Vol. 68, p. 453 (1981).

Woerde, H. M., L. J. Bostelaar, A. Heek, and W. M. Sachtler; Journal of Catalysis, Vol. 76, pp. 316-319 (1982).

Yang, S. H., and C. N. Satterfield; Journal of Catalysis, Vol. 81, 168-178 (1983).

Yang, S. H., and C. N. Satterfield; Ind. Eng. Chem. Proc. Des. Dev., Vol. 23, No. 1 (1984).

Zielinski, J. Z.; Journal of Catalysis, Vol. 76, pp. 157-163 (1982).

# APPENDIX A

# REACTOR SYSTEM

## Experimental Apparatus

The experimental apparatus was shown in Figure 1. It consisted of two fixed bed, reactors connected in series as described by Tarhan (1983) and Bhan (1983). The reactors were equipped with heating systems and temperature programmer/controllers. The apparatus also included oil and gas feed systems and two sampling systems. A brief description of the reactor system will be given here. More details are available in Bhan (1983) and Beazer (1984).

## The Reactors

The reactors consisted of 1.27 cm O.D. and 0.089 cm thick 316 stainless steel tubes. Reactor 1 was 43.2 cm and reactor 2 was 45.7 cm long. 0.32 cm stainless steel tubes, with one end welded shut, were used as thermowells. Parker fittings were used to secure the thermowells radially inside the reactors and to connect the reactors to the rest of the system.

Two monolithic aluminum blocks were bolted around each reactor as heating elements. Heat was supplied by bands fitted around the assembled blocks. Power was supplied through two temperature programmer/controllers for separate temperature control of each reactor. Iron constantan thermocouples were placed in drilled holes in the aluminum blocks. Output signals from the thermocouples were fed to the temperature programmer/controllers for precise temperature control. The reactor sysem was insulated with felt and glass fiber material.

## Oil Feed System

The oil feed system consisted of a stainless steel feed tank, a RUSKA positive displacement pump and a safety line. The feed tank was equipped with two heating bands and a thermowell. An iron constantan thermocouple was used to monitor feed temperature; a variac was used for control.

A RUSKA positive displacement pump was used to feed residue into the reactor, and the pump was operated at a pressure of 10.3 MPa and a rate of 35 ml of oil/h. The pump was refilled with residue every 24 h. The pump and feed lines were heated with flexible heating tape.

The feed line was equipped with a pressure transmitter connected to a shut-off switch. The pump was automatically turned off at pressures above 17 MPa. The feed system was also protected by a safety line equipped with a surge tank and two rupture discs. The discs were rated at 18.4 MPa and 21.8 MPa, respectively.

## Gas Feed System

Hydrogen gas from a cylinder manifold was metered through a high pressure flow meter and a 0-20.8 MPa Heise pressure gauge. A "Mity-Mite" regulator at the cylinder manifold was used to control system hydrogen pressure. Two check valves were placed on the reactor side of the hydrogen line to prevent residue flow in.

The upstream pressure of the system was monitored by the Heise pressure gauge. The downstream pressure was indicated by guages 43 and 44 connected to sample bombs 1 and 2, respectively (Figure 2). The Heise gauge reading was considered system pressure and was controlled by the "Mity-Mite" regulator.

Gas flow rate was maintained by means of the micrometer valve 10 and monitored by a Matheson low pressure rotameter. The low pressure rotameter was calibrated by connection to a 0-500 $cm^3$ bubble-flow-meter. A 60 vol% monoethanolamine scrubber and liquid traps were placed between valve 10 and the low pressure rotameter.

## Temperature Measurement

Temperatures were measured inside the catalyst beds, outside reactor walls, and outside feed and sampling lines. Three iron constantan thermocouples were placed along 10.2 cm intervals to measure outside wall temperatures for each reactor. Axial temperatures for each bed were measured with three thermocouples, 0.0254 mm diameter, placed at 7.62, 17.78 and 30.48 cm inside the thermowell. Iron constantan thermocouples were placed at selected points outside feed lines, sample bombs, and sample lines. Output from the thermocouples was fed to an Omega digital indicator through a multipoint temperature selector switch.

## Sampling Systems

This system consisted of four sample bombs (SB). The top of the first was connected to the bottom end of the second reactor. The bottom of this bomb was connected to the second sample bomb with the high pressure valve 3. Liquid and gaseous products from the first bomb passed into the second bomb where they were separated. Gases from the second bomb passed into the third and fourth bombs in series where the entrained liquid was removed. For liquid recovery from sample bomb 3, sample bombs 2 and 3 were connected from the bottom through valve 7.

Gases from bomb 4 flowed through the metering valve, the gas scrubber, liquid traps and the low pressure rotameter before exhausting into the hood.

## Gas Detectors

A combustible gas detector, MSA model 501, was installed in the laboratory with detectors located over the hydrogen cylinder-manifold and the reactors. An audible alarm with a red light would turn on once combustibles' level in the room reaches 40% of the lower explosive limit.

A portable hydrogen sulfide detector was used during catalyst sulfiding. Warning alarm would sound once $H_2S$ concentrations exceeded 20 ppm. This alarm also provided digital output of the instantaneous, average and maximum $H_2S$ concentrations.

## Inert Gas Purging Facilities

For start-up and sampling purposes, nitrogen was directly supplied to the bottom of sample bomb 2 from the supply cylinder. Nitrogen pressure was set by a pressure regulator on the cylinder. Nitrogen flowed into the sample bomb through valve 6, a check valve and valve 4. Valve 8 was used to vent the nitrogen to the atmosphere.

# APPENDIX B

# EXPERIMENTAL PROCEDURE

## Catalyst Preparation and Loading

For each reactor, the catalyst was packed in the middle section between two layers of glass beads. Glass beads were used to minimize end effects, improve liquid distribution and as catalyst support. The catalyst beds were designed for minimum pressure drop. The catalyst was packed according to its volume. The reactors were prepared from top to bottom according to the following procedure:

1. The thermowell was fitted centrally inside the reactor. A 50-mesh screen with a 0.32 cm diameter hole in the center was slid down the thermowell until it touched the top end of the reactor.

2. The top of the reactor was fitted with the appropriate Parker fittings. The reactor was held upside down.

3. Glass beads were poured into the reactor while gently tapping it for uniform packing. Glass beads were packed to a height of 7.62 cm in the top section.

4. While gently tapping, 8.75 $cm^3$ of catalyst were poured into the reactor.

5. A 1.27 cm redistributor was slid down the thermowell until it touches the catalyst.

6. While gently tapping, 8.75 $cm^3$ catalyst were packed into the reactor. A total of 17.5 $cm^3$ of catalyst were used in each reactor for all runs.

7. Glass beads were poured inside the reactor to a height of 5.08 cm.

8. A 50-mesh size screen with a 0.32 cm diameter hole in the center was slid down the thermowell until it touches the glass beads.

9. The rest of the reactor was fitted with a 0.95 cm stainless steel pipe to hold the catalyst bed in place (this was used instead of glass beads to minimize pressure drop).

10. The packed reactor was fitted with 1.27-0.67 cm Parker reducer so that it could be connected to the rest of the system.

Each fitting in the reactor system was pressure tested with nitrogen. Pressure testing was carried out at 11.09 MPa which was 693.33 kPa higher than operating pressure.

## Catalyst Sulfiding

A mixture of 5 vol% hydrogen sulfide in hydrogen ($H_2S/H_2$) was used for sulfiding. A total of 20 theories of sulfur (Jespen and Rase, 1981) with respect to the catalyst combination of CVR6 were passed through the catalyst beds in each run. Sulfiding was carried out as follows:

1. The hydrogen sulfide detector was turned on.

2. Valve 1 was closed to protect the gas feed system from hydrogen sulfide corrosion.

3. Valves 24, 14, 4, 7, and 8 were closed.

4. Valves 3, 9, 10, and 15 were opened.

5. Valve 2 was opened and $H_2S/H_2$ flow was started through the reactors at a pressure of 555 kPa and a flow rate of 800 $cm^3/min$.

6. Reactor heating was started at a rate of 50°C/h.

7. After about 4 h and when the temperature of the reactors reached 200°C, the pressure was increased to 1387.5 kPa. The same heating rate was maintained.

8. After about 3 h and when the temperature reached 350°C, this temperature was held constant for three hours.

9. After a total sulfiding period of 10 h, the $H_2S/H_2$ flow was cut-off by closing the main cylinder valve.

10. After the gas flowed out of the system (this was indicated by the gas pressure regulator and pressure gauge 43), valve 2 was closed.

11. The system was flushed with nitrogen by opening valve 1 and the main valve of the nitrogen cylinder.

## Start-Up Procedure

When catalyst sulfiding was complete, the temperature programmer/controllers were set at 370°C; 10°C lower than the operating temperature. The residue feedstock was charged into the feed tank and the RUSKA pump rate was set at 35 $cm^3$ of oil/h. The following start-up steps were followed:

1. Valve 23 was opened and the RUSKA pump was traversed to charge the residue into the pump.

2. Valves 23 and 24 were closed, and valve 22 was opened.

3. The feed out was traversed until the pressure of the pump was 10.3 MPa.

4. Valve 3 was closed.

5. The reactor was pressurized with hydrogen to a pressure of 10.3 MPa by opening valve 1 and setting the "Mity-Mite" regulator.

6. Valves 5, 7, 8, 9, and 14 were closed.

7. Valves 4 and 15 were opened.

8. Valve 6 was opened and the sample bombs were pressurized with nitrogen to 10.06 MPa.

9. Valves 4 and 6 were closed.

10. Valves 3 and 9 were opened.

11. The hydrogen flow rate was adjusted at 1040 $cm^3/min$ (1781 $m^3$ $H_2/m^3$ oil) by means of the needle valve 10 and the bubble-flow-meter.

12. The RUSKA pump was started and valve 24 was opened.

13. The temperature programmer/controllers were adjusted at 380°C.

## Normal Operation

During normal operation, maximum variations in temperature and pressure of 5°C and 100 kPa were considered tolerable. The temperature profile inside the reactor and along reactor walls, feed and sample lines' temperatures, pressure readings, pump scale reading, inlet and off gas flow rates, and hydrogen cylinder pressure were recorded every hour on the hour.

Valve throttle positions during normal operation were as follows:

Opened valves: 1, 3, 9, 10, 15, 22, and 24.

Closed valves: 2, 4, 5, 6, 7, 14, and 23.

## Sampling Procedure

Samples were collected every 6 h from the accumulated product in the sample bombs. Precautions were taken to minimize possible operational disturbances. The following steps were followed:

1. Valves 3 and 9 were closed.

2. Pressure in sample bombs 2, 3, and 4 (gauge 44) was reduced to atmospheric by opening valve 8 very slowly.

3. The pressure of the nitrogen purge cylinder was adjusted to 1040 kPa. Valves 6 and then 4 were opened to allow nitrogen flow into sample bombs 2, 3, and 4.

4. After purging for 5 minutes, valve 8 was closed until pressure in the sample bombs (gauge 44) rose to 1040 kPa. Valve 6 was closed.

5. A sample jar was placed in the sample port downstream valve 5. Valve 5 was opened very gently to allow the accumulated product to flow out.

6. Valve 7 was opened and let any collected liquid in bomb 3 to flow out.

7. Valves 5 and 7 were closed.

8. Valve 6 was opened to pressurize the sample bombs to 9.71 MPa.

9. Valves 4 and 6 were closed.

10. Valves 3 and 9 were opened.

11. After bringing the system back to normal operating, valve throttle positions were checked.

12. The collected sample was labeled.

## Feed Pump Recharging

The RUSKA pump's full capacity was 1000 ml of residue. The pump was recharged every 24 h. The following steps were taken:

1. One liter of residue was charged into the feed tank and heated to 100°C.

2. Tank lid was bolted and the tank was pressurized with nitrogen to 1730 kPa.

3. Valve 24 was closed and pump pressure was reduced to atmospheric. Valve 22 was closed.

4. Valves 23 was opened and the residue was charged into the pump by traversing the pump to suck the feedstock.

5. Valve 23 was closed and valve 22 was opened.

6. The pump was traversed until the discharge pressure gauge indicated 10.4 MPa.

7. The pump was started and valve 24 was opened.

8. Valve throttle positions were checked.

## Shut-Down Procedure

After a run duration of 72 h, the following shut-down procedure was carried out:

1. The RUSKA feed pump was turned off.

2. Valve 24 was closed.

3. The temperature programmer/controllers were turned off.

4. The pump was depressurized and the left over liquid was drained.

5. When temperature inside the catalyst beds dropped down to 250°C, hydrogen flow was stopped and the reactors were depressurized to 1730 kPa. Nitrogen purge was started.

6. When the reactors cooled down to room temperature, the sampling procedure was followed to collect the last product sample.

7. The reactors were depressurized and the oil and gas feed lines, and sample bomb 1 were disconnected.

8. Reactor insulation and heating system were removed.

9. Each reactor was cut and its catalyst was separated into 4 sections.

10. The catalyst samples and the top and bottom glass bead layers were labeled and kept for analysis.

# APPENDIX C

## MAJOR EQUIPMENT AND CHEMICALS

## Equipment

1. Reactors: 316 stainless steel tubing, 1.27 cm (1/2 in) OD, 0.089 cm (0.035 in) wall thickness. Top zone 43.2 cm (17 in) long, bottom zone 45.7 cm (18 in) long. Vendor: Precision Fitting & Gauge Company, Tulsa, Oklahoma.

2. Thermowells: 316 stainless steel tubing, 0.318 cm (1/8 in) OD, 76.2 cm (30 in) long with one end welded. Vendor: Precision Fitting & Gauge Company, Tulsa, Oklahoma.

3. Reactor Fittings: Parker union crosses, 1.27 cm (1/2 in). Parker reducing unions, 1.27 to 0.635 cm (1/2 to 1/4 in). Parker reducing unions, 0.635 to 0.318 cm (1/4 to 1/8 in). Parker tube end reducers, 1.27 to 0.635 cm (1/2 to 1/4 in). Parker union tees, 1.27 cm (1/2 in). Vendor: Precision Fitting & Gauge Company, Tulsa, Oklahoma.

4. Heating Blocks: Two aluminum blocks, each 10.2 (4 in) diameter. Top 38.1 cm (15 in) long and bottom 40.6 cm (16 in) long.

5. Band Heaters: 11.4 cm (4.5 in) diameter, 0.48 cm (3/16 in) gap, 120 volts, 400 watts. Vendor: Thermal Corporation, Huntsville, Alabama.

6. Bed Thermocouples: Iron-constantan, 0.025 and 0.05 cm (0.01 and 0.02 in) OD, 304 stainless steel sheath, grounded sensor tip, 91.4 cm (36 in) long, J-type. Vendor: Omega Engineering, Inc.

7. Wall Thermocouples: Iron-constantan, 0.159 cm (1/16 in), 304 stainless steel sheath, grounded sensor tip, 30.4 cm (12 in) long, J-type. Vendor: Omega Engineering, Inc.

8. Multiple Selector: 40 points selector connected to a temperature indicator. Vendor: Omega Engineering, Inc.

9. Temperature Controller/Programmers: Two controllers, one for each reactor zone. Model PC-6010-B. Vendor: Valley Forge Instrument Company, Inc., Phoenixville, Pennsylvania.

10. Powerstats: Input 120 volts, output 0-140 volts, 10 amperes, type 116. Vendor: The Superior Electric Company, Bristol, Connecticut.

11. Heating Tapes: Briskheat heavy insulated tape, 115 volts, 2.54 cm (1 in), and 1.27 cm (1/2 in) wide, 61 cm (2 ft) to 183 cm (6 ft) long. Vendor: Fisher Scientific Company.

12. Insulation Material: Fiberglass. Vendor: ACE Hardware Store, Stillwater, Oklahoma.

13. Pressure Gauges: Heise - Bourdon tube gauge, 0-20.6 MPa (0-3,000 psig). Vendor: Heise Bourdon Tube Company, Inc., Newtown, Connecticut. Crosby, Aschcroff, and Matheson gauges 0-20.6 MPa (0-3,000 psig). Vendors: Crosby, Ashcroft, and Matheson Company, Inc, respectively.

14. Pressure Regulator: Mity-Mite type, internally loaded, inlet pressure 34.5 MPa (5,000 psig), outlet pressure 20.7 MPa (3,000 psig), 0.635 cm (1/4 in) inlet and outlet connections. Vendor: Whitey Company.

15. Sample Bombs: 0.3 $m^3$, 12.4 MPa (1,800 psig), 304 stainless steel, model 6-645-232. Vendor: Matheson Company.

16. Surge Bomb: 2.25 $m^3$, 12.5 MPa (1,800 psig), 304 stainless steel, model 806. Vendor: Matheson Company.

17. Rupture Disks: 0.635 cm (1/4 in), bursting pressure 12.4 and 15.9 MPa (1,800 and 2,000 psig) at 22°C (72°F). Vendor: Autoclave Engineering.

18. Pump: RUSKA positive displacement pump, 1 $m^3$ barrel capacity, feed rates from 0.0025 to 0.56 $m^3$, 82.8 MPa (12,000 psig) maximum. Model 2236 WII-SXTR. Vendor: RUSKA Instrument Corporation, Houston, Texas.

19. Feed Tank: 21.6 cm (8.5 in) OD, 19.1 cm (7.5 in) in height, stainless steel tank.

20. Hydrogen Sulfide Detector: Concentration range 0 to 50 ppm, model 10 HS. Vendor: Sierra Labs, Inc., Palo Alto, California.

21. Hydrogen Detector: Combustible gas alarm, model I-501. Vendor: MSA Instrument Corporation.

## Chemicals

1. Hydrogen: 99.5% purity, 15.7 MPa (2,300 psig). Vendor: Sooner Supplies, Inc., Stillwater, Oklahoma.

2. Nitrogen: 99.5% purity, 15.7 MPa (2,300 psig). Vendor: Sooner Supplies, Inc., Stillwater, Oklahoma.

3. Hydrogen Sulfide: 5 vol% in hydrogen, 15.7 MPa (2,300 psig). Vendor: Jimmie Jones Company, Stillwater, Oklahoma.

4. Toluene: Reagent grade. Vendor: Fisher Scientific Company.

# VITA

HASAN MOHAMAD QABAZARD

Candidate for the Degree of

Master of Science

Thesis: THE EFFECT OF CATALYST ZONING ON HYDRODEMETALATION OF A PETROLEUM RESIDUE

Major Field: Chemical Engineering

Biographical:

Personal Data: Born in Al-Jibla, Kuwait, August 24, 1955, the son of Mohamad and Rabab Qabazard.

Education: Attended AL-Da'eyah School, Kuwait; received the Degree of Bachelor of Science in Chemical Engineering from The University of Tennessee, Knoxville, March, 1979; Completed requirements for the Degree of Master of Science in Chemical Engineering at Oklahoma State University in December, 1986.

Professional Experience: Process Engineer, Petrochemicals Industries Company, Shuaiba, 1979; Process Engineer, Kuwait Oil Company, Ahmadi, 1980-81; Deputy Managing Director, Arabian Light Metals Company, Ahmadi, 1982; Research Associate, Kuwait Institute for Scientific Research, Shuwaik, 1983-84; Research Assistant, School of Chemical Engineering, Oklahoma State University, Stillwater, January, 1985-May, 1986; 2nd Lieutenant on the Kuwait Army Reserve Force.

Membership in Scholarly and Professional Societies: Omega Chi Epsilon, Tau Beta Pi, Kuwait Engineers Society, American Society for Metals, Chevron Pilot Plant Committee, Oklahoma Society of Professional Engineers, The National Society of Professional Engineers.